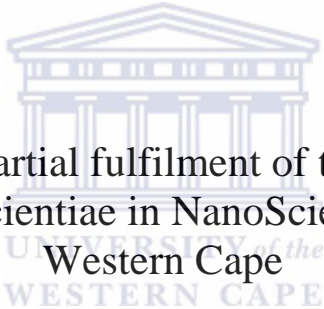# Synthesis of silver nanoparticles and investigating their antimicrobial effects

By

Zimasa N. Sithole

BSc (Honours) Biotechnology

A thesis submitted in partial fulfilment of the requirements for the Degree of Magister Scientiae in NanoScience, University of the Western Cape

Supervisor:	Professor Marla I. Tuffin
Co-supervisor:	Professor Leslie F. Petrik

December 2014

Abstract

Water is essential for life, yet access to safe drinking water is still a major concern worldwide due to waterborne diseases. The current study proposes silver nanoparticles (AgNPs) as an antibacterial agent. Silver nanoparticles were synthesised using different reductants and stabilisers, and the resulting structures were characterised with Ultra-violet visible (UV-vis) spectroscopy, transmission electron microscopy (TEM), energy-dispersive spectroscopy (EDS) analysis. The antibacterial properties of the AgNPs were tested against a panel of 5 indicator organisms: *Cupriavidus metallidurans, Staphylococcus epidermidis, Mycobacterium smegmatis, Bacillus cereus and* a multi-drug resistant *Escherichia coli* 1699.

Spherical AgNPs that absorbed at around 400 nm, with diameters ranging between 18.8-26.4 nm or 5.4-13.1 nm were prepared by ascorbic acid or sodium borohydride respectively. The optimum processing conditions that produced 6 ± 1.8 nm spherical nanoparticles included maintaining the temperature at 0 °C, the pH at 9.78 and the $NaBH_4$/Ag/PVP ratio at 16:1:10. Exposing AgNPs to light for 6 hours did not alter the particle size rather it changed the particles shape from spherical to icosahedral. Stirring caused particles to agglomerate, however, no agitation resulted in the formation of irregular structures of different sizes.

Sensitivity to the AgNPs ranged between 25 % and 100 % reduced bacterial growth depending on the strains used and the concentration of the AgNPs. The Gram negative bacteria were more sensitive to AgNPs than Gram positive bacteria. However silver ions were more toxic than AgNPs for all but one of the strains tested, *B. cereus* was completely resistant to both Ag^+ and AgNPs. *C. metallidurans* and *E.coli* (1699) showed a dose dependent sensitivity to AgNPs and the minimum inhibitory concentrations were established at 50 and 20 mg/L AgNPs respectively. *C. metallidurans* and *E.coli* (1699) were also eradicated by 10 mg/L Ag^+. The *E. coli* TEM images showed accumulation of AgNPs within the cells, cell shrinking and leakage of cellular components. This suggests that AgNPs have a similar toxicity effect on bacterial cells as Ag^+.

Keywords: safe drinking water, waterborne diseases; water disinfection; antimicrobial agent; nanotechnology, nanoparticles, silver nanoparticles; redox reaction; stabilising agents
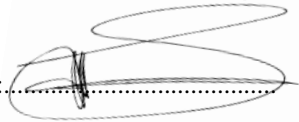
Declaration

I declare that *Synthesis of silver nanoparticles and investigating their antimicrobial effects,* is my own work, that it has not been submitted for any degree or examination in any other university, and that all the sources I have used or quoted have been indicated and acknowledged by complete references.

Full name: Zimasa Ntombizam Sithole   Date: 2014

Signed:...

Acknowledgements

Contents

LIST OF ABBREVIATIONS

AgNPs   Silver nanoparticles

CPG   Casamino-acid peptone glucose

DNA   Deoxyribonucleic acid

EDS   Energy-dispersive X-ray spectroscopy

EMU   Electron microscope unit

HRTEM   High Resolution Transmission Electron Microscopy

IMBM   Institute for Microbial Biotechnology and Metagenomics

LB   Luria broth

MIC   Minimum inhibitory concentration

OD   Optical density

PBS   phosphate buffered saline

PIA   polysaccharide intercellular adhesion

PVP   polyvinyl-pyrrolidone

RNA   Ribonucleic acid

ROS   reactive oxygen species

TEM   Transmission Electron Microscopy

TSB   Tryptic soy broth

UV-vis spectroscopy   Ultraviolet-visible (UV-vis) spectroscopy

WHO   World Health Organization

List of Figures

Chapter 4

List of Tables

Chapter 1

LITERATURE REVIEW

1.1. Introduction

This chapter accentuates the problems arising when people utilise unsafe water and the consequences thereof. It further addresses emerging pathogens; their resistance to antibacterial agents and the inefficiency of conventional disinfection methods. An innovative nanotechnology as a disinfection method is presented. The chapter further reviews the general literature on synthesis, characterisation and application of silver nanoparticles. The problem statement, the objectives and research question of the current study concludes this chapter.

1.2. Water stress and scarcity

Safe drinking-water is essential to sustain life and its availability may have tangible health benefits (Eisenberg *et al*., 2007). Hundreds of years ago water was available in abundance and considered an infinite resource in a world with fewer inhabitants and minimal pollution. The negative impacts of modern civilisation and industrialisation such as global warming, population growth and pollution have contributed to bringing about water stress and scarcity (Rijsberman, 2006; Gleick, 2003). A water stressed region is defined as an area that has an annual water supply below 1700 m^3/capita/year. Water scarcity results when the annual rain fall of a specific region is insufficient to sustain its population (Jiang, 2009; Rijsberman, 2006). Water stress and scarcity may occur as a result of natural causes such as climate change. Two thirds of the African countries including South Africa are already characterised

as water stressed with an annual water supply of 1000 m^3/ capita/year (Rijsberman, 2006). The World Resources Institute estimates this to increase, that 48 % of the world's projected population in 2025 will be living under water stress and scarcity conditions (Rijsberman, 2006; Johnson *et al*., 2001).

1.3. Waterborne diseases

Appending to the burden of water scarcity, 60 % of Africa's open water sources are regarded as unsafe resulting in over 1000 deaths per million population annually. The World Health Organisation (WHO) defines safe drinking water as: water utilised for domestic purposes that presents with microbial, chemical and physical contaminants below the WHO guidelines or national standards on drinking water quality (WHO, 2011; Eisenberg *et al*., 2007). Consumption and utilization of unsafe water may result in waterborne outbreaks. A waterborne outbreak is defined as an incident where a number of people suffer waterborne illness with epidemiological evidence linking to a common water source. Microbial pollutants exceed the other water contaminants and the consumption of pathogen contaminated water may result in a waterborne disease (Morones *et al*., 2005; Sondia & Salopek-Sondib, 2004; Lok *et al*., 2006; Goering *et al*., 2007).

1.3.1. Waterborne pathogens

Waterborne diseases are caused by pathogens transmitted into the body through ingesting, or by mucosal and skin contact, with contaminated water (Morones *et al*., 2005; Sondia & Salopek-Sondib, 2004; Lok *et al*., 2006; Goering *et al*., 2007). The infection can be encountered when bathing, drinking or using contaminated water when preparing food. Waterborne illnesses manifested by gastroenteritis-like symptoms include watery or perfuse diarrhoea, vomiting, fever and they may be severe, causing otitis, cholera, haemolytic

uraemic syndrome, renal failure and ultimately death (Goering *et al*., 2007). Waterborne pathogens comprises of bacteria, fungi, viruses and protozoa (Guggenbichler *et al*., 1999; Sambhy *et al*., 2006; Dibrov *et al*., 2002; Goering *et al*., 2007; Parka *et al*., 2009; Rai *et al*., 2009; Rosarin & Mirunalini, 2011). The World Health Organisation narrows the list of virulent waterborne bacterial pathogens to include *Burkholderia pseudomallei, Campylobacter jejuni*, *C. coli, Escherichia coli –EHEC, Francisella tularensis, Legionella* spp., *Leptospira, Mycobacteria* (nontuberculous), *Staphylococcus spp., Salmonella Typhi, Salmonellae, Shigella* spp. *Bacillus spp* and *Vibrio cholera* (WHO, 2011). The aquatic environment, soil and vegetation are natural habitats for these organisms. However, these organisms are abundant in faeces of warm-blooded animals, hence faecal contaminated water is the main source of infection.

1.3.1.1. Bacillus spp.

Bacillus is a genus of heterogenic group of gram positive, endospore-forming, rod-shaped, facultative anaerobic bacteria. This endospore-forming ability permits the bacteria to tolerate harsh conditions better than the non-sporulating bacterial enteropathogens. Under stressful environmental conditions, the bacterium produces oval endospores that can stay dormant until the environment becomes comfortable and then they germinate to their vegetative form that is most infective. The bacteria proliferate in a wide range of environments including the soil, water and foods. Some species are pathogenic to humans and are found in abundance within the gut of warm blooded animals; hence they are transmitted through fecal-oral route. *Bacillus cereus* is the most virulent foodborne pathogen of all *Bacillus* species. *B. cereus* produces heat-labile enterotoxins and a heat-stable emetic toxin that are respectively responsible for the diarrheal and vomiting type of illnesses (McIntyre *et al*., 2008). Other *Bacillus* species such as *B. subtilis*, *B. pumilus*, *B. anthracis* and *B. licheniformis* have

generally been considered of little significance in food poisoning incidents but their ability to produce both enterotoxins and emetic toxin has been increasingly recognized (McIntyre *et al.*, 2008; From *et al.*, 2005; Apetroaie-Constantin *et al.*, 2008). They have an infection dose of a million colony forming units per gram of sample. The symptoms manifest within 15 minutes to 11 hours post infection and may last a day. Symptoms include vomiting, abdominal cramps, diarrhoea, nausea, headaches and sweating. The intoxication is usually self-limiting (McIntyre *et al.*, 2008). The infection may be severe and cause bovine mastitis, severe systemic and pyogenic infections, gangrene, septic meningitis, cellulitis, panophthalmitis, liver failure, lung abscesses, infant death, and endocarditis (Apetroaie-Constantin *et al.*, 2008). Thermal disinfection may not be ideal in disinfecting endorespore forming bacteria since high temperatures induce the formation of heat stable spores and slow cooling may favour the formation of the enterotoxin.

1.3.1.2.   *Escherichia coli*

E. coli is a Gram negative, facultative anaerobic bacillus. The bacterium is found in the soil and fresh produce but is present in abundance in the intestine of warm-blooded animals. Hence it is an ideal indicator of faecal contamination. Indicator organisms are non-pathogenic organisms that are present in abundance in faeces therefore are used to measure potential faecal contamination of environmental samples. Faecal contaminated samples pose a hazard due to the presence of pathogens that are transmitted through the faecal-oral route such as *Vibrio cholerea, Salmonella typhi,* and *Leptospira spp*. *E. coli* is normally harmless and forms the normal flora in the gut where it produces vitamin K_2. Some serotypes, such as Enterohemorrhagic *E. coli* (O157:H7), Enteroinvasive *E. coli* and Enterotoxigenic *E. coli*, have gained virulent genes, through horizontal gene transfer, that cause serious food intoxication and food poisoning in human. Poor hygiene, improper cooking of food, faecal contaminated domestic and irrigation sources may result in foodborne illnesses. In 2006 *E.*

coli O157:H7 contaminated spinach and lettuce caused 205 foodborne illnesses that claimed the lives of 3 citizens in Atah and New Mexico (Grant *et al*., 2008). *E. coli* O157:H7 caused 3,950 outbreaks of foodborne illnesses episodes and 53 deaths in northern Germany in 2011 (Bielaszewska *et al*., 2011).

1.3.1.3.   Mycobacteriaceae

Mycobacterium is a genus in the family of Mycobacteriaceae. They are aerobic, nonmotile, straight or slightly curved bacilli. The bacteria have a long incubation period that can extend up to 3 weeks. Mycobacteria have a distinct waxy, thick, acid-alcohol-fast and hydrophobic cell wall rich in mycolic acid. Mycolic acids are interconnected to the peptidoglycan layer by polysaccharides and arabinogalactan. The cell wall also presents with high lipid content that accounts for hydrophobicity and allows these bacteria to adhere to surfaces easily and form biofilms (Falkinham, 2003). The cell wall makes a substantial contribution to the resilience of this genus. They are naturally resistant to a number of antibiotics that disrupt cell-wall biosynthesis, such as penicillin. Furthermore the cell walls aid in the resistance to acid, alkalis, detergents, oxidative bursts and lysis (von Reyn *et al*., 1993; Falkinham *et al*., 2001). The bacteria can be found in a number of environments such as water, aerosols, soil, mud, plants and can replicate in free-living amoebae (von Reyn *et al*., 1993; Falkinham *et al*., 2001). The genus comprises of some non-pathogen strains such as *M. smegmatis* and other well known pathogens such as *M. avium, M. intracellulare, M. leprae* and *M. tuberculosis* (Falkinham, 2003). Over the years *Mycobacteria* were susceptible to the antibiotics clarithromycin and rifamycin, but antibiotic-resistant strains have emerged. *M. avium* is a potential pathogen occurring in drinking water systems and it is known to resist chlorine better than many other microbes (Torvinen *et al*., 2007; Taylor *et al*., 2000; Falkinham, 2003). The incidences of *M. avium* and *M. intracellulare* infections have exponentially increased from 1.5 to 9.0 cases per 100,000 population during 1997-2003 in Canada

(Falkinham, 2011). The infections are mostly virulent to the immunodeficient (e.g., HIV/AIDS) and immunosuppressed (e.g. cancer and transplant) patients and elderly people. These bacterial strains dwell in household plumbing systems where they exist in biofilms (von Reyn *et al*., 1993; Falkinham, 2011). Taylor *et al.,* (2000) concluded that *M. avium* is highly resistant to ozone- and chlorine-based disinfectants.

1.3.1.4. *Staphylococcus epidermidis*

Staphylococcus epidermidis are nonmotile, capsulated, gram-positive cocci that are approximately 0.5 to 1.5 micrometers in diameter that arrange themselves into grape-like clusters when viewed with a microscope (Mack *et al*., 1996). The normally colonize the human and animal skin and mucous membranes (Mack *et al*., 1996; Kalishwaralal *et al*., 2008). *S. epidermidis* is normally a non-pathogenic bacteria and it forms part of the human skin flora. Opportunistically the bacteria may manifest skin infection and systemically spread to cause endocarditis or sepsis in immunocompromised patients. The bacterium has the ability to form biofilms hence the burden in surgical implants, contact lenses, prostheses and catheters (Kalishwaralal *et al*., 2008). The capsule comprises of polysaccharide intercellular adhesion (PIA) which aids the bacterium to bind to the already existing biofilm, which is an antimicrobial resistance strategy employed by the bacteria. The biofilm sanctuary protects the bacteria from disinfection and supplies these pathogens with nutrients abundantly, therefore allowing the microorganism to persist for longer (Lehtola *et al*., 2007; Steed & Falkinham, 2006; Falkinham, 2003). Biofilm is a slime of bacteria communities living in aggregates in a mass of self-produced matrix; these cells adhere to each other on a surface (Guggenbichler *et al*., 1999; Furno *et al*, 2004). This slime is a polymeric accumulation of microorganisms, nucleic acids, proteins, and polysaccharides. Species which live in this community are more virulent and difficult to eradicate than those living in isolation (Guggenbichler *et al*., 1999;

Furno *et al*, 2004; Goering *et al*., 2007). Chloride and antibiotics cannot easily diffuse in the mesh of PIA hence the inefficacy in eradication biofilms (Stewart & Costerton, 2001; Mah & O'Toole, 2009). There are emerging strains that are developing resistance to first line antibiotics such as penicillin, amoxicillin, and methicillin.

1.3.2. The burden of waterborne diseases

Waterborne diseases claim approximately 1.8 million lives annually of which 84 % are children under five years of age (Tiwari *et al*., 2008; WHO, 2011). Tiwari *et al.,* (2008) estimated that a child dies from waterborne diseases every 15 seconds in Africa. The most susceptible people are immune compromised patients, elderly people over 65 years of age and those infected with HIV/AIDS (Goering *et al*., 2007). The burden of waterborne diseases may be under-estimated in accordance with the absence of proper surveillance and abuse of broad-spectrum antibiotics, where antibiotics are administered without identifying the causative agent. Contaminated surface water may contribute other water related diseases such as vector-borne diseases and food poisoning, therefore broadening the mortality to 5 million annually (Gleick, 2003). Waterborne disease results in healthcare expenses and lost productivity days therefore threatening the food security, economic development and quality of life (Jiang, 2009; Rijsberman, 2006; Johnson *et al*., 2001).

1.3.2. Risk factors that may escalate the burden of waterborne diseases

Sewage discharge without sufficient treatment is the main source of organic impurities in surface water (WHO, 2011). Poor hygiene, improper water disinfection methods and open defecation increase the risk of waterborne diseases (Eisenberg *et al*., 2007; Tiwari *et al*., 2008). The majority of Africa's population has a low socioeconomic status and lives in the rural regions where open defecation is still practised (Tiwari *et al*., 2008). Improving water quality in recreational water and domestic-water supply in rural Africa is currently

challenging. Hence there are so many deaths resulting from waterborne diseases (WHO, 2011). South Africa has improved the quality of drinking water and accordingly the amount of waterborne outbreaks has decreased (Kahinda *et al*., 2007).

1.4. Antimicrobial agents

Water contamination has evolved over the years hence water purification technologies such as distillation, reverse osmosis, ultra-violet light, slow sand filtration, rapid sand filtration, anodic oxidation, chlorine dioxide, thermal treatment, chlorination and silver based filters have been developed (Burch & Thomas, 1998). These techniques have disadvantages such as producing off-taste water; some of the compounds are carcinogenic, expensive and may contribute to climate change by using enormous amounts of energy (Burch & Thomas, 1998). Some methods are inefficient at eradicating biofilms, heat stable toxins and endospore forming bacteria (Burch & Thomas, 1998; Goering *et al*., 2007; Morones *et al*., 2005; Dibrov *et al*., 2002). South African municipal water disinfection infrastructures prefer thermal and chlorine treatment techniques as they are easy to conduct and cheaper (Burch & Thomas, 1998; Momba *et al*., 2009). However these technologies also have disadvantages and the epidemiology of waterborne diseases raises global public health concerns about emerging pathogens that are resistant to the conventional water purification techniques (WHO, 2011).

1.4.1. Thermal treatment

Thermal treatment may stimulate endospore-forming bacteria to change from vegetative cells to endospores. Endospores are reproductive structures that bacteria form when environmental conditions are fatal to the bacteria. When the environmental conditions are comfortable; the spore germinates into vegetative cells that are infective (Goering *et al*., 2007). The treatment is also ineffective against bacteria that produce heat-stable toxins. The mode of action of these pathogens involves the production of heat stable toxins which can survive very high

temperatures and if ingested cause food intoxication (Morones *et al*., 2005; Dibrov *et al*., 2002; Goering *et al*., 2007). The toxin attaches to the intestinal mucosa and causes massive loss of water into the intestinal tract which will be later lost by the body through diarrhea (Dibrov *et al*., 2002; Goering *et al*., 2007).

1.4.2. Chlorine treatment

Scientists have realised that chlorination is not effective in eradicating bacteria in biofilms (Furno *et al*., 2004; Lehtola *et al*., 2007; Steed & Falkinham, 2006; Furno *et al*., 2004; Goering *et al*., 2007). Some bacterial pathogens, such as *Mycobacterium* spp., *Vibrio* spp. and *Campylobacter* spp, form biofilms in water purification systems as a survival strategy (Buswell *et al*., 1998, Lehtola *et al*., 2007). Conversely chlorine interacts with salts and compounds that can be found in water therefore producing harmful by-products (Pontius, 1990).
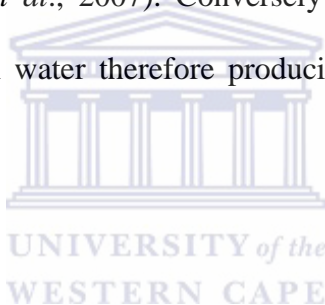
1.4.3. Metal treatment

Essential metals (such as calcium, potassium, magnesium, manganese and sodium) are required nutrients and function as catalysts for biochemical reactions, stabilizers of protein structures, bacterial cell walls and maintain the osmotic balance. There are other metals that are nonessential and have no biological role (such as silver, aluminium, cadmium, lead and mercury) and which are toxic to microorganisms. Silver is considered to be the most toxic element to microorganisms: Ag >Hg >Cu >Cd >Cr >Pb >Co >Au >Zn >Fe >Mn >Mo >Sn therefore is considered an alternative to antibiotics (Sondia & Salopek-Sondib, 2004). Silver has been used as antimicrobial agents in medicine for many years (Fox & Modak, 1974; Furno *et al*, 2004; Morones *et al*., 2005; Sambhy *et al*., 2006; Lok *et al*., 2006; Rai *et al*., 2009; Parka *et al*., 2009; Rosarin & Mirunalini, 2011). These non-essential metals have a greater affinity to thiol-containing groups and oxygen sites than the essential metals. Bruins

et al., (2000) described the mode of action of toxic and non-essential metals to include covalent or ionic interactions of the metals with essential cellular processes therefore damaging cell membranes, altering conformational structure of nucleic acids and proteins therefore interfering with enzyme specificity, disrupting cellular functions, and damaging the structure of DNA. Silver is a broad-spectrum biocide that hinders cell replication and eradicates a wide range of microorganisms including fungi, viruses, bacteria and protozoa (Morones *et al.*, 2005; Fox & Modak, 1974; Rosarin & Mirunalini, 2011; Furno *et al.*, 2004). However bacteria have adapted to metals through a variety of chromosomal, transposon, and plasmid-mediated resistance systems. These resistance mechanisms include exclusion by permeability barrier, intra- and extra-cellular sequestration, active transport efflux pumps, enzymatic detoxification, and reduction in the sensitivity of cellular targets to metal ions. When metals are present in small quantities they are transported into the cell by nonspecific uptake systems (Nies & Silver, 1995). However, in situations where metal ions are in excess, synthesis of specific ion efflux systems can occur to exclude nonessential metals.

As an example, *C. metallidurans* has two large plasmids, pMOL28 and pMOL30, which carry genes that code for heavy metal resistance which are expressed when the microorganism grows in a metal stressed environment. *C. metallidurans* mediates its resistance to heavy metals by trans-membrane transporter protein complexes, which export cations from the cytoplasm to the exterior of the cell (efflux) and reductive precipitation (Mergeay *et al.*, 2003; Reith *et al.*, 2009; Rojas *et al.*, 2011). Some bacteria have cell surface electron-transport systems or enzyme-reducing systems that allow bacteria to detoxify and regulate the movement of metal ions by changing their valence or charge through oxido-reduction in order to regulate and resist the metal (Wakatsuki, 1995). Reith *et al.*, (2009) revealed that the *C. metallidurans* has the ability to reduce ionic gold to elemental gold therefore producing gold nanoparticles. Some facultative anaerobes have also been shown to

reduce Cr (VI) through their electron-transport systems containing cytochromes (Wang & Shen, 1995). Mullen *et al.* (1989) showed that *B. cereus* grown in the presence of 1 mM AgNO$_3$ could bio-remediate and detoxify 89 % of silver ions and produced colloidal aggregates that accumulated in the cell surface and occasionally in the cytoplasm (Mullen *et al.*, 1989). Other *Bacillus* species have also been reported to produce silver nanoparticles such as *B. licheniformis* (Beveridge *et al.*, 1982; Kalishwaralal *et al.*, 2008), *B. cereus* PGN1 (Ganesh Babu *et al.*, 2009), *B. subtilis* (Beveridge *et al.*, 1980) but the mechanism of this reaction is not yet clear. The plasmid-mediated resistance systems have been shown to be transferable to organisms that are naturally metal sensitive (such as *Staphylococcaus* sp., *Escherichia coli*, *Pseudomonas aeruginosa*, and *Bacillus* sp) through conjugation or transduction gene transfer. Like the development of antibiotic resistance, human activities can create environments of high selection for metals and lead to metal resistance (Ji & Silver, 1995). However, there is a contradiction in literature whether there is significant microbial resistance to silver in environments where silver is routinely used; such as, burns units in hospitals, silver-coated catheters and dental settings (amalgams contain 35 % silver).

1.5. Innovative technologies

Nanotechnology

Science is faced with a challenge of inventing rapid, specific, portable and sensitive water purification technologies. Nanotechnology has the potential to produce materials that can be used for small-scale or point-of-use systems, which do not need a connected central infrastructure and could be used in emergency responses following disasters.

Nanotechnology is the study and application of nanomaterials. It has the potential to produce water treatment systems that efficiently disinfect water while producing fewer pollutants than

traditional methods, and may require less labour, capital, land and energy. A nanomaterial is defined as a naturally occurring or artificially synthesised substance composed of particles, either in unbound state, aggregated or agglomerated, with a size distribution of one or more external dimensions ranging from 1 nm to 100 nm (Sahoo *et al*., 2009; Rosarin & Mirunalini, 2011). Nanomaterials are fabricated by either *bottom-up* or *top-down* approaches as demonstrated in Figure 1.2 (Sahoo *et al*., 2009; Rosarin & Mirunalini, 2011).
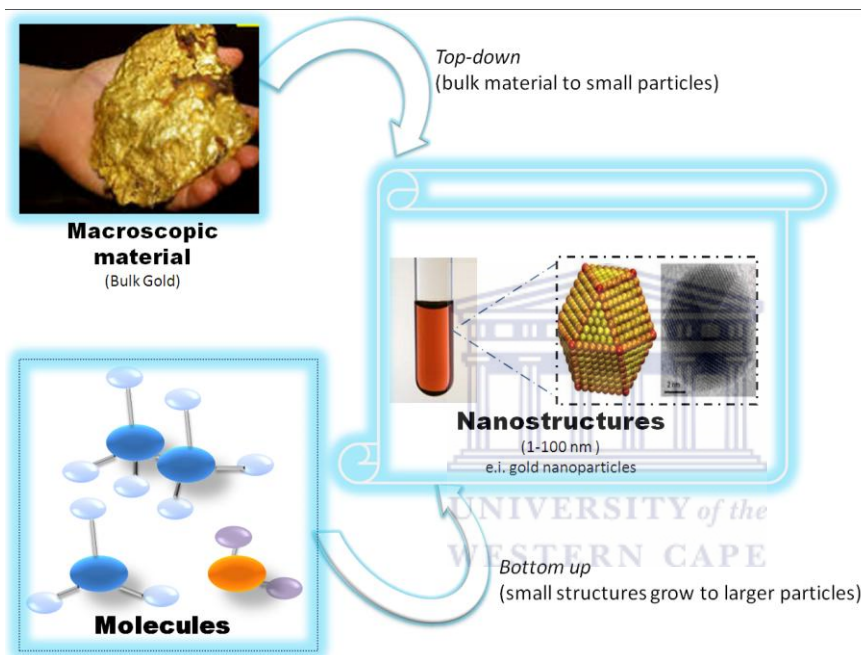
Figure 1.1: Illustration of top-down approach vs the bottom-up approach in the synthesis of nanoparticles.

The *top-down* approach involves the breakdown of a bulk material into the nanoscale size without changing the elemental composition of the bulk material, an example may be laser ablation (Sahoo *et al*., 2009; Rosarin & Mirunalini, 2011). While the *bottom-up* approach fabricates nanoparticles by collecting, consolidating and fusing individual atoms and molecules to nanosized particles, an example could be chemical reduction (Rosarin & Mirunalini, 2011). The *bottom-up* approach has the potential to engineer homogenous nanostructures with less defects and controlled size distribution (Rosarin & Mirunalini,

2011). Nanoparticles can either occur naturally or be artificially synthesised (chemical reduction). These nano structures have an increased surface area to volume ratio that results in enhanced quantum mechanical effects (Thembela *et al.*, 2006; Sahoo *et al.*, 2009). Decreasing bulk material size to the nanoscale has resulted in enhanced optical, electrical, catalytic and toxic properties of that material (Thembela *et al.*, 2006, Rai *et al.*, 2009; Sahoo *et al.*, 2009; Rosarin & Mirunalini, 2011).

1.6. Silver nanoparticles

1.6.1. Synthesis of silver nanoparticles

The bottom-up approach synthesis of silver nanoparticles involves the reduction of ionic silver to elemental silver and then these silver atoms self-assemble to form particles between 1 nm and 100 nm. There are several methods to prepare silver nanoparticles such as chemical reduction of silver ions in aqueous solutions with or without surfactants, electrochemical reduction, heat evaporation, and thermal decomposition in organic solvents, polyol process, photoreduction in reverse micelles, biological, radiochemical and chemical reduction (Sahoo *et al.*, 2009). The chemical reduction method has been predominantly studied because it has the potential to produce nanoparticles of controlled size, shape and dispersion cheaply, and in a short period of time (Sahoo *et al.*, 2009). The synthesis of silver nanoparticles by wet chemical method initially involves the dissociation of silver nitrate ($AgNO_3$) into a silver ion (Ag^+) and a negative nitrate ion (NO^{3-}). Then in order to convert the silver ions into solid silver, Ag^+ has to be reduced by receiving an electron from a donor (Cao, 2004; Chou *et al.*, 2005). The equation below illustrates the reduction of the silver ions by addition of an electron. Subsequently silver atoms self-assemble and continue growing until the equilibrium between the final nanoparticles and the Ag^+ of the solution is reached (Chou *et al.*, 2005).

$$Ag^+_{(aq)} + e^- \rightarrow Ag_{(s)}$$
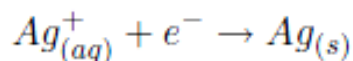
Optimising the reaction parameters such as, pH, temperature, amount of reducing agent and the presence of a stabilising agent is predicted to control the particle size, shape and dispersion.

1.6.1.1. Effect of stabilising agent in the synthesis of silver nanoparticles

A stabilising agent is a substrate that ideally prevents particle agglomeration. Stabilising agents form a protective shell that coats the nanoparticle and this layer increases the zeta potential therefore prevents nanoparticle agglomeration (Irwin *et al*., 2010). Stabilising agents include surfactants, polymers or ions that are responsible for increasing the zeta potential between particles therefore preventing agglomeration, hence controlling the particle size and dispersion in a colloidal system (Sahoo *et al*., 2009). The polymer (stabilising agent) attaches to the particle at one end therefore the polymer looks like tentacles on the particle. The alkaline pH and the presence of citrate as a dispersing agent has promoted the formation of mono-dispersed spherical silver nanoparticles (Qin *et al*., 2010). Likewise the use of polymer polyvinyl-pyrrolidone (PVP) as a stabilising agent has produced small particles with a uniform size distribution (Irwin *et al*., 2010). PVP is one of the known polymers that have high affinity for silver metal. This hydrophobic polymer covalently links to the silver metal by its pyridyl groups. The polymer binds to the AgNPs and forms a micelle around the nanoparticles. PVP is partially charged therefore causing inter-particle repulsion. Polymer molecules require a good solvent to perform at their utmost capability. If the solvent permits the stabilising agent to stretch away from the particle then the solvent is effective, whereas if the solvent makes the stabilising agent collapse on the surface of the particle then the solvent

is poor. These polymer molecules collapse when the nanoparticles are suspended in a poor solvent such as the acidic pH of the ascorbic acid based synthesis.

1.6.1.2. The effect of temperature on the synthesis of silver nanoparticles

Sahoo *et al*., (2009) synthesised AgNPs using sugars and found that increasing the temperature from 30 °C to 60 °C increases the nanoparticle size. The increase in temperature is directly proportional to the reaction rate and may cause agglomeration of the particles since the time will not be conducive to allow coating of the Ag^+ by the stabilisers (Jiang *et al*., 2011). Temperatures below 30 ºC tended to produce spherical particles smaller than 30 nm in size whereas temperatures between 30 ºC–60 ºC favoured the formation of triangular shaped nanoparticles between 40 nm and 100 nm in size (Jiang *et al*., 2011). Heating a solution with reduced silver ions supplies the silver atoms with enough kinetic energy to penetrate the polymer layer, favouring particle agglomeration (Cao, 2004). Therefore heating can be used to produce larger particles but the method of heating is important. Microwave heating is preferred to a hot plate due to homogeneous heat transfer to the solution instead of the localised heating produced by a hot plate.

1.6.1.3. Effect of pH on the synthesis of silver nanoparticles

When a substance wich is either positively or negatively charged is exposed to an electrolyte either the OH^- or H^+ adheres to its surface through the electrostatic interaction, therefore altering the surface charge. Point of Zero Charge (pzc) is a surface characteristic of a material and it is defined as the pH at which the surface of a material has a net neutral or zero charge. The point of zero charge of silver is estimated to be at pH 5.5 (Overbreek, 1952; Hunter, 1987; Shaw, 1992). Qin *et al.,* (2010) synthesised silver nanoparticles, where silver nitrate was reduced by ascorbic acid at different pH's and demonstrated that increasing the pH from 6 to 10.5 could alter the particle size from 73 nm to 31 nm. The alkaline pH and the presence

of a citrate as a dispersing agent promoted the formation of mono-dispersed spherical silver nanoparticles (Qin *et al*., 2010). Sahoo *et al.,* (2009) also agrees that alkaline pH (8.5-9.0) yielded smaller mono-dispersed nanoparticles at a faster rate than the acidic pH.

1.6.1.4.   Synthesis of silver nanoparticles with different shapes

Several studies have predicted that silver nanoparticles with different shapes have diverse affects on the bacteria (Lkhagvajav *et al*., 2011; Morones *et al*., 2005; Dibrov *et al*., 2002; Goering *et al*., 2007). Jiang *et al.,* (2011) exposed silver nanoparticle spheres to light and produced different shaped nanoparticles. Different shapes were formed at different maturation stages; for example spherical discs are immediately formed whereas triangle platelets form as the reaction progressed at elevated temperatures of about 40 $^{\text{o}}$ C and after 48 hours of exposure the suspensions were a three-dimensional icosahedral structure (Jiang *et al*., 2011).
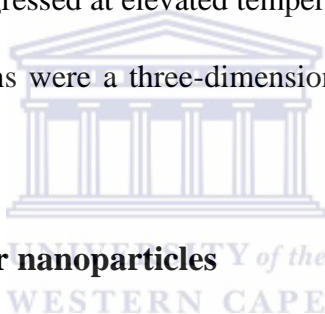
1.6.2. Mode of action of silver nanoparticles

The large surface area exposed in silver nanoparticles increases their interaction with the microorganisms therefore enhances the antimicrobial effect compared to other bulk silver ion counterparts (Morones *et al*., 2005; Sondia & Salopek-Sondib, 2004; Rai *et al*., 2009; Rosarin & Mirunalini, 2011; Furno *et al*., 2004; Lok *et al*., 2006). Silver nanoparticles have shown the ability to penetrate biofilms and have cidal effects even to virulent biofilm communities (Furno *et al*., 2004). The bactericidal effect of silver nanoparticles is not very well understood (Lkhagvajav *et al*., 2011; Dibrov *et al*., 2002). It is predicted to disrupt cellular metabolism, the electron transfer system, the transportation of substrate in the microbial cell membrane and suppresses respiration therefore hindering cellular development and replication and ultimately causing cell death (Fox & Modak, 1974; Sondia & Salopek-Sondib, 2004; Dibrov *et al*., 2002) [Figure 1.3].

Cell wall [1]
Cell membrane [2]
Cytoplasm [3]
Plasmid [4]
Ribosomes [5]
Nucleoid (DNA) [6]
RNA [7]
Peptides [8]
Proteins [9]
Silver nanoparticle [10]
Silver ions [11]
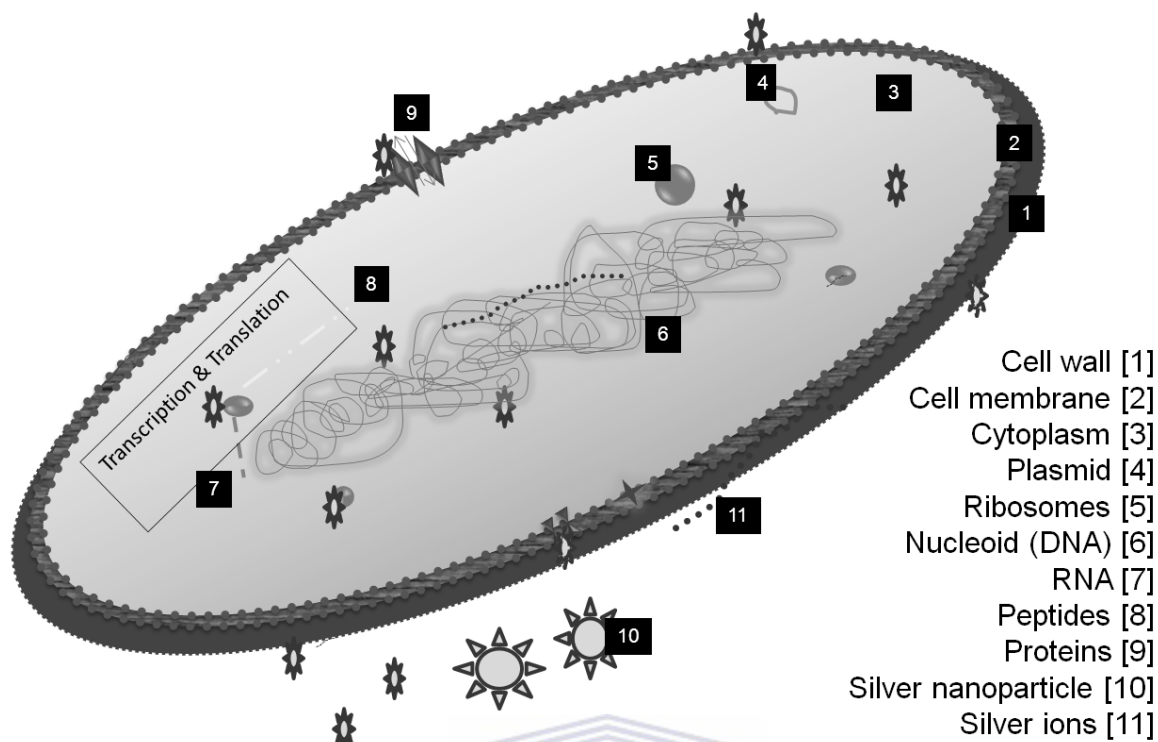
Figure 1.2: The predicted silver nanoparticles mode of action in a bacterial cell.

The nanoparticles react with cell membrane components and the constituents of the solution they are suspended in and get oxidised to produce silver ions. Silver ions interact with multiple cellular compartments; including protein, nucleic acids, ribosomes, cell membrane and the cell wall, in that way they could evade the emergence of microbial resistance (Morones *et al*., 2005; Sambhy *et al*., 2006; Parka *et al*., 2009; Rosarin & Mirunalini, 2011; Furno *et al*., 2004). Silver ions directly inhibit the production of antioxidants leading to elevated reactive oxygen species (ROS) concentrations (Choi & Hu, 2008), which may cause nucleic acid and protein oxidation, activating apoptosis (Sondia & Salopek-Sondib, 2004; Dibrov *et al*., 2002; Parka *et al*., 2009; Rosarin & Mirunalini, 2011). Silver or silver ions bind to the sulfhydryl (SH-) groups of some enzymes therefore inhibiting their enzymatic activity (Lkhagvajav *et al*., 2011; Dibrov *et al*., 2002). Dibrov *et al.,* (2002) revealed that submicromolar concentration of silver ions (Ag^+) targets the sodium translocating NADH:

ubiquinone oxidoreductase therefore inhibiting energy-dependent sodium ions (Na^+) transport in membrane vesicles of *Vibrio cholerae*. Low micromolar concentrations of Ag^+ causes proton (H^+) leakage therefore collapsing the proton motive force, respiration-generated membrane electric potential and pH gradient across the mitochondrial membrane, therefore disrupting the bacterial metabolism (Dibrov *et al*., 2002). This causes loss of energy which may result in cell death. Literature has confirmed that AgNPs have cidal effects against a range of microorganisms including *Escherichia coli, Staphylococcus aureus, Candida albicans, Bacillus subtilis, Salmonella typhimurium, Pseudomonas aeruginosa, Vibrio cholerae* and *Klebsiella pneumoniae* (Dibrov *et al*., 2002; Lkhagvajav *et al*., 2011).

The mode of entry of the nanoparticles into a bacterial cell has not yet been identified, but silver nanoparticles have been found inside the cells. Lkhagvajav *et al.,* (2011) suggested that the bacteriocidal effect is dependent on the ability of the nanoparticle to bind to the microorganisms and the high surface area available for interaction. Particles smaller than 40 nm have an increased surface area available for the interaction which is directly proportional to the greater bactericidal effect they have, as compared to particles larger than 40 nm (Lkhagvajav *et al*., 2011). The silver nanoparticles between 1 and 10 nm showed direct interaction with the bacteria cell wall. These small particles have the ability to react with, and penetrate, the cell membrane because of their higher surface to volume ratio. Particles smaller than 5 nm have enhanced electronic effects that can change the local electronic structure of the bacterial surface (Pal *et al*., 2007). Morones *et al.,* 2005 predicted that smaller particles can penetrate the cell membrane more easily than large nanoparticles. Some researchers have implied that different particle shapes such as, octahedral, multiple-twinned icosahedral, decahedral, tubes, spheres and triangle shaped nanoparticles may have diverse effects on the bacteria (Pal *et al*., 2007; Jiang *et al*., 2011).

1.6.3. Application and developments of silver nanoparticles based products

There are over 100 silver nanoparticles based products in the market. Sweet and Singleton (2011) reviewed commercially available products that contain silver nanoparticles such as textiles, medical devices, food preservatives, water purifying systems and surface coatings. There is a portable drinking water purifying system that is designed by incorporating silver nanoparticles into a blotter paper (Dankovich & Gray, 2011; You *et al*., 2011). Nanobiocides such as metal nanoparticles have been successfully incorporated into nanocomposites and their slow release into the water to directly kill microbes yet maintain an acceptable human silver dose of 100 mg/L in water was sustained (Rai *et al*., 2009). Table 1.1 lists some of the silver nanoparticles based products currently on the market.

Table 1.1: Antimicrobial uses of AgNPs.

AgNP-containing products	Reference
Textiles and clothing	Leung & Ko, (2011)
Medical implants	Furkert *et al.,* (2011); Lu *et al.,* (2011)
Surface coating (work surfaces, kitchens)	Galeano *et al.,* (2003); Sreekumari *et al.,* 2005
Food preservation	Del Nobile *et al.,* (2004);Fernandez *et al.,* (2010)
Purification of drinking water	Dankovich & Gray, 2011
Wastewater treatment	Musee *et al.,* (2011)
Household items (e.g., washing machines, deodorants)	Kim *et al.,* (2010)

Silver nanoparticles immobilised in silica spheres were found to be an efficient catalyst in the reduction of dye by sodium borohydride. The increase in the amount of silver nanoparticles reduced the reaction time by two thirds (Jiang *et al*., 2004). In addition, many nanoparticles function as catalysts as their high energy surfaces are more reactive than the surfaces of bulk materials due to the large surface curvature. Smaller nanoparticles exhibit quantum confinement, which occurs when the physical dimensions of the nanoparticles are smaller than the mean free path of the electrons.

1.6.4. Toxicity of silver nanoparticles

As expected for every rising technology there are issues that are in question regarding nanotechnology such as: toxicity, ecological impact and the global economics (Rosarin & Mirunalini, 2011). Hence the implementation of these developments is slow because nanotechnology is under advocacy and regulation. Prolonged contact with or ingestion of silver compounds is known to cause Argyria, which is a phenomenon where silver deposits underneath the skin and results in gray to gray-black staining of the skin and mucous membranes (Rai et. al., 2009; Rosarin & Mirunalini, 2011). The small size, larger surface to area ratio, high mobility and reactivity of AgNPs poses more harm to human beings (Borm & Kreyling, 2004) and the ecosystem (DuránI *et al*., 2010). The Guidelines for drinking-water quality (1996) limits the amount of silver exposure to 0.1 mg/L, a concentration that gives a total dose over 70 years of 10 g, which can be tolerated without risk to health. Hussain *et al*., (2005) evaluated the acute toxicity of 15 or 100 nm AgNPs invitro using a rat liver derived cell line (BRL 3A). A dose-dependent cytotoxicity, impaired mitochondrial function and cell shrinkage were observed after 24 hours. Cytotoxicity increased with a decrease in particle size. Burd *et al*., (2007) also reported a dose dependent cytotoxicity of silver ion or metallic nanocrystalline silver on monolayer cell culture, a tissue explant culture model and a mouse expurgated wound model. Nanoparticles can be inhaled, (Oberdorster *et al*., 2001), orally ingested (Jani *et al*., 1990) and absorbed through skin contact (Kreilgaard *et al*., 2002); post uptake the nanoparticles can spread to different body tissues. Takenaka *et al*., (2001) reported detection of AgNPs in the lung, liver, kidney, spleen, brain, heart, and blood of rats post inhalation of 4-10 nm ultrafine particles. However, with so many silver nanoparticle-based products in the market there have been no toxicity incidences reported (DuránI *et al*., 2010). Small quantities of silver nanoparticles have been administered in human cells and have been shown to inactivate HIV and prevent the propagation of the virus (Rosarin & Mirunalini,

2011). Braydich-Stolle *et al*., (2005) investigated the effect of silver nanoparticles on a mouse spermatogonial stem cell line and discovered that the nanoparticles disrupted the cell morphology, mitochondrial function and also caused membrane leakage therefore interfering with cellular metabolism. The ingestion and constant contact with silver nanoparticles can affect the normal flora and be cidal to the essential bacteria that produce vitamin K in the gut.

1.6.5. Characterization techniques used to analyse silver nanoparticles

This section reviews the characterisation techniques used to determine the structure and properties of silver nanoparticles

1.6.5.1.   UV-visible spectroscopy

UV-vis spectroscopy is a useful tool in studying electronic transition of species that absorb at near infrared through the visible to the UV region of electromagnetic spectrum with transition energy in the approximate range between 10^2 and 10^3 kJ mol^{-1}. These species absorb this light then undergo an electron transition whereby a valence electron gets excited from ground state to the excited state (i.e. from lower energy to higher energy). Optical excitation of electrons across the band gap is strongly allowed, producing an abrupt increase in absorption at the wavelength corresponding to the band gap energy. The energy required to promote an electron from valence band to the conduction band for most metals is in the same energy region, thus UV-vis spectroscopy is a powerful technique to study the interband electronic transition of these metals. Ultraviolet-visible spectroscopy (UV-vis) is used to determine the optical properties of a solution. Light is sent through the sample and the amount of light absorption and scattering patterns are measured. The technique concurrently examines the colour and the current of a material then measures the wavelength at which the maximum absorption (λmax) band occurs. Elemental silver absorbs energy in the form of photons between 350 nm and 450 nm whereas ionic silver does not absorb at this wavelength

(Vigneshwaran *et al*., 2006). The degree of light absorption and scattering is dependent on the size of the AgNPs. Evanoff and Chumanov, (2004) stated that AgNPs with UV-vis spectra that depict a dipole resonant mode maximally absorb light and none or minute amounts are transmitted, scattered or reflected. Literature seconds this conclusion since the extinction spectra and the absorbance of small nanoparticles is similar whereas the extinction spectra of larger nanoparticles have higher amplitude than the absorption spectra of the same nanoparticles (Kumbhar *et al*., 2005). Absorption peaks occurring at lower wavelengths imply a blue-shifted absorption edge resulting from quantum confinement of the excitons present in the sample. The excitons present in the sample cause a more discrete energy spectrum of the individual nanoparticles. If no visible absorption is seen in the visible region, the system can be said to be a non-linear optical (NLO) material. Kumbhar *et al.,* (2005) investigated optical properties of different sized AgNPs and the extinction spectra of those AgNPs are represented in Figure 1.6. The AgNPs with diameters ranging between 1 and 60 nm have one plasmon peak belonging to a dipolar mode, because particles smaller than 60 nm maximally absorbed light with minimum light scattering. Evanoff and Chumanov (2004), stated that the extinction spectrum of particles smaller than 60 nm is mainly contributed by absorbed light. The increase in particle size causes red shift in the dipole mode peak from 400 nm to 600 nm. In addition to the dipole mode, particles larger than 60 nm have a shoulder at about 450 nm called octupole mode and as the particle size increases above 100 nm the extinction spectra shows a quadropole mode around 550 nm [Fig 1.4]. The absorption spectrum of AgNPs broadens as the nanoparticle size distribution increases therefore contributing to a wider full width at half-maximum (FWHM).
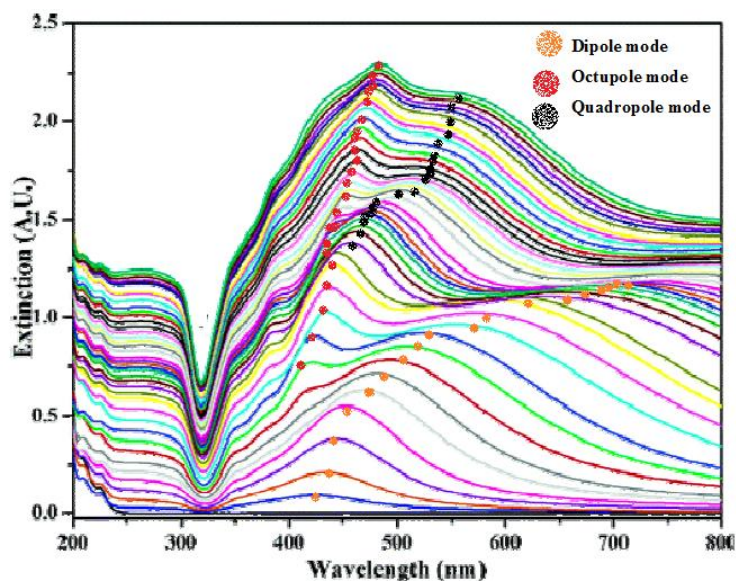
Figure 1.3 : UV-Vis spectra of different sized AgNPs ranging from 10 nm (bottom blue line) to 215 nm (top green line) dispersed in water. (Adapted from Kumbhar *et al.,* 2005)

1.6.5.2. Transmission electron microscopy and Energy Dispersive Spectroscopy

Transmission electron microscopy (TEM) measures the interaction of transmitted electrons as they pass through an ultra-thin specimen. The principle involves projection of an electron beam that is primarily focused by a series of magnetic lenses into the specimen, then the electrons will be absorbed and scattered as they interact with the specimen. Subsequently the transmitted electrons will be focused by the objective lenses then detected by the detector which creates an image visualised by the CCD cameras (Lambert & Mulvey, 1996). Then the transmitted electrons give an image with useful information about the morphology of a material. The particle to particle interaction will be conveyed by the dispersion or agglomeration of the particles that make up the specimen. The technique analyses the crystal structure, particle shape and size of the silver nanoparticles (Chen *et al*., 2010; Rosarin & Mirunalini, 2011, Zhang *et al*., 2003; Chen *et al*., 2010; Rai *et al*., 2009).

1.7. Proposal

1.7.1. Problem Statement

The world is faced with the burden of emerging waterborne pathogens, which are more virulent and resistant to conventional disinfection methods. This necessitates the development of broad-spectrum antimicrobial agents that are effective against emerging pathogens while delaying the emergence of resistance. With the increased environmental and economic concern these new disinfection methods should be cheap and not emit greenhouse gases. These "point of use" disinfection techniques should not require specialised infrastructure or trained personnel, as most of the areas affected by waterborne disease outbreaks are in the rural areas where there is a lack of proper municipal water treatment systems.

Innovative techniques such as a nanocomposite containing filtering systems have been developed. Silver nanoparticles and their nanocomposites have a potential to be broad-spectrum antimicrobial agents as they have cidal effects against a wide range of pathogenic microorganisms and a wide mode of action (deactivate proteins, retards DNA replication, formation of reactive oxygen species and ion imbalance) thus can prolong the emergence of resistance.

The literature has predicts that small AgNPs are more toxic and there has been research in trying to optimise the synthesis of such nanoparticles. However, the ideal nanoparticle remains elusive. This study serves to bridge the gap through changing the parameters asserted by literature to synthesise silver nanoparticles with high cidal effects against a wide range of bacterial species. Although the antimicrobial effect of silver nanoparticles has been studied, a comparison of their superiority to the conventional disinfection methods or to antibiotics has not been conducted. In the present study, the synthesised silver nanoparticles will be tested on a range of bacteria. To date the binding, localisation and accumulation of AgNPs is not clear

so transmission electron microscopy (TEM) will be employed to visualise the accumulation of AgNPs.

1.7.2. Aim

The present study is aimed at investigating the efficiency of silver nanoparticles as an antibacterial agent.

1.7.3. Objectives of study

The present study aims to investigate the effects of silver nanoparticles on several bacterial strains with the specific objectives:

- To optimise the synthesis of small stable silver nanoparticles

- To produce homogeneously shaped and dispersed AgNPs colloids

- To compare bacterial growth retardation in response to AgNPs

- To establish the minimum inhibitory concentration of the AgNPs

- To compare the cidal efficacy of silver nanoparticles over silver compounds

- To investigate the entry and mode of action of silver nanoparticles

- To investigate the binding and accumulation of AgNPs on the bacteria

1.7.4. Primary Research Questions

- What reaction parameters are responsible for a certain shape or size of AgNPs?

- What is the minimum cidal or static concentration of silver nanoparticles?

- Are AgNPs more toxic that Ag^+?

- Do silver nanoparticles enter the microorganism?

- What is the mode of entry and action of silver nanoparticles in a bacterial cell?

1.7.5. Hypotheses

Low temperatures, alkaline pH and abundant reducing and stabilising agents produce small particles. Silver nanoparticles have enhanced bactericidal effect as compared to silver ions. The mode of action of AgNPs is distinct to that of Ag^+.

1.7.6. Model organisms

A model organism is defined as a non-human species sharing a common ancestor, or with similar metabolic pathway, developmental pathways and genetic makeup with the organisms in question. The biological phenomena of model organisms have been extensively studied and they are safe to handle in a biosafety level 1 laboratory. They are used when it is unfeasible or unethical to work with pathogenic strains. To evaluate the hypothesis of the current study the model bacterial strains that were used are *Escherichia coli* 1699, *Staphylococcus epidermidis, Bacillus cereus, Mycobacterium smegmatis* and *Cupriavidus metallidurans* (CH34).

B. cereus is physiologically and biochemically similar to virulant spore-forming bacteria such as *B. thuringiensis* and *B. anthracis*. Therefore *B. cereus* will aid in investigating the efficiency of silver nanoparticles in eradicating spore-forming bacteria. *S. epidermidis* will be used to examine the efficiency of silver nanoparticles in inhibiting the growth of biofilm-forming bacteria.

Mycobacterium smegmatis is structurally and genetically similar to *Mycobacteriaceae spp* Often *Mycobacteriaceae* are associated with resistance since they have longer incubation periods and possess a cell wall that is highly impermeable to antimicrobial agents. Rodgers *et al.,* (1999) stated that that *Mycobacterium* can resist heavy metals therefore *M. smegmatis*, will be used to test this hypothesis and the ability of silver nanoparticles to enter the mycobacterium distinct cell wall.

E. coli is an indicator of faecal contamination, where the presence of 100 cfu/ml of *E. coli* in a water sample poses a hazard of the presence of pathogens such as *Vibrio cholerea, Salmonella typhi* and *Leptospira spp*. The sensitivity of the indicator organism may reflect the efficiency of the antimicrobial agent in eradicating pathogens. The *E. coli* 1699 strain used in this study has been genetically engineered to be resistant to over 50 antibiotics.

Cupriavidus metallidurans (CH34) is not pathogenic to humans but it is known to adapt in areas contaminated with heavy metal stress such as Ag (I), Zn(II), Cd(II), Co(II), Ni(II), Cu(II), CrO, Hg(II) and Pb(II) amongst others (Mergeay *et al*., 2003; Rojas *et al*., 2011). It is a gram-negative, facultative anaerobic chemolithoautotroph. This extremophile is also involved in heavy metal remediation and sensing. The predicted mode of action of AgNPs includes the oxidation of AgNPs therefore, release silver ions (Ag^+) which then interact with the microorganism. In trying to examine this prediction a bacterial strain that is known to resist Ag^+ by reducing them into Ag, *C. metallidurans,* will be exposed to AgNPs. *C. metallidurans* will be used as a model organism to investigate the mode of action of silver nanoparticles and degree of emergence of efflux if the silver nanoparticles accumulate.

Chapter 2

Methodology

This chapter details the research design used in this study such as synthesis and characterization of silver nanoparticles (AgNPs), and it further describes methods that were chosen in the investigation of the antibacterial properties of these nanoparticles. Additionally the chapter portrays the motive for the choice of methods and techniques used in the study. Figure 2.1 describes the experimental approach followed in pursuit of the objectives of this study.

AgNO$_3$

Ascorbic acid
(Reductant)

Parameters varied:
- ❖ *Amount of reductant*
- ❖ *Stabilising agent*
- ❖ *Temperature*
- ❖ *pH*

Sodium borohydride
(Reductant)

Characterization (**UV-vis spectroscopy**)

Optimum synthesis
(Small AgNPs with narrow size distribution were further characterized using **HR-TEM**)

Shape altering (Effect of light)
[HR-TEM analysis]

Pre-concentration
[HR-TEM analysis]

UNIVERSITY *of the*
WESTERN CAPE

Up-scaling the start material

Centrifugation

Freeze-drying

Antimicrobial testing on:
- ❖ *Cupriavidus metallidurans*
- ❖ *Staphylococcus epidermidis*
- ❖ *Mycobacterium smegmatis*
- ❖ *Bacillus cereus*
- ❖ multi-drug resistant *Escherichia coli* 1699

Minimum inhibitory concentration
(Ag$^+$, By-products or AgNPs)

Growth curves of strains sensitive to AgNPs

TEM imaging of the strain most sensitive to AgNPs

Figure 2.1: Schematic representation of the experimental approach.

2.1. Materials

2.1.1. Chemicals and Bacterial strains used in this study

2.1.1.1. Bacterial strains used in the study

The *E. coli* (1699) and *M. smegmatis* were obtained in an agreement with a collaborator, Dr. Victoria Knight-Connoni, Cubist Pharmaceuticals. The *C. metallidurans* (ATCC 43123 / DSMZ 2839) was a DSMZ acquisition. The *S. epidermidis* and *B. cereus* (ATCC10702I) were obtained at IMBM, UWC, South Africa.

2.1.1.2. Chemicals used in the study

Silver nitrate (99.80 %), sodium borohydride (99.90 %), ascorbic acid (99.00 %), sodium chloride (99.80 %) and sodium hydroxide (99.9 %) were purchased from Kimix Chemicals. Nitric acid (65.00 %), tryptone powder, casein peptone (99.90 %) and Peptone powder (99.90 %) were purchased from Merck Chemicals. Yeast extract, citric acid, D-(+)-glucose (99.5 %) Hydrochloric acid (37.00 %), Polyvinylpyrrolidone, ethanol, sodium chloride, osmium tetroxide, glutaraldehyde (25 %), resin, acetone and Tryptic soy broth were purchased from Sigma Aldrich. Casamino acid was purchased from Becton, Dickson and Company.

2.1.2. Sample Storage

Silver nanoparticle solutions were stored in sealed polyethylene containers to avoid any moisture uptake. The bacterial glycerol stocks were stored at -80 °C. Solutions were prepared fresh and were stored at 4 °C before analyses or antibacterial tests.

2.2 Silver nanoparticles synthesis

The theory of silver nanoparticles synthesis involves the reduction of silver ion to zero valent silver atoms, then these silver atoms self assemble into nanostructures (1 to 100 nm). Silver

nitrate (AgNO$_3$) was used as the silver precursor. The silver ions (Ag$^+$) were reduced by chemical reduction using ascorbic acid or sodium borohydride as reducing agents. The silver nanoparticles were synthesised using two methods: section 2.2.1 describes the first method which used ascorbic acid as a reducing agent and section 2.2.2 describes the second method which used sodium borohydride as a reducing agent. Literature suggests that controlling the reaction parameters can influence the quality of the silver nanoparticles. In each method, the reaction parameters such as the amount of reducing agent, the amount of stabilising agent, the temperature and the pH were individually varied to investigate the influence that these parameters have on the size and shape of the silver nanoparticles.

2.2.1. AgNP synthesis through the reduction of silver ions by ascorbic acid

The silver nanoparticles were synthesised according to the recipe described by Qin *et al.,* (2010). The syntheses of silver nanoparticles were carried out by using ascorbic acid as reducing agent. Citric acid or Polyvinylpyrrolidone (PVP) was used as stabilising agents.

2.2.1.1. Investigating the effect of reducing agent

The effect of the reducing agent on the silver nanoparticles size was investigated by varying the concentration of ascorbic acid used to reduce the silver ions. Other reaction parameters such as the temperature, the pH and the amount of stabilising agent (citric acid) were kept constant. The synthesis was controlled at 30 ^{o}C, pH 10.5 and 2.781 x 10^{-3} M citric acid. Table 2.1 summarises the reaction conditions and molar ratio of citric acid/Ag and that of ascorbic acid/Ag.

Table 2.1: Investigating the effect of ascorbic acid.

Sample ID	Ag (µg/mL)	Ascorbic acid: Ag	Citric acid: Ag	Temperature (^{o}C)	pH
AA1	100	1	3	30	10.5
AA2	100	3	3	30	10.5
AA3	100	4	3	30	10.5

The initial concentration of ascorbic acid used to achieve the ascorbic acid/Ag molar ratio of 1, 3 and 4 were 4.635×10^{-4} M, 1.39×10^{-3} M and 1.85×10^{-3} M ascorbic acid respectively. An aqueous solution (10 mL) containing ascorbic acid and 2.781×10^{-3} M citric acid was adjusted to pH 10.5 by adding 0.1 M NaOH solution. Then the solution was left shaking in a 30 °C water-bath for 30 minutes. Subsequently 100 µL of 0.1 M $AgNO_3$ was added drop-wise and the mixture was allowed to shake for 15 minutes after adding silver. The resulting samples, labelled AA1, AA2 and AA3 for the ascorbic acid/Ag molar ratio of 1, 3 and 4 respectively, were analysed by UV-vis spectroscopy.

2.2.1.2. Investigating the effect of stabilising agent

An efficient stabilising agent produces stable and a small silver nanoparticle size with a narrow particle size distribution. In an attempt to select an efficient stabilising agent, the synthesis of silver nanoparticles was carried out in the presence of either citric acid or Polyvinylpyrrolidone (PVP).

2.2.1.2.1. Investigating the effect of citric acid

The effect of the stabilising agent on silver nanoparticles was investigated by varying the concentration of citric acid. Other reaction parameters such as the temperature, the pH and the amount of ascorbic acid used were kept constant. The synthesis was controlled at 30 °C, pH 10.5 and 4.635×10^{-4} M ascorbic acid. Table 2.2 summarises the reaction conditions and molar ratio of citric acid/Ag and that of ascorbic acid/Ag of samples AA4, AA5 and AA6.

Table 2.2: Investigating the effect of citric acid.

Sample ID	Ag (µg/mL)	Ascorbic acid: Ag	Citric acid: Ag	Temperature (°C)	pH
AA4	100	1	0	30	10.5
AA5	100	1	3	30	10.5
AA6	100	1	10	30	10.5

The citric acid/Ag molar ratio varied at 0, 3 and 10 for sample AA4, AA5 and AA6. The initial concentration of citric acid used to achieve the citric acid/Ag molar ratio of 0, 3 and 10

were 0 M, 2.781 x 10^{-3} M and 9.27 x 10^{-3} M citric acid respectively. An aqueous solution (10 mL) containing 4.635 x 10^{-4} M ascorbic acid and citric acid was adjusted to pH 10.5 by adding 0.1 M NaOH solution. Then the solution was left shaking in a 30 °C water-bath for 30 minutes. Subsequently 100 µL of 0.1 M AgNO$_3$ was added drop-wise and the mixture was allowed to shake for 15 minutes after adding silver. The resulting samples were analysed by UV-vis spectroscopy. The resulting samples, labelled AA4, AA5 and AA6 for the citric acid/Ag molar ratio of 0, 3 and 10 respectively, were analysed by UV-vis spectroscopy.

2.2.1.2.2. Investigating the effect of Polyvinylpyrrolidone

The effect of the stabilising agent on the silver nanoparticle size was investigated by varying the concentration of PVP used in the synthesis of silver nanoparticles. Other reaction parameters such as the temperature, the pH and the amount of ascorbic acid used were kept constant. The synthesis was controlled at 30 °C, pH 10.5 and 4.635 x 10^{-4} M ascorbic acid. The PVP/Ag molar ratio was varied at 0, 3 and 10 for sample AA4, AA7 and AA8. Table 2.3 summarises the reaction conditions and molar ratio of citric acid/Ag and that of ascorbic acid/Ag used in the synthesis of samples AA4, AA7 and AA8.

Table 2.3: Investigating the effect of Polyvinylpyrrolidone.

Sample ID	Ag (µg/mL)	Ascorbic acid: Ag	PVP	Temperature (°C)	pH
AA4	100	1	0	30	10.5
AA7	100	1	3	30	10.5
AA8	100	1	10	30	10.5

The initial concentration of PVP used to achieve the PVP/Ag molar ratio of 0, 3 and 10 were 0 M, 2.781 x 10^{-2} M and 9.27 x 10^{-2} M PVP respectively. A 10 mL of 4.635 x 10^{-4} M ascorbic acid aqueous solution was adjusted to pH 10.5 by adding 0.1 M NaOH solution. Then the solution was left shaking in a 30 °C water-bath for 30 minutes. Subsequently 100 µL aqueous solution containing 0.1 M AgNO$_3$ and PVP was added drop-wise to the shaking ascorbic acid solution and the mixture was allowed shake for 15 minutes after adding silver. The resulting

samples, labelled AA4, AA7 and AA8 for the PVP/Ag molar ratio of 1, 3 and 4 respectively, were analysed by UV-vis spectroscopy.

2.2.1.3. Investigating the effect of temperature

This set of experiments investigated the effect of temperature on the size of AgNPs. Silver nanoparticles were synthesised by chemical reduction with ascorbic acid and stabilised by citric acid at pH 10.5 at varying temperature of 25 $^{\circ}$C, 30 $^{\circ}$C or 50 $^{\circ}$C for sample AA9, AA10 and AA11 respectively. Other reaction parameters such as the pH, the amount of ascorbic acid and the amount of citric acid were kept constant. The synthesis was controlled at pH 10.5, 2.781 x 10^{-3} M citric acid and 4.635 x 10^{-4} M ascorbic acid. Table 2.4 summarises the reaction conditions and molar ratio of citric acid/Ag and that of ascorbic acid/Ag used in the synthesis of samples AA9, AA10 and AA11.
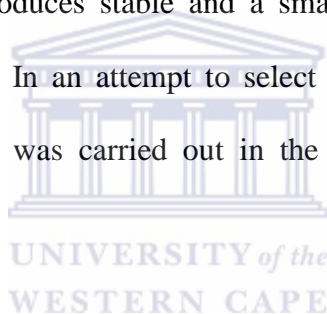
Table 2.4: Investigating the effect of temperature.

Sample ID	Ag (µg/mL)	Ascorbic acid: Ag	Citric acid: Ag	Temperature ($^{\circ}$C)	pH
AA9	100	1	3	25	10.5
AA10	100	1	3	30	10.5
AA11	100	1	3	50	10.5

An aqueous solution (10 mL) containing 4.635 x 10^{-4} M ascorbic acid and 2.781 x 10^{-3} M citric acid was adjusted to pH 10.5 by adding 0.1 M NaOH solution. Then the solution was left shaking for 30 minutes in a 25 $^{\circ}$C, 30 $^{\circ}$C or 50 $^{\circ}$C water-bath respectively. Subsequently 100 µL of 0.1 M AgNO$_3$ was added drop-wise and the mixture was allowed to shake for 15 minutes after adding silver. The resulting samples, labelled AA9, AA10 and AA11 for 25°C, 30 $^{\circ}$C and 50 $^{\circ}$C respectively, were analysed by UV-vis spectroscopy.

2.2.1.4. Investigating the effect of pH

This set of experiments investigated the influence of pH on the size of AgNPs. Silver nanoparticles were synthesised by chemical reduction with ascorbic acid and stabilised by

citric acid at 30 °C while varying the pH. Other reaction parameters such as the temperature, the amount of ascorbic acid and the amount of citric acid were kept constant. The synthesis was controlled at 30 °C, 2.781 x 10^{-3} M citric acid and 4.635 x 10^{-4} M ascorbic acid. The pH was controlled at pH 5.5, 9 or 10.5 for sample AA12, AA13 and AA14 respectively. Table 2.5 summarises the reaction conditions and molar ratio of citric acid/Ag and that of ascorbic acid/Ag used in the synthesis of samples AA12, AA13 and AA14.

Table 2.5: Investigating the effect of pH.

Sample ID	Ag (μg/mL)	Ascorbic acid: Ag	Citric acid: Ag	Temperature (°C)	pH
AA12	100	1	3	30	5.5
AA13	100	1	3	30	9
AA14	100	1	3	30	10.5

An aqueous solution (10 mL) containing 1.39 x 10^{-3} M ascorbic acid and 2.781 x 10^{-3} M citric acid was adjusted to pH 5.5, 9 or 10.5 respectively by adding 0.2 M citric acid or 0.1 M NaOH solution. Then the solution was left shaking in a 30 °C water-bath for 30 minutes. Subsequently 100 μL of 0.1 M $AgNO_3$ was added drop-wise and the mixture was allowed to shake for 15 minutes after adding silver. The resulting samples, labelled AA12, AA13 or AA14 for pH 5.5, 9 and 10.5 respectively, were analysed by UV-vis spectroscopy.

2.2.2. AgNP synthesis through the reduction of silver ions by sodium borohydride

The silver nanoparticles were synthesised according to the recipe described in Solomon *et al* (2007). The syntheses of silver nanoparticles were carried out by using sodium borohydride as reducing agent and citric acid or Polyvinylpyrrolidone (PVP) was used as stabilising agents.

2.2.2.1. Investigating the effects of reducing agent

This set of experiments investigated the effect of varying the amount of sodium borohydride on the size and shape of AgNPs. The temperature, the pH and the amount of PVP were kept constant. The synthesis was controlled at 0 °C, pH 9.78 and 9.27×10^{-3} M PVP. Ag^+ was reduced using sodium borohydride at $NaBH_4$/Ag molar ratio of 3, 10 or 16 for sample BB1, BB2 and BB3 respectively. The initial concentration of sodium borohydride used to achieve the $NaBH_4$/Ag molar ratio of 3, 10 and 16 were 4.635×10^{-4} M, 1.39×10^{-3} M and 1.85×10^{-3} M sodium borohydride respectively. The solutions were prepared and chilled to ice temperature and the reaction was carried out on ice. Table 2.6 summarises the reaction conditions and molar ratio of PVP/Ag and that of $NaBH_4$/Ag used in the synthesis of samples BB1, BB2 and BB3.

Table 2.6: Investigating the effect of sodium borohydride.

Sample	Silver (µg/mL)	NaBH4:Ag	PVP:Ag	Temperature (°C)	pH
BB1	100	3	10	0	9.78
BB2	100	10	10	0	9.78
BB3	100	16	10	0	9.78

An aqueous solution (30 mL) containing 3.7×10^{-3} M, 1.23×10^{-2} M or 1.98×10^{-2} M $NaBH_4$ for sample BB1, BB2 or BB3 respectively, was adjusted to pH 9.78 by adding 0.1 M NaOH. The solution was poured into an Erlenmeyer flask, and then the flask was placed in an ice bath on a stir plate. The solution was stirred and cooled for 20 minutes. Then 10 mL of aqueous 3.8×10^{-3} M $AgNO_3$ was added into the stirring $NaBH_4$ solution at approximately 1 drop per second. Stirring was discontinued immediately after adding silver nitrate. Then 0.0148 g PVP was added into AgNPs solution and then the solution was stirred to dissolve the PVP. The resulting samples were analysed by UV-vis spectroscopy.

2.2.2.2. Investigating the effect of the stabilising agent

2.2.2.2.1. Investigating the effect of citric acid

This set of experiments investigated the effect of varying the amount of citric acid on the size and shape of AgNPs. The temperature, the pH and the amount of sodium borohydride were kept constant. The synthesis was controlled at 0 ^{o}C, pH 9.78 and 1.98×10^{-2} M NaBH$_4$. AgNPs was stabilised using citric acid at citric acid/Ag molar ratio of 0, 3 and 10. The initial concentration of citric acid used to achieve the citric acid/Ag molar ratio of 0, 3 or 10 were 0 M, $2.781x10^{-3}$ M and $9.27x10^{-3}$ M citric acid respectively. The solutions were prepared and chilled to ice temperature and the reaction was carried out on ice. Table 2.7 summarises the reaction conditions and molar ratio of citric acid/Ag and that of NaBH$_4$/Ag used in the synthesis of samples BB4, BB5 and BB6.

Table 2.7: Investigating the effect of citric acid.

Sample	Silver (µg/mL)	NaBH4: Ag	Citric acid: Ag	Temperature (^{o}C)	pH
BB4	100	16	0	0	9.78
BB5	100	16	3	0	9.78
BB6	100	16	10	0	9.78

A 30 mL 1.98×10^{-2} M NaBH$_4$ aqueous solution was adjusted to pH 9.78 by adding 0.1 M NaOH. The solution was poured into an Erlenmeyer flask, and then the flask was placed in an ice bath on a stir plate. The solution was stirred and cooled for 20 minutes. Then 10 mL of aqueous 3.8×10^{-3} M AgNO$_3$ solution was added into the stirring NaBH$_4$ solution at approximately 1 drop per second. Stirring was discontinued immediately after adding silver nitrate. Then 0 g, 23.2 mg or 7.79 mg citric acid was added into AgNPs solution sample BB4, BB5 and BB6 respectively. Subsequently the solution was stirred to dissolve the citric acid. The resulting samples were analysed by UV-vis spectroscopy.

2.2.2.2.2. Investigating the effect of Polyvinylpyrrolidone

This set of experiments investigated the effect of varying the amount of Polyvinylpyrrolidone (PVP) on the size and shape of AgNPs. The temperature, the pH and the amount of sodium borohydride were kept constant. The synthesis was controlled at 0 $^{\circ}$C, pH 9.78 and 1.98×10^{-2}M NaBH$_4$. AgNPs were stabilised using PVP at PVP/Ag molar ratio of 0, 3 and 10. The initial concentration of PVP used to achieve the PVP/Ag molar ratio of 0, 3 or 10 were 0 M, 2.781×10^{-3} M and 9.27×10^{-3} M PVP respectively.   The solutions were prepared and chilled to ice temperature and the reaction was carried out on ice. Table 2.8 summarises the reaction conditions and molar ratio of PVP/Ag and that of NaBH$_4$/Ag used in the synthesis of samples BB4, BB7 and BB8.

Table 2. 8: Investigating the effect of PVP.

Sample	Silver (µg/mL)	NaBH4:Ag	PVP:Ag	Temperature ($^{\circ}$C)	pH
BB4	100	16	0	0	9.78
BB7	100	16	3	0	9.78
BB8	100	16	10	0	9.78

The pH of 1.98×10^{-2} M NaBH$_4$ aqueous solution (30 mL) was adjusted to pH 9.78 by adding 0.1 M NaOH. The solution was poured into an Erlenmeyer flask, and then the flask was placed in an ice bath on a stir plate. The solution was stirred and cooled for 20 minutes. Then 10 mL of aqueous 3.8×10^{-3} M AgNO$_3$ solution was added into the stirring NaBH$_4$ solution at approximately 1 drop per second. Stirring was discontinued immediately after adding silver nitrate. Then 0 g, 4.5 mg or 14.8 mg PVP was added into AgNPs solution in sample BB4, BB7 and BB8 respectively. Subsequently the solution was stirred to dissolve the PVP. The resulting samples were analysed by UV-vis spectroscopy.

2.2.2.3. Investigating the effects of temperature

This set of experiments investigated the effect of temperature on the size and shape of AgNPs. The pH and the amount of sodium borohydride and the amount of PVP were kept

constant. The synthesis was controlled at pH 9.78, 1.98×10^{-2} M NaBH$_4$ and 9.27×10^{-3} M PVP. Table 2.9 summarises the reaction conditions and molar ratio of PVP/Ag and that of NaBH$_4$/Ag used in the synthesis of samples BB9 and BB10.

Table 2.9: Investigating the effect of temperature.

Sample	Silver (µg/mL)	NaBH4: Ag	PVP: Ag	Temperature (^{o}C)	pH
BB9	100	16	10	0	9.78
BB10	100	16	10	25	9.78
BB11	100	16	10	50	9.78

In the preparation of sample BB10, the solutions were prepared and allowed to cool in ice for 30 minutes prior to the synthesis and the synthesis was also carried out on ice [Fig 2.2 (A)]. In the preparation of sample BB11, the solutions were prepared at room temperature and the synthesis was carried out at 25°C, [Fig 2.2 (B)].
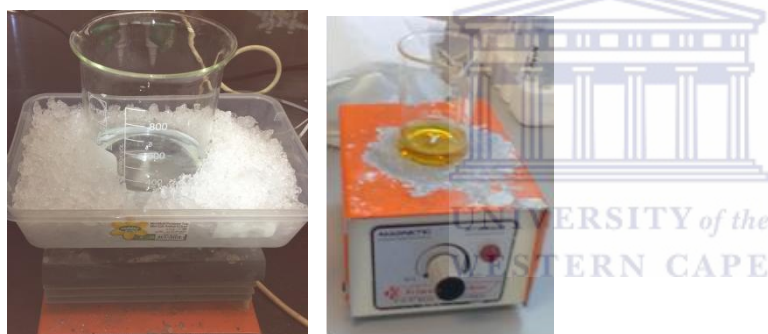
Figure 2.2: Setup for the experiment for AgNPs synthesised at different temperature.
A) The synthesis carried out at 0 ^{o}C. B) The synthesis carried out at 25 ^{o}C.

Preparation of BB9: The pH of 1.98×10^{-2} M NaBH$_4$ aqueous solution (30 mL) was adjusted to pH 9.78 by adding 0.1 M NaOH. The solution was poured into an Erlenmeyer flask, and then the flask was placed in an ice bath on a stir plate. The solution was stirred and cooled for 20 minutes. Then 10 mL of aqueous 3.8×10^{-3} M AgNO$_3$ solution was added into the stirring NaBH$_4$ solution at approximately 1 drop per second. Stirring was discontinued immediately after adding silver nitrate. The resulting samples were analysed by UV-vis spectroscopy.

Preparation of BB10: The pH of 1.98×10^{-2} M NaBH$_4$ aqueous solution (30 mL) was adjusted to pH 9.78 by adding 0.1 M NaOH. The solution was poured into an Erlenmeyer flask, and then the flask was placed on a stir plate at room temperature. The solution was stirred for 20

minutes. Then 10 mL of aqueous 3.8×10^{-3} M AgNO$_3$ solution was added into the stirring NaBH$_4$ solution at approximately 1 drop per second. Stirring was discontinued immediately after adding silver nitrate. Then 14.8 mg PVP was added into AgNPs solution and then the solution was stirred to dissolve the PVP. The resulting samples were analysed by UV-vis spectroscopy.

2.2.2.4. Investigating the effects of pH

This set of experiments investigated the effect of varying pH on the size and shape of AgNPs. The temperature, the amount of PVP and the amount of sodium borohydride were kept constant. The synthesis was controlled at 0 ^{o}C, 9.3×10^{-3} M PVP and 1.98×10^{-2} M NaBH$_4$. The pH at which the reaction occurred was controlled at pH 5.5, 9.78 or 10.5 for BB11, BB12 and BB13 respectively. The solutions were prepared and chilled to ice temperature and the reaction was carried out on ice. Table 2.10 summarises the reaction conditions and molar ratio of PVP/Ag and that of NaBH$_4$/Ag used in the synthesis of samples BB11, BB12 and BB13.

Table 2.10: Investigating the effect of pH.

Sample	Silver (µg/mL)	NaBH4: Ag	PVP: Ag	Temperature (^{o}C)	pH
BB12	100	16	10	0	5.5
BB13	100	16	10	0	9.78
BB14	100	16	10	0	10.5

The pH of a 30 mL 1.98×10^{-2} M NaBH$_4$ aqueous solution was adjusted to pH 5.5, 9.78 or 10.5 by adding 0.2 M citric acid and 0.1 M NaOH. The solution was poured into an Erlenmeyer flask, and then the flask was placed in an ice bath on a stir plate. The solution was stirred and cooled for 20 minutes. Then 10 mL of aqueous 3.8×10^{-3} M AgNO$_3$ solution was added into the stirring NaBH$_4$ solution at approximately 1 drop per second. Stirring was discontinued immediately after adding silver nitrate. Then 0.0148 g PVP was added into AgNPs solution and then the solution was stirred to dissolve the PVP.

The UV-vis spectroscopy was used to screen all the AgNPs synthesised by varying the synthesis conditions. The optimum synthesis parameters that produced a spectrum with a narrow full width at half maximum and highest absorbance intensity was chosen in all down-stream investigations.

2.2.3. Investigating the effect of light

From the UV-Vis spectra of the AgNPs, the sample with the smallest particle and narrowest size distribution was exposed to a beam of light. The AgNPs solution (500 mL) was poured into a beaker, and then the beaker was placed on a stir plate. The nanoparticle solution was stirred and exposed to light using an OSRAM Vitalux lamp (300 W and 230 V) for 1, 3, 6 or 12 hours and the samples were labelled S1, S2, S3 and S4 respectively. In another set of experiments the nanoparticle solution was exposed to light using an OSRAM Vitalux lamp (300 W and 230 V) without stirring for 1, 3, 6 or 12 hours and the samples were labelled S5, S6, S7 and S8 respectively
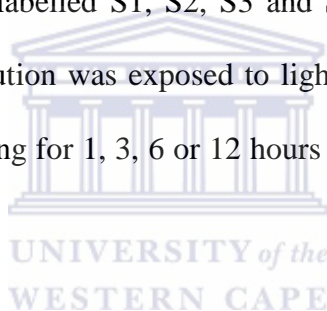
2.3. Silver nanoparticles concentration and purification

This section investigated ways to concentrate and purify the AgNPs to suite their biological application.

2.3.1. Increasing the starting material to scale-up the concentration of silver from 0.1 mg/ml to 1 mg/ml

The preparation of sample BB14 was carried out at 0 $^{\circ}$C, pH 9.78, with a Ag/sodium borohydride/PVP molar ratios of 1:16:10. The pH of 0.198 M 1.98×10^{-2} M $NaBH_4$ aqueous solution (30 mL) was adjusted to pH 9.78 by adding 0.1 M NaOH. The solution was poured into an Erlenmeyer flask, and then the flask was placed in an ice bath on a stir plate. The solution was stirred and cooled for 20 minutes. Then 10 mL of aqueous 3.8×10^{-2} M $AgNO_3$

solution was added into the stirring NaBH$_4$ solution at approximately 1 drop per second. Stirring was discontinued immediately after adding silver nitrate. Then 0.148 g PVP was added into the AgNPs solution and the solution was stirred to dissolve the PVP. The resulting samples were analysed by UV-vis spectroscopy.

2.3.2. Concentrating the nanoparticles using the freeze-dry and centrifuge techniques

Silver nanoparticles (40 mL) were freshly synthesised into a 50 mL greiner tube. The nanoparticles were synthesised at pH 9.78, at a temperature of 0 ^{o}C and Ag/NaBH$_4$/PVP molar ratio of 1:16:10. Thirty- millilitres of 1.98×10^{-2} M NaBH$_4$ aqueous solution was adjusted to pH 9.78 by adding 0.1 M NaOH. The solution was poured into an Erlenmeyer flask, and then the flask was placed in an ice bath on a stir plate. The solution was stirred and cooled for 20 minutes. Then 10 mL of aqueous 3.8×10^{-3} M AgNO$_3$ solution was added into the stirring NaBH$_4$ solution at approximately 1 drop per second. Stirring was discontinued immediately after adding silver nitrate. Then 14.8 mg PVP was dissolved in the AgNPs solution.

The AgNPs solution was emptied into a 50 mL greiner tube, then the tube was sealed with a parafilm (with poked holes) and frozen at -80 ^{o}C for 6 hours. Subsequently the tube was placed in a freeze drier and the liquid was removed at -50°C for 120 hour. Another batch of silver nanoparticles (40 mL) were freshly synthesised as described above and emptied into a 50 mL greiner tube. The nanoparticle solution was centrifuged at 1300 rpm for 30 minutes.

2.4.   Characterization of silver nanoparticles

The synthesized silver nanoparticles were characterized using microscopic and spectroscopic techniques. High resolution transmission electron microscopy (HR-TEM) was the microscopic technique used while the spectroscopic techniques were ultraviolet-visible

spectroscopy (UV-vis) and Energy-dispersive X-ray spectroscopy (EDS). In the section that follows, a description of the principles, practical aspects as well as instrumentation of all the techniques used in this study is given.

2.4.1. Ultraviolet visible spectroscopy

In the production of silver nanoparticles: silver ions were reduced to zero valent silver atoms, which then self-assembled into silver nanoparticles. Therefore UV-visible spectroscopy could qualitatively and quantitatively analyse the silver nanoparticles. This technique predicts the particle size, distribution and quantifies the concentration of silver using the Beer-Lamberts Law. Freshly prepared samples were used for UV-vis analysis. UV-Vis spectroscopy measurements were recorded over a range of 200-600 nm using 3 cm^3 quartz cuvettes with Nicolette Evolution 100 Spectrometer (Thermo Electron Corporation, UK).

2.4.1.1.   Silver nanoparticles size prediction using UV-vis spectroscopy interpretation models
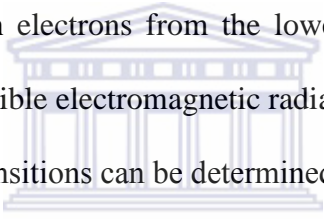
The absorption of light at a particular wavelength is determined by the ratio of transmitted light and incident light (I/Io). Therefore absorbance can be expressed as:

$$A = -\log\left(\frac{I}{I_0}\right)$$

This expression implies that each molecule in a solution absorbs a certain amount of light, therefore absorbance is directly proportional to the abundance of particles in a solution. Beer-Lambert Law states that absorbance of a solution is directly proportional to the concentration of the absorbing species in the solution and the path length.

$$A = -\log_{10}\left(I_0 \big/ I\right) = \varepsilon.c.L$$

The parameter A = describes the absorbance, I_0 = is the intensity of incident light, I = is the intensity of the transmitted light, ε = is the molar absorptivity or extinction coefficient at wavelength (λ_{max}) =1.85 X 10^{10} M^{-1} cm^{-1} and L = is the path length. Typically the light path is a constant equal to the quartz cell length of 1 cm, while the concentration (c) may vary. The law is true for stable homogeneous samples where the physical and chemical state of the sample does not change. Therefore Beer-Lambert Law is used for estimation of concentration the silver nanoparticles. UV-vis absorption spectroscopy is also an effective technique used to study particle growth of nanocrystals giving useful information on the size and particle size distribution. Nakaoka and Nosaka, (1997) illustrated the relationship between the radius of a particle and its absorption band. The conduction band energy represents the amount of energy required to excite the conduction electrons from the lowest energy state to higher energy states as influenced by the UV-visible electromagnetic radiation. A good estimation of energy resulting from these electronic transitions can be determined by Plank's law:

$$\Delta E = h\nu = h\left(\frac{c}{\lambda_{max}}\right)$$

Where E = is the energy of light (eV), h = 6.626 x 10^{-34} J s^{-1} is Planks constant, ν = frequency of light, c = 2.998 x 10^8 m s^{-1} is the speed of light and λ_{max} = maximum wavelength (nm). Then the particle size can be derived using the effective mass approximation model (Beri *et al.*, 2010):

$$Eg = \frac{h^2}{8a^2}\left(\frac{1}{m_e} + \frac{1}{m_h}\right)$$

Where Eg = is the energy band gap (eV), a = is the particle size, h = 6.626 x 10^{-34} is the Plank's constant, m_e = $0.17m_o$ is the electron mass, m_h = $1.44m_o$ is the hole mass (m_o = 9.1095 x 10^{-31} kg, is the mass of a stationary electron).

2.4.1.2. Prediction of silver nanoparticles size distribution using UV-vis spectroscopy

The peak width will be used to determine the particle size distribution and compare the different synthesis methods used in this study. The full width at half maximum (FWHM) is discribed in Figure 2.3.
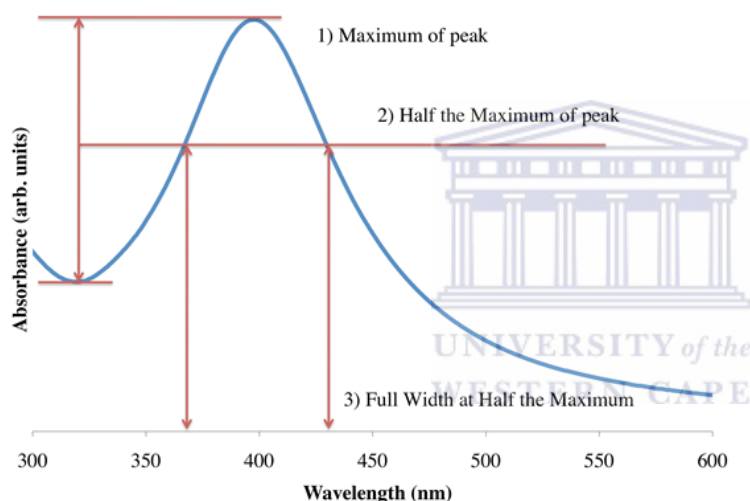
Figure 2.3: Deriving full width at half maximum (FWHM) from a UV-vis spectra.

The FWHM was measured using the following steps: primarily, a line was drawn connecting the maximum of the peak to the baseline (amplitude), then a 90° perpendicular line was drawn in the centre of the amplitude. Then the two points of intersection between the perpendicular line and the peak were noted. The wavelength difference between the two points of intersections was recorded as the FWHM.

2.4.2. Transmission electron microscopy

High resolution transmission electron microscopy (HRTEM) analyses the morphology and crystallography of the atoms that makeup that particular particle. HRTEM is an imaging tool

that directly images nanoparticles therefore providing more information on the quality, size, shape, arrangement of the particles and the inter-particle interaction on the scale of atomic diameter. The aim of carrying out HRTEM analysis was to confirm the size and morphology of the nanocrystals, check if they are agglomerated or dispersed as well as their chemical composition. The TEM sample preparation was performed by placing a drop of the silver nanoparticle solution onto S147-4 lacey carbon film 400 mesh copper grids and drying the mounted sample under an electric bulb for 15 min then allowing the sample to dry maximally for 18 hours. Then the HR-TEM images were acquired using a Tecnai G2F2O X-Twin MAT 200 kV Field Emission Transmission Electron Microscope from FEI (Eindhoven, Netherlands). The TEM images were analysed using ImageJ software. The actual size distribution of the silver nanoparticles was derived from a histogram which was obtained by measuring the diameter of all the particles; about 200 particles were taken into account to establish the histogram.
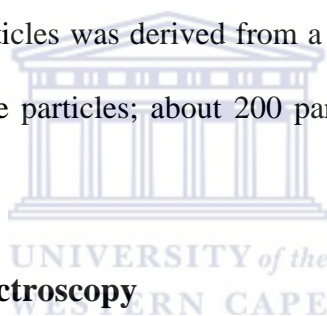
2.4.3. Energy Dispersive Spectroscopy

The HR-TEM is coupled with an integral motorized Energy Dispersive Spectroscopy (EDS) detector, which allows for insertion and removal into the TEM column for X-ray collection. The localised EDS determined the elemental composition of a sample. EDS was used to measure the purity and quality of the silver nanoparticles. EDS spectra were collected at $\alpha=15°$ and $\beta=0°$ for every analysis. Bright field images from the regions of interest were obtained with the sample at zero tilt. The desired counts per second were between 1000 - 4000 and the detector dead time was maintained between 30 % - 40 %.

2.5. Investigating the antibacterial properties of silver nanoparticles

The nanoparticles with uniform size distribution and morphology were chosen for further analysis. The antibacterial activity of the silver nanoparticles was investigated on *Escherichia coli* 1699, *Staphylococcus epidermidis, Bacillus cereus, Mycobacterium smegmatis, Cupriavidus metallidurans*. Chloramphenicol was used as a positive control in order to demonstrate growth inhibition. The sample preparation, medium preparation, minimum inhibitory concentration procedure, growth curve procedures and TEM analysis procedure are detailed below.

2.5.1. Media Preparation

Tryptic soy broth (TSB) medium was prepared by dissolving 30 g of tryptic soy broth in 800 mL of distilled water and made up to the final volume of 1 litre. Casamino acid-Peptone-Glucose (CPG) medium was prepared by dissolving 1 g of casamino acid, 10 g of peptone powder and 5 g of glucose in 800 mL of distilled water and made up to the final volume of 1 litre. The Luria broth (LB) medium was prepared by dissolving 10 g tryptone powder, 5 g yeast extract and 10 g NaCl in 800 mL of distilled water and made up to the final volume of 1 litre. The solutions were autoclaved for 20 minute at 121 °C and allowed to cool to room temperature.

2.5.2. Growth of Bacteria

2.5.2.1.   Overnight cultures

Overnight cultures were prepared by aliquoting 5 mL of media into sterile McCartney glass bottles and inoculated from a -80 °C glycerol stock. The bacteria were inoculated in the respective media *E. coli* in LB*, C. metallidurans* in CPG, and *M. smegmatis, S. epidermidis*

and *B. cereus* in TSB [Table 2.11]. The cultures were incubated at 37 ºC with shaking at 250 rpm, overnight.

Table 2.11: The bacteria used in this study and their corresponding growth media.

Name of the media	Bacterial strains
Luria broth (LB)	*E. coli*
Casamino-acid peptone glucose	*C. metallidurans*
Tryptic soy broth	*B. cereus*
	M. smegmatis
	S. epidermidis

2.5.2.2. Minimum inhibitory concentration of silver nanoparticles

Antibacterial activity of the AgNPs at different silver concentrations was determined by a microtitre well plate method (Jaiswal *et al*., 2010).

The nanoparticles could not be purified from the by-products of the synthesis such as boron, sodium, nitrites and the alkaline pH. In order to be precise about the silver nanoparticles' cidal effects, control experiments were performed. The equation below predicts the by-products in the synthesis of AgNPs using sodium borohydride.

$$AgNO_3 + NaBH_4 \longrightarrow Ag + \tfrac{1}{2}H_2 + \tfrac{1}{2}B_2H_6 + NaNO_3$$

Experimental controls in respect to the expected amount of the by-product in a silver nanoparticles colloidal suspension were performed. The by-product stock solution contained 19.77 mM $NaBH_4$, 9.27 mM PVP and 0.927 mM $NaNO_3$ and was freshly prepared and stored at 4 °C prior to use. An additional control, silver nitrate, was included in order to test the efficacy/toxicity of the silver nanoparticles in relation to silver ions. AgNPs (100 mg/L) stock solution was also freshly prepared and stored at 4 °C prior to use. Bacteria were cultured in microtitre well plates with varying concentrations of the stock solutions (by-products, Ag^+ or AgNPs) [Table 2.12].

In the preparation of 0, 10, 20, 30, 40, 50, 60 and 70 mg/L of treatment titration (Ag^+, AgNPs or by-products) respective volumes of sterile distilled water (175, 155, 135, 115, 95, 75, 55 and 34 µL) were added into a 96-well plate. Subsequently 0, 20, 40, 60, 80, 100, 120 and 140

µL of the treatment (AgNPs, Ag+ or by-products) were added (0, 10, 20, 30, 40, 50, 60 and 70 mg/L treatment) in the respective wells. Separately, 5 µL of the overnight culture was inoculated into 20 µL of ten times concentrated bacterial growth media. Then 25 µl of the inoculums (10X growth media inoculated with bacteria from the overnight culture) was added on the respective wells [Table 2.12]. The experiment was done in triplicates.

Table 2.12: A representation of amount of materials added in each well in a 96 well plate in the minimum inhibitory concentration experiment

Stock solution (v/v)	0	0.05	0.1	0.15	2	2.5	3	3.5
Treatment agent (µL) (AgNPs; $AgNO_3$ and by-products)	0	20	40	60	80	100	120	140
dH_2O (µL)	175	155	135	115	95	75	55	35
10X bacterial growth media (µL)	20	20	20	20	20	20	20	20
Overnight culture (µL)	5	5	5	5	5	5	5	5

The cultures were incubated at 37 °C while shaking at 250 rpm and then optical density (OD) readings were taken before the incubation and after 24 hours of incubation. To determine the minimum inhibitory concentration (MIC) an OD (t = 0 and t = 24 hours) vs time bar graph was plotted. The MIC reported is the minimum concentration of AgNPs, Ag^+ or by-product which resulted in complete lack of growth.

2.5.2.3.   Growth curves

Fresh medium (100 ml media in 250 ml Erlenmeyer flask in triplicate) was inoculated with 50 µl of the overnight culture, and the flasks were incubated at 37 °C while shaking at 250 rpm for 24 hours. The population growth (optical density) was then monitored every 2 hours by spectrophotometric reading at 600 nm.

2.6. Structural characterisation of bacteria using transmission electron microscope (TEM)

TEM was used to visualise the surface damage caused by silver nanoparticles on the bacteria and possible nanoparticle attachment and accumulation as has been demonstrated by Morones *et al., (*2005).

2.6.1. Cell treatment and harvesting

An overnight culture was prepared as in section 2.5.2.1. Fifty microlitres of overnight culture was inoculated into 100 ml of fresh media in a 250 ml Erlenmeyer flask. At mid-logarithmic growth (OD = 0.45) the bacterial culture was treated with 20 mg/L silver nanoparticles and the culture incubated at 37 °C for an hour. The bacteria were harvested by aliquoting the culture in 2 mL eppendorf tubes and pelleting the cells at 1300 rpm for 10 minutes. Prior to the fixation step, the cells were washed by resuspending the pellet in water and then centrifuging for another 10 minutes at 1300 rpm.
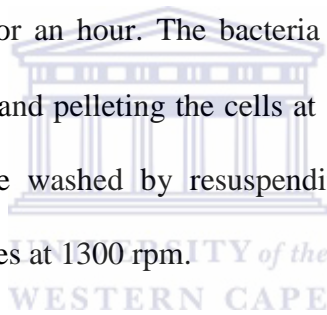
2.6.2. Cell fixation

The cells were fixed by adding 2.5% glutaraldehyde in phosphate buffered saline (PBS) buffer and the cells were incubated at 4 °C overnight. Cells were collected by centrifugation (10,000 rpm, 5 min) and washed twice with 0.1 M PBS buffer (by centrifugation at 10000 rpm for 15 sec). For final fixing of cells, 1% osmium tetroxide in PBS was added and samples were held at 25 °C for 1 hour. Subsequently the cells were washed twice with 0.1 M PBS (centrifuge at 10000 rpm for 10 min in between the washing steps) followed by two washings with ddH$_2$O (centrifuge at 10000 rpm for 10 min). Thereafter the cells were dehydrated with ethanol.

2.6.3. Dehydration

The pellet was washed with 30 % ethanol then centrifuged at 10000 rpm for 10 min and the liquid was discarded. Sequentially the same was done for the 50 %, 60 %, 70 %, 80 %, 90 %, 95 %, 100 % ethanol dehydration steps preceding the 100 % acetone wash. The dehydrated cells were flooded with a mixture of resin/ acetone ratio of 1:1 and incubated at 25 °C overnight.

2.6.4. Resin treatment

The cells were centrifuged at 10000 rpm for 5 min and the liquid was discarded. The pellet was flooded with a mixture of resin/acetone ratio of 3:1 and incubated at 25 °C in a rotator for 5 hours. The liquid was discarded prior to the addition of 100 % resin and the cells were incubated at 25 °C in a rotator overnight. The cells were transferred into a mould and put in an oven (60 °C) overnight. The polymerised cells settling in the apex of the mould were cut into sections using a diamond knife.
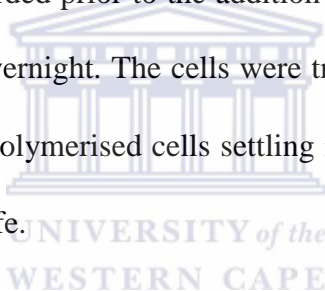
2.6.5. Transmission electron microscopy and energy dispersive spectroscopy analysis

The thin layers of sample (cut as described above) were fixed to a TEM copper grid and TEM sample analysis was performed. Electron micrographs of untreated cells and AgNP-treated bacteria were taken using a Zeiss EM 900 transmission electron microscope (Zeiss, Germany). EDS Spectra were collected at $\alpha=15°$ and $\beta=0°$. Bright field images from the regions of interest were obtained with the sample at zero tilt. The desired counts per second were between 1000 - 4000 and the detector dead time was maintained between 30 % - 40 %.

Chapter 3

Characterisation of silver nanoparticles

3.1. Introduction

The synthesis of small and uniformly sized nanoparticles still remains a challenge, hence this study aimed to synthesise small and uniform nanoparticles. These nanostructures exhibit unique properties due to their large surface to volume ratios compared to bulk materials or individual molecules in suspension. Silver Nanoparticles were synthesized by a wet chemical technique through the reduction of silver ions by ascorbic acid or sodium borohydride as described in section 2.2 previously. Then the reaction conditions, including temperature, pH and the amount of reducing agent and that of stabilising agent, were varied to control the nanoparticles size and size distribution. This chapter is divided into five parts: Firstly, the Ultraviolet-visible spectra analysis of AgNPs (synthesised by ascorbic acid or sodium borohydride while varying the reaction conditions mentioned previously) is presented. Secondly, a comparative analysis of the two reducing agents (ascorbic acid and sodium borohydride) is given. Thirdly, the size of AgNPs synthesised by sodium borohydride is confirmed using transmission electron microscopy. Fourthly, the EDS analysis of AgNPs resulting from the synthesis that produced small and uniform AgNPs is presented. Lastly, the stability, concentrating, purification and isolation studies will be detailed.

3.2. Characterisation of silver nanoparticles using Ultraviolet-visible spectroscopy

When an object is subjected to a beam of light it absorbs some photons while others get transmitted, scattered or reflected; therefore measuring the interaction of light with the object

can predict the presence and size of that object. The absorption patterns of AgNPs, with peaks between 350 - 450 nm confirmed successful synthesis of AgNPs (Vigneshwaran *et al.*, 2006). Full width at a half maximum (FWHM) described in section 2.4.1, predicts the variation in particle size distribution. The maximum absorbance (λ_{max}) indicates the wavelength at which the nanoparticles absorb and a shift towards longer wavelengths represents an increase in average particle size.

3.2.1. Characterisation of AgNPs synthesised by ascorbic acid using ultraviolet-visible spectroscopy

The resulting AgNPs synthesised using ascorbic acid and sodium borohydride as described in section 2.2.1 and 2.2.2 respectively were characterised using UV-vis spectroscopy. The average particle size and their distribution were determined as detailed in section 2.4.1.1 and 2.4.1.2 respectively.

3.2.1.1.   The effect of ascorbic acid on the size of AgNPs

The effect of the reducing agent on the silver nanoparticle's size was investigated by varying the concentration of ascorbic acid (4.635 x 10^{-4} M, 1.39 x 10^{-3} M and 1.85 x 10^{-3} M ascorbic acid for AA1, AA2 and AA3 respectively). Other reaction parameters were controlled at 30 ⁰C, pH 10.5 and 2.781 x 10^{-3} M citric acid as described in section 2.2.1.1. Figure 3.1 shows the UV-vis spectra of AA1, AA2 and AA3. Table 3.1 presents the size and particle size distribution of AgNPs in samples AA1, AA2 and AA3.

Figure 3.1: The UV-vis spectra of samples AA1, AA2 and AA3 showing the effect of varying the concentration of the reductant, ascorbic acid.

Table 3.1: Analysis of UV-vis spectra of samples AA1, AA2 and AA3.

Sample ID	Varied synthesis condition (Molar ratio)		λ_{max}	Absorbance intensity (u.a)	FWHM	Particle size (nm)
AA1		1:1	430 nm	1.5	110	22.6
AA2	Ag: Ascorbic acid	1:3	430 nm	1.1	170	22.6
AA3		1:4	435 nm	1.4	115	24.5

The particle size distributions, represented by the full width at a half maximum (FWHM), was independent of the amount of ascorbic acid since Sample AA1, AA2 and AA3 had 110 nm, 170 nm and 115 nm FWHM respectively. However, the particle size increased as the amount of ascorbic acid increased, sample AA1, AA2 and AA3 produced 22.6, 22.6 and 24.5 nm AgNPs respectively. Low concentrations of ascorbic acid (sample AA1) produced smaller AgNPs, with a narrow particle size distribution.

3.2.1.2.   The effect of stabilising agent on the size of AgNPs

3.2.1.2.1.   The effect of citric acid on the size of AgNPs

The effect of the stabilising agent on the silver nanoparticles size was investigated by varying the concentration of citric acid (0 M, 2.781 x 10^{-3} M and 9.27 x 10^{-3} M citric acid for AA4,

AA5 and AA6 respectively). Other reaction parameters were controlled at 30 °C, pH 10.5 and 4.634 x 10^{-4} M ascorbic acid as described in section 2.2.1.2.1. Figure 3.2 shows the UV-vis spectra of AA4, AA5 and AA6. Table 3.2 presents the size and particle size distribution of AgNPs in samples AA4, AA5 and AA6.

Figure 3.2: The UV-vis spectra of samples AA4, AA5 and AA6 showing the effect of varying the amount of stabilising agent, citric acid.

Table 3.2: Analysis of UV-vis spectra of samples AA4, AA5 and AA6.

Sample ID	Varied synthesis condition (Molar ratio)		λ_{max}	Absorbance intensity (u.a)	FWHM	Particle size (nm)
AA4		0	430 nm	1.5	105	22.6
AA5	Ag: Citric acid	1:3	435 nm	2.5	115	22.5
AA6		1:10	440 nm	1.1	125	26.4

The quantity of AgNPs (absorbance intensity) was affected by high or low amounts of citric acid therefore sample AA5 yielded more AgNPs with absorbance intensity of 2.5 u.a. Minute amounts of citric acid (sample AA5) preserved the AgNPs, producing a particle size of 22.5 nm AgNPs. However, high concentrations of citric acid (sample AA6) collapsed the stability of the AgNPs resulting in increased particle size from 22.6 nm (uncoated AgNPs) to 26.4 nm. Citric acid creates a negatively charged thick electric double layer around the particle in low

ionic strength water, therefore causing inter-particle repulsion. However, high concentration can vastly affect optimum pH that aids in the reduction efficiency of ascorbic acid or the stability of AgNPs.

3.2.1.2.2. The effect of PVP on the size of AgNPs

The effect of the stabilising agent on the silver nanoparticles size was investigated by varying the concentration of PVP (0 M, 2.781 x 10^{-3} M and 9.27 x 10^{-3} M PVP for AA4, AA7 and AA8 respectively). Other reaction parameters were controlled at 30 ^{o}C, pH 10.5 and 4.634 x 10^{-4} M ascorbic acid as described in section 2.2.1.2.2. Figure 3.3 shows the UV-vis spectra of AA4, AA7 and AA8. Table 3.3 presents the size and particle size distribution of AgNPs in samples AA4, AA7 and AA8.
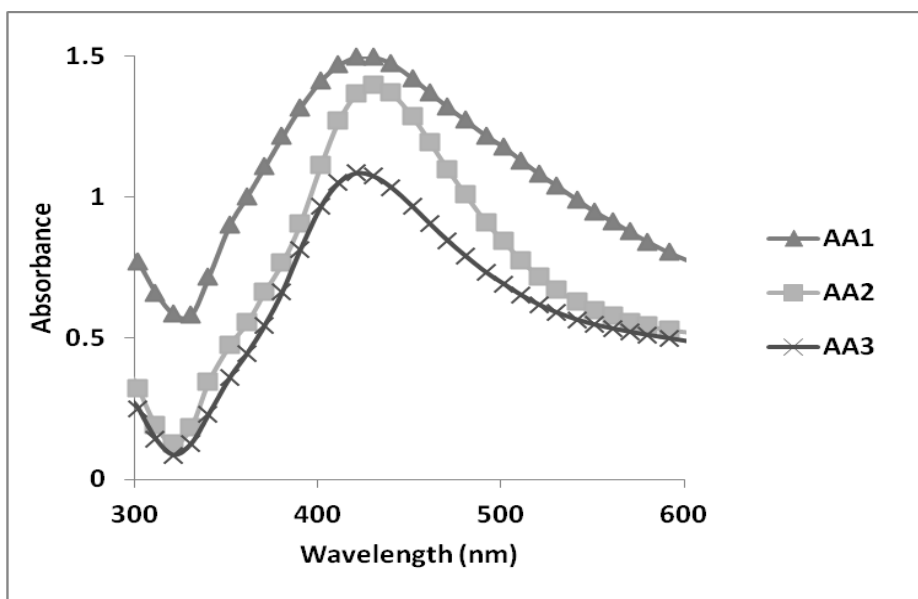

Figure 3.3: The UV-vis spectra of samples AA4, AA7 and AA8 showing the effect of varying the amount of stabilising agent, PVP.

Table 3.3: Analysis of UV-vis spectra of samples AA4, AA7 and AA8.

Sample ID	Varied synthesis condition (Molar ratio)		λ_{max}	Absorbance intensity (u.a)	FWHM	Particle size (nm)
AA4		0	430 nm	1.5	105	22.6
AA7	Ag: PVP	1:3	435 nm	0.4	200	25.5
AA8		1:10	None	None	None	None

PVP was not a good stabilising agent for the AgNPs synthesised by ascorbic acid. The addition of PVP caused a shift in the UV-vis spectrum to longer wavelengths from 430 nm to 435 nm, depicting agglomeration of particles. Furthermore, minute amounts of PVP (sample AA7) depleted the number of AgNPs (absorbance intensity of naked AgNPs (1.5 u.a.) which decreased to 0.4 u.a. following addition of PVP). Increasing the amount of PVP completely agglomerated the particles, hence sample AA8 did not absorb in this region. The PVP collapsed the strength of the solution to hold the AgNPs in dispersion therefore caused a decrease in Gibbs energy and causing particle agglomeration.

3.2.1.3. The effect of temperature on the size of AgNPs

The effect of the temperature on the silver nanoparticles size was investigated by varying the temperature (25, 30 and 50 $^{\circ}$C for AA9, AA10 and AA11 respectively). Other reaction parameters were controlled at pH 10.5, 2.781×10^{-3} M citric acid and 4.634×10^{-4} M ascorbic acid as described in section 2.2.1.3 Figure 3.4 shows the UV-vis spectra of AA9, AA10 and AA11. Table 3.4 presents the size and particle size distribution of AgNPs in samples AA9, AA10 and AA11.
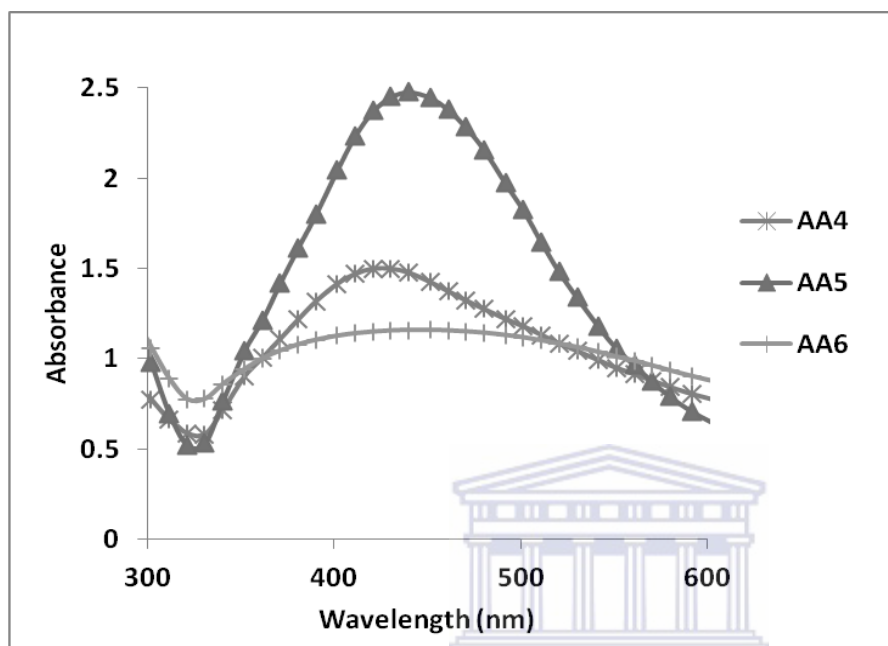

Figure 3.4: The UV-vis spectra of samples AA9, AA10 and AA11 showing the effect of varying the temperature.

Table 3.4: Analysis of UV-vis spectra of samples AA9, AA10 and AA11.

Sample ID	Varied synthesis condition		λ_{max}	Absorbance intensity (u.a)	FWHM	Particle size (nm)
AA9		25	None	None	None	None
AA10	Temperature (^{o}C)	30	435 nm	1.5	115	24.5
AA11		50	None	None	None	None

AA9 and AA11 proved that temperature is very crucial in the synthesis of AgNPs by ascorbic acid. The Ag$^+$ were not reduced at 25 ^{o}C (AA9) and 50 ^{o}C (AA11) whereas the synthesis at 30 ^{o}C (AA10) successfully produced AgNPs. Controlling the temperature at 30 ^{o}C (AA10) produced 24.5 nm AgNPs. The reduction of Ag$^+$ by ascorbic acid is an endothermic reaction therefore 30 ^{o}C supplied enough energy for the reaction to occur. Very high temperatures are associated with increasing the rate of a reaction which facilitated particle agglomeration hence the sample did not absorb in the UV-visible region.

3.2.1.4.   The effect of pH on the size of AgNPs

The effect of the pH on the silver nanoparticles size was investigated by varying the pH (pH 5.5, 9.78 and 10.5 for AA12, AA13 and AA14 respectively). Other reaction parameters were controlled at 30 ^{o}C, 2.781 x 10^{-3} M citric acid and 4.634 x 10^{-4} M ascorbic acid as described in section 2.2.1.4. Figure 3.5 shows the UV-vis spectra of AA12, AA13 and AA14. Table 3.5 presents the size and particle size distribution of AgNPs in samples AA12, AA13 and AA14.
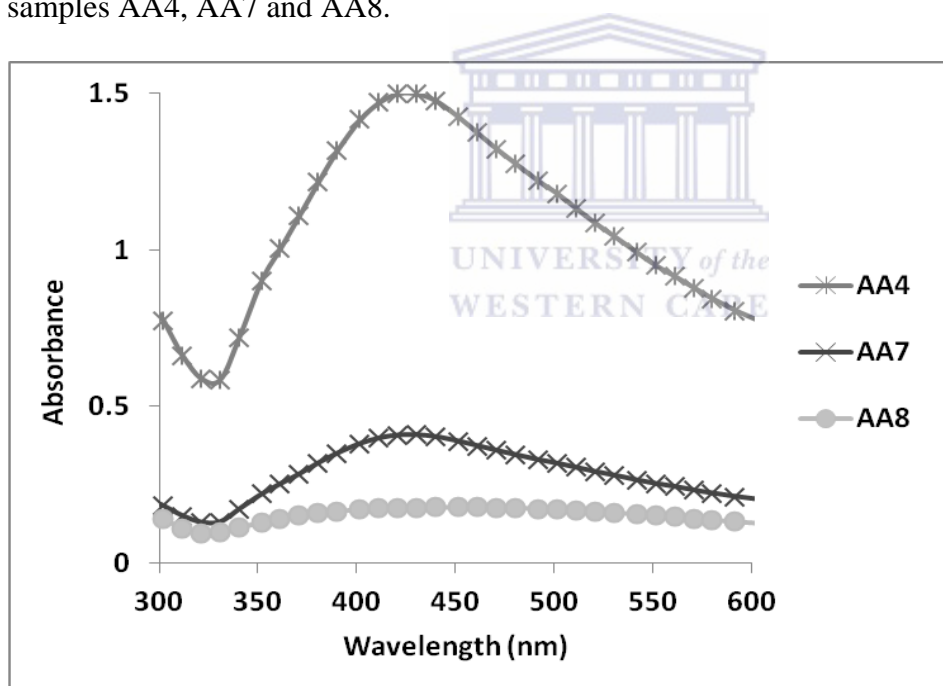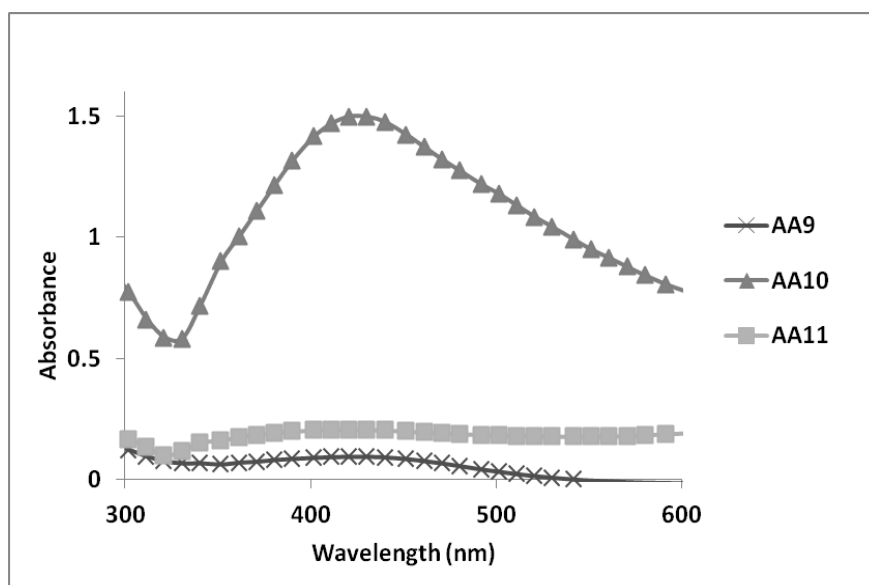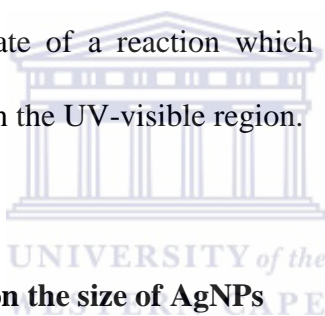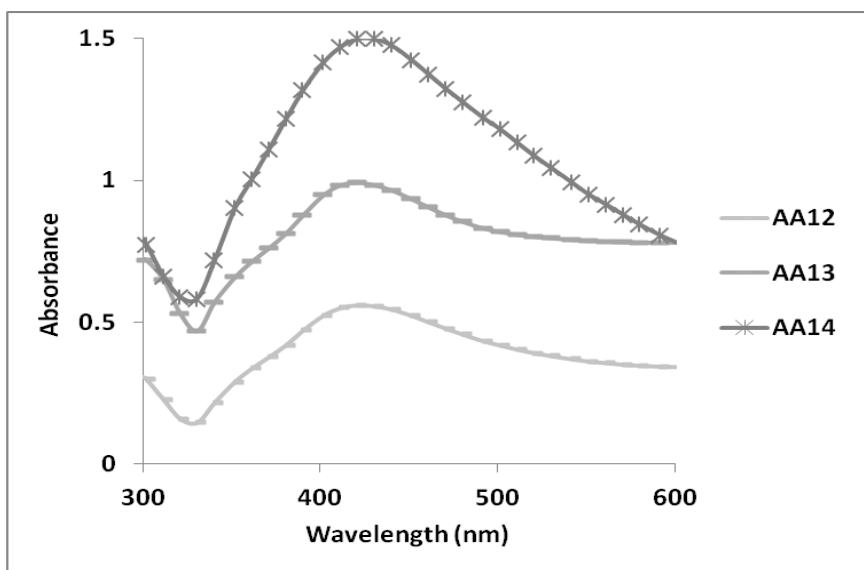
Figure 3.5: The UV-vis spectra of samples AA12, AA13 and AA14 showing the effect of pH variation.

Table 3.5: Analysis of UV-vis spectra of samples AA12, AA13 and AA14.

Sample ID	Varied synthesis condition		λ_{max}	Absorbance intensity (u.a)	FWHM	Particle size (nm)
AA12		5.5	420 nm	0.55	125	18.8
AA13	pH	9.78	425 nm	1	125	20.7
AA14		10.5	435 nm	1.5	115	24.5

There was a Red shift in the absorption peak as the pH increased, AgNPs produced at pH 5.5, pH 9.78 and 10.5 absorbed at 420, 425 and 435 nm respectively. The particle size also increased as the pH increased producing 18.8 nm, 20.7 nm and 24.5 nm AgNPs at pH 5.5 (AA12), 9 (AA13) and 10.5 (AA14) respectively. pH 10.5 (sample AA14) yielded more AgNPs (1.5 a.u. absorbance intensity) with uniform particle size distribution (FWHM = 115 nm) compared to both pH 5.5 (sample 12) and pH 9.78 (sample 13).

3.2.2. Characterisation of AgNPs synthesised by sodium borohydride using ultraviolet-visible spectroscopy

The AgNPs were synthesised through the reduction of $AgNO_3$ by sodium borohydride while varying the concentration of the reducing (sodium borohydride) and stabilising (citric acid or PVP) agent, temperature and pH.

3.2.2.1. The effect of sodium borohydride on the size of AgNPs

The amount of sodium borohydride was varied (4.635×10^{-4} M, 1.39×10^{-3} M and 1.85×10^{-3} M sodium borohydride in sample BB1, BB2 and BB3 respectively) in order to investigate the effect of sodium borohydride on the silver nanoparticles size. Other reaction parameters were controlled at 0 ^{o}C, pH 9.78 and 29.27×10^{-3} M PVP as described in section 2.2.2.1. Figure 3.6 and Table 3.6 shows the UV-vis spectra and the measured size and particle size distribution of AgNPs in samples BB1, BB2 and BB3.

Figure 3.6: The UV-vis spectra of samples BB1, BB2 and BB3 showing the effect varying the amount of the reductant, sodium borohydride.

Table 3.6: Analysis of UV-vis spectra of samples BB1, BB2 and BB3.

Sample ID	Varied synthesis condition (Molar ratio)		λ_{max}	Absorbance intensity	FWHM	Particle size (nm)
BB1		1:1	385 nm	2.8	130	7.3
BB2	Ag:NaBH4	1:10	390 nm	2.7	100	7.33
BB3		1:16	390 nm	3.15	90	7.33

Changing the amount of sodium borohydride did not show a significant difference in the size of AgNPs (BB1, BB2 and BB3 yielded 7.33 nm, 7.33 nm and 7.3 nm AgNPs respectively) produced, rather it improved the particle size distribution (BB1, BB2 and BB3 yielding

AgNPs with a FWHM of 130 nm, 100 nm and 90 nm respectively). Sample BB3 also had a maximum yield (3.15 a.u.) and the narrowest particle size distribution.

3.2.2.2. The effect of stabilising agent of the size of AgNPs

3.2.2.2.1. The effect of citric acid on the size of AgNPs

The effect of citric acid as a stabiliser on the size of silver nanoparticles was investigated by varying its concentration (0 M, 2.781×10^{-3} M and 9.27×10^{-3} M citric acid in sample BB4, BB5 and BB6 respectively). Other reaction parameters were controlled at 0 °C, pH 9.78 and 1.85×10^{-3} M sodium borohydride as described in section 2.2.2.2.1. Figure 3.7 and Table 3.7 show the UV-vis spectra and the measured size and particle size distribution of AgNPs in samples BB4, BB5 and BB6.

Figure 3.7: The UV-vis spectra of samples BB4, BB5 and BB6 showing the effect of varying the concentration of stabilising agent, citric acid.

Table 3.7: Analysis of UV-vis spectra of samples BB4, BB5 and BB6.

Sample ID	Varied synthesis condition (Molar ratio)		λ_{max}	Absorbance intensity	FWHM	Particle size (nm)
BB4		0	385 nm	2.65	75	5.4
BB5	Citric acid: Ag	3	390 nm	1.2	60	6.7
BB6		10	None	None	None	None

The stabilising agent (citric acid) had an effect on the quality of AgNPs produced. The addition of citric acid to the borohydride system caused depletion of the nanoparticles as shown by the absorbance intensity (2.65, 1.2 and 0 a.u. in samples BB4, BB5 and BB6 respectively) but low concentrations of citric acid improved particle size distribution (FWHM = 75 nm and 60 nm for samples BB4 and BB5 respectively). A Red shift in the absorption spectra following the addition of citric acid (sample BB5) is an indication of agglomeration therefore increasing the size of the particles (5.4 and 6.7 nm in samples BB4 and BB5 respectively).

3.2.2.2.2. The effect of PVP on the size of AgNPs

The effect of PVP as a stabiliser on the size of silver nanoparticles was investigated by varying its concentration (0 M, 2.781×10^{-3} M and 9.27×10^{-3} M PVP in sample BB4, BB7 and BB8 respectively). Other reaction parameters were controlled at 0 $^{\circ}$C, pH 9.78 and 1.85×10^{-3} M sodium borohydride as described in section 2.2.2.2.2. Figure 3.8 and Table 3.8 show the UV-vis spectra and the measured size and particle size distribution of AgNPs in samples BB4, BB7 and BB8.
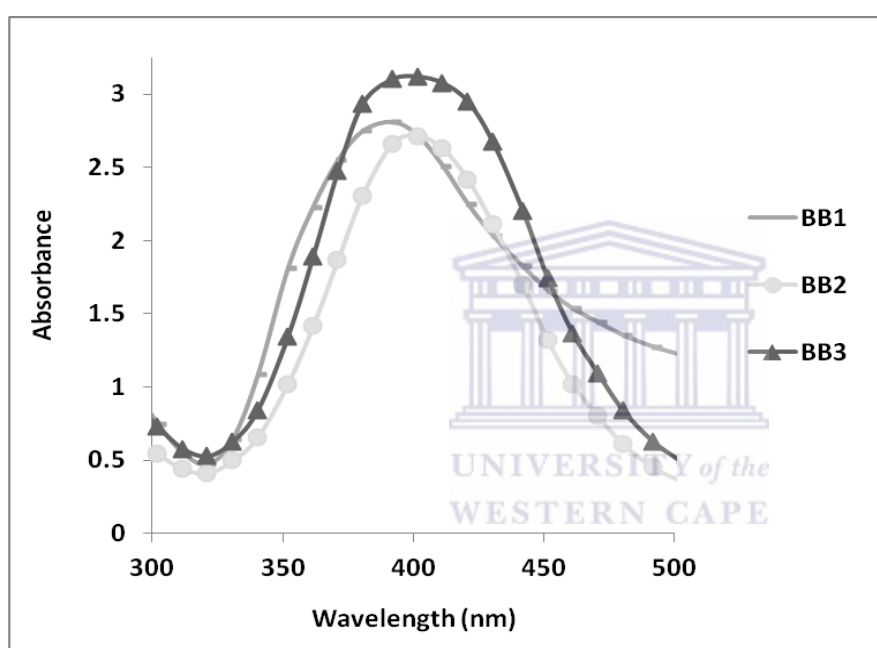

Figure 3.8: The UV-vis spectra of samples BB4, BB7 and BB8 showing the effect of varying the amount of stabilising agent, PVP.

Table 3.8: Analysis of UV-vis spectra of samples BB4, BB7 and BB8.

Sample ID	Varied synthesis condition (Molar ratio)		λ_{max}	Absorbance intensity (u.a.)	FWHM	Particle size (nm)
BB4		0	385 nm	2.65	75	5.4
BB7	Ag:PVP	1:3	390 nm	2.45	85	7.3
BB8		1:10	390 nm	3.15	90	7.3

The addition of PVP increased the particles size from 5.4 nm (BB4) to 7.3 nm (BB7 and BB8) and also broadened the particle size distribution (FWHM = 75, 85 and 90 nm for samples BB4, BB7 and BB8 respectively).

3.2.2.3. The effect of temperature on the size of AgNPs

The effect of temperature on the size of silver nanoparticles was investigated by controlling the synthesis temperatures at 0 °C, 25 °C and 50 °C for samples BB9, BB10 and BB11 respectively. Other reaction parameters were controlled at pH 9.78, 9.27×10^{-3} M PVP and 1.85×10^{-3} M sodium borohydride as described in section 2.2.2.3. Figure 3.9 and Table 3.9 show the UV-vis spectra and the measured size and particle size distribution of AgNPs in samples BB9, BB10 and BB11.
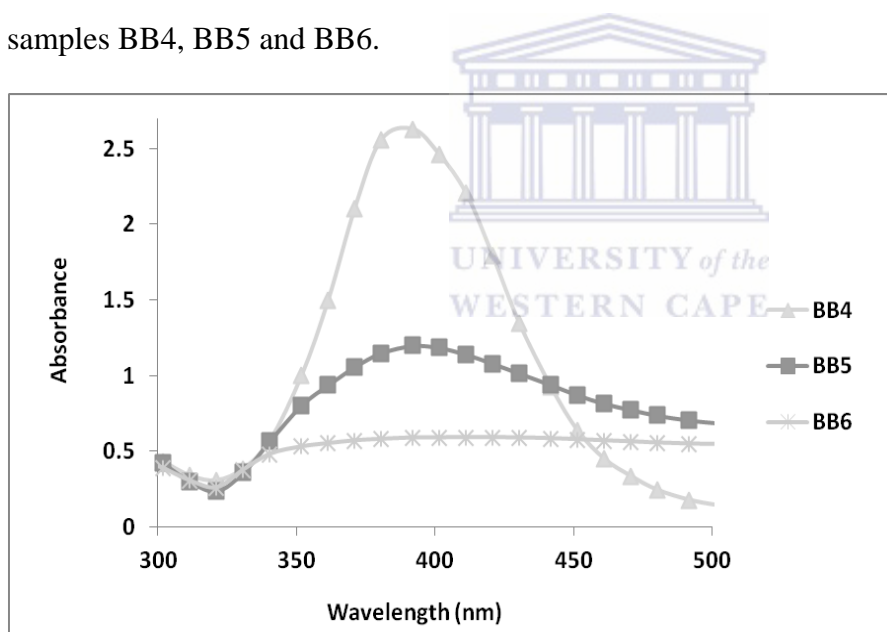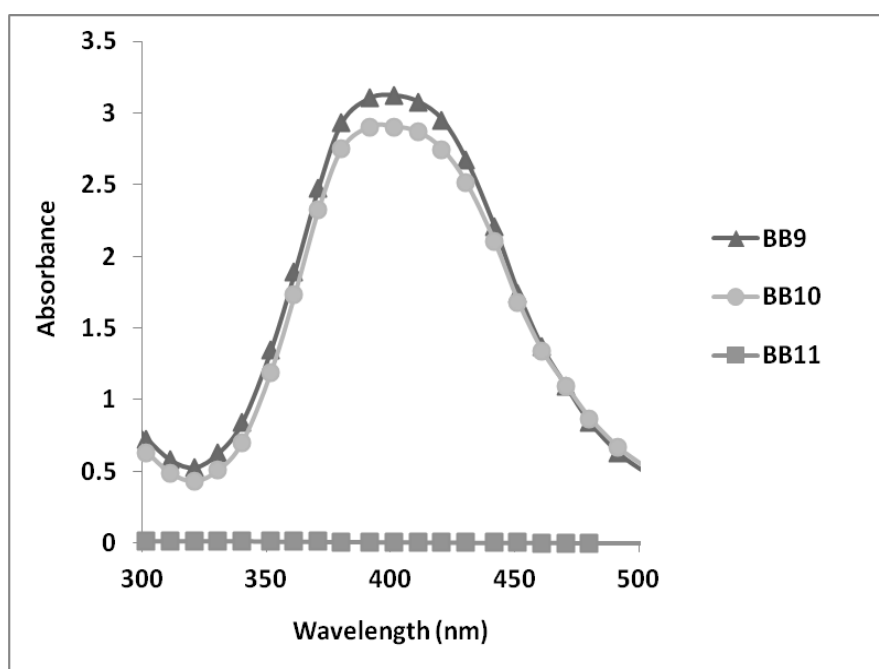

Figure 3.9: The UV-vis spectra of samples BB9, BB10 and BB11 showing the effect of varying the temperature.

Table 3.9: Analysis of UV-vis spectra of samples BB9, BB10 and BB11.

Sample ID	Varied synthesis condition		λ_{max}	Absorbance intensity	FWHM	Particle size (nm)
BB9		0	390 nm	3.15	90	7.3
BB10	Temperature (^{o}C)	25	390 nm	2.95	95	7.3
BB11		50	None	None	None	None

Temperature is very crucial in the synthesis of AgNPs by sodium borohydride. The synthesis carried out at 0 ^{o}C (BB9) and 25 ^{o}C (BB10) produced 7.3 nm AgNPs although sample BB10 had a wider size distribution (FWHM = 95 nm) than BB9 (FWHM = 90 nm). The nanoparticles produced at 50 ^{o}C (BB11) did not absorb in the wavelength range for silver nanoparticles.

3.2.2.4. The effect of pH on the size of AgNPs

The effect of pH on the size of silver nanoparticles was investigated by controlling the synthesis pH at 5.5, 9.78 and 10.5 for samples BB12, BB13 and BB14 respectively. Other reaction parameters were controlled at 0 ^{o}C, 9.27×10^{-3} M PVP and 1.85×10^{-3} M sodium borohydride as described in section 2.2.2.4. Figure 3.10 and Table 3.10 show the UV-vis spectra and the measured size and particle size distribution of AgNPs in samples BB12, BB13 and BB14.
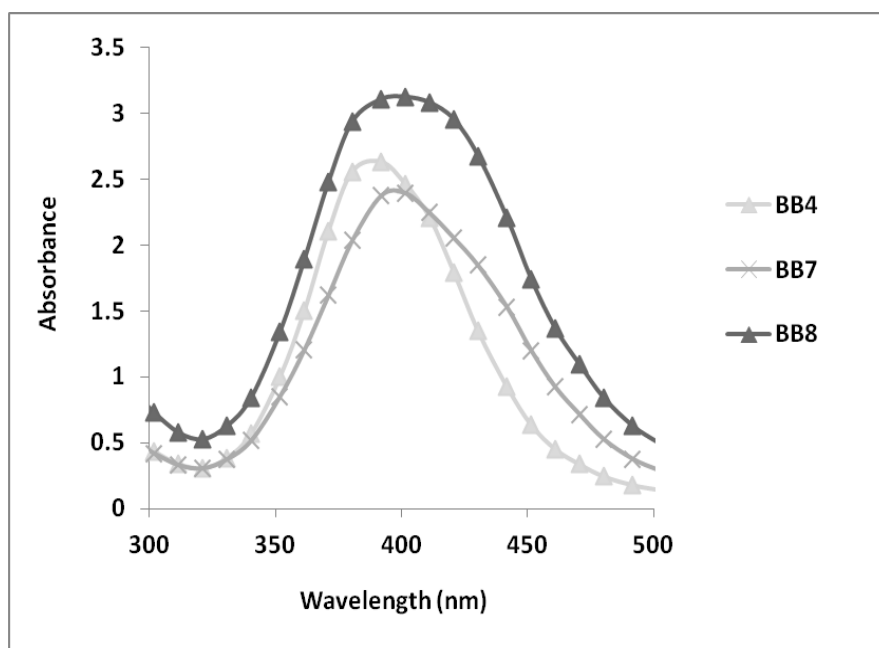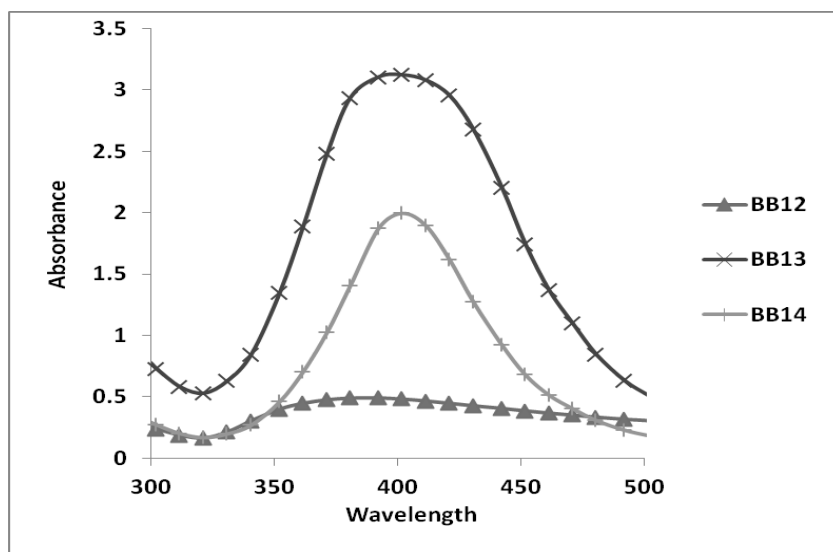

Figure 3.10: The UV-vis spectra of samples BB12, BB13 and BB14 showing the effect of varying pH.

Table 3.10: Analysis of UV-vis spectra of samples BB12, BB13 and BB14.

Sample ID	Varied synthesis condition		λ_{max}	Absorbance intensity	FWHM	Particle size (nm)
BB12		5.5	385 nm	0.5	200	5.4
BB13	pH	9.78	390 nm	3.15	85	7.3
BB14		10.5	405 nm	2	90	13.1

The particle size increased as the pH increased producing 5.42 nm, 7.33 nm and 13 nm AgNPs at pH 5.5 (BB12), 9.78 (BB13) and 10.5 (BB14) respectively. Sample BB13 had a fine size distribution (FWHM = 85 nm) compared to the sample BB12 (FWHM = 200 nm) and BB14 (FWHM = 90 nm). Sample BB13 also had the highest yield of AgNPs with an absorbance intensity of 3.15 u.a.

3.2.3. Comparative study of silver nanoparticles synthesised with sodium borohydride and ascorbic acid

Figure 3.11 and 3.11 show the size and particle size distribution (FWHM) of AgNPs synthesised by ascorbic acid (sample AA1 to AA14) and sodium borohydride (BB1 to BB14) respectively. The reaction conditions were varied as described in section 2.2.
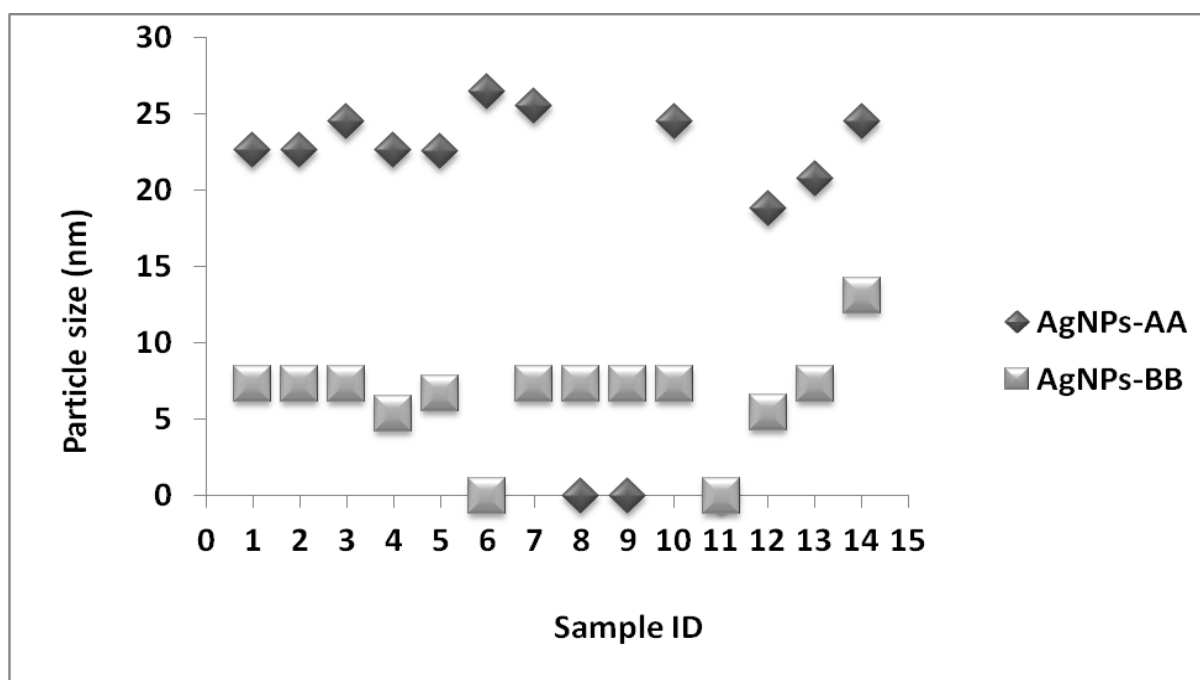
Figure 3.11: The size of AgNPs synthesised through reduction by ascorbic acid (AgNPs-AA) and sodium borohydride (AgNPs-BB).
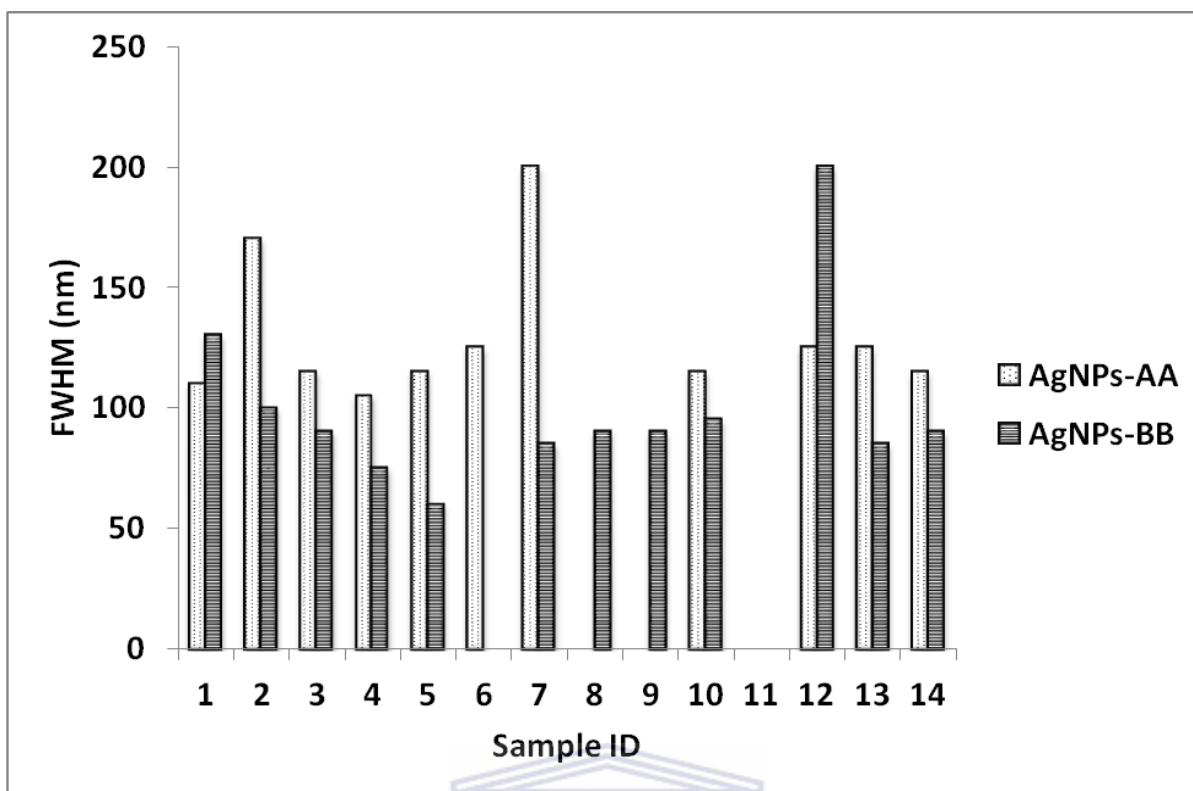
Figure 3.12: The peak width of the UV-vis spectra of AgNPs synthesised through reduction by ascorbic acid (AgNPs-AA) and sodium borohydride (AgNPs-BB).

The reduction of silver ions with ascorbic acid produced silver nanoparticles ranging between 18.8 and 26.4 nm; whereas the nanoparticles produced by sodium borohydride ranged between 5.4 nm and 13.1 nm. The UV-vis spectra of AgNPs synthesised by ascorbic acid had a FWHM ranging between 105 nm and 200 nm; whereas the FWHM of nanoparticles produced by sodium borohydride ranged between 60 nm and 130 nm. Therefore sodium borhydride produced nanoparticles with small and uniform AgNPs compared to ascorbic acid.

Some parameters (amount of reducing and stabilising agent, temperature and pH) were able to control the AgNPs size and particle size distribution. The increase in the amount of reducing agent in the sodium borohydride synthesis caused a gradual narrowing of particle size distribution (samples BB1, BB2 and BB3 had 130, 100, and 90 nm FWHM). Ascorbic acid produced AgNPs were best stabilised with citric acid compared to PVP whereas the sodium borohydride produced AgNPs were best stabilised with PVP compared to citric acid.

The AgNPs stabilised with either citric acid or PVP (samples AA5, AA6, BB5 and BB6,) were larger in size compared to the non-stabilised AgNPs (samples AA4 and BB4).The 1:3 (Ag: citric acid) molar ratio yielded more AgNPs (sample AA5 with the absorbance intensity of 2.5 u.a) compared to the non-stabilised AgNPs (sample AA4 with the absorbance intensity of 1.5 u.a) in the ascorbic acid synthesis. Ascorbic acid could only synthesis AgNPs at 30 ^{o}C whereas sodium borohydride had successfully produced AgNPs at 0 ^{o}C and 25 ^{o}C with the maximum yield at 0 ^{o}C. The particle size was influenced by pH in both the ascorbic acid and sodium borohydride based syntheses. Acidic pH conditions (pH 5.5) resulted in smaller AgNPs compared to the alkaline pH (9-10.5) on both syntheses. However, the acidic pH resulted in AgNPs with a wide particle size distribution compared to the alkaline pH on both syntheses.

The synthesis condition that produced smaller, uniform particles and the highest absorption intensity was chosen to compare the efficacy of each reducing agent (ascorbic acid or sodium borohydride). Sample AA5, synthesised at pH 10.5, the temperature of 30 ^{o}C, and Ag/ascorbic acid/citric acid molar ratio of 1:4:3; was chosen because it produced small and uniform AgNPs in the ascorbic acid based synthesis. Sample BB3, synthesised at pH 9.78, the temperature of 0 ^{o}C, and Ag/$NaBH_4$/PVP molar ratio of 1:10:10; was chosen because it produced small and uniform AgNPs in the sodium borohydride based synthesis. Figure 3.13 shows the TEM images and EDS spectra of AgNPs synthesised by sodium borohydride (BB3) or ascorbic acid (AA5).
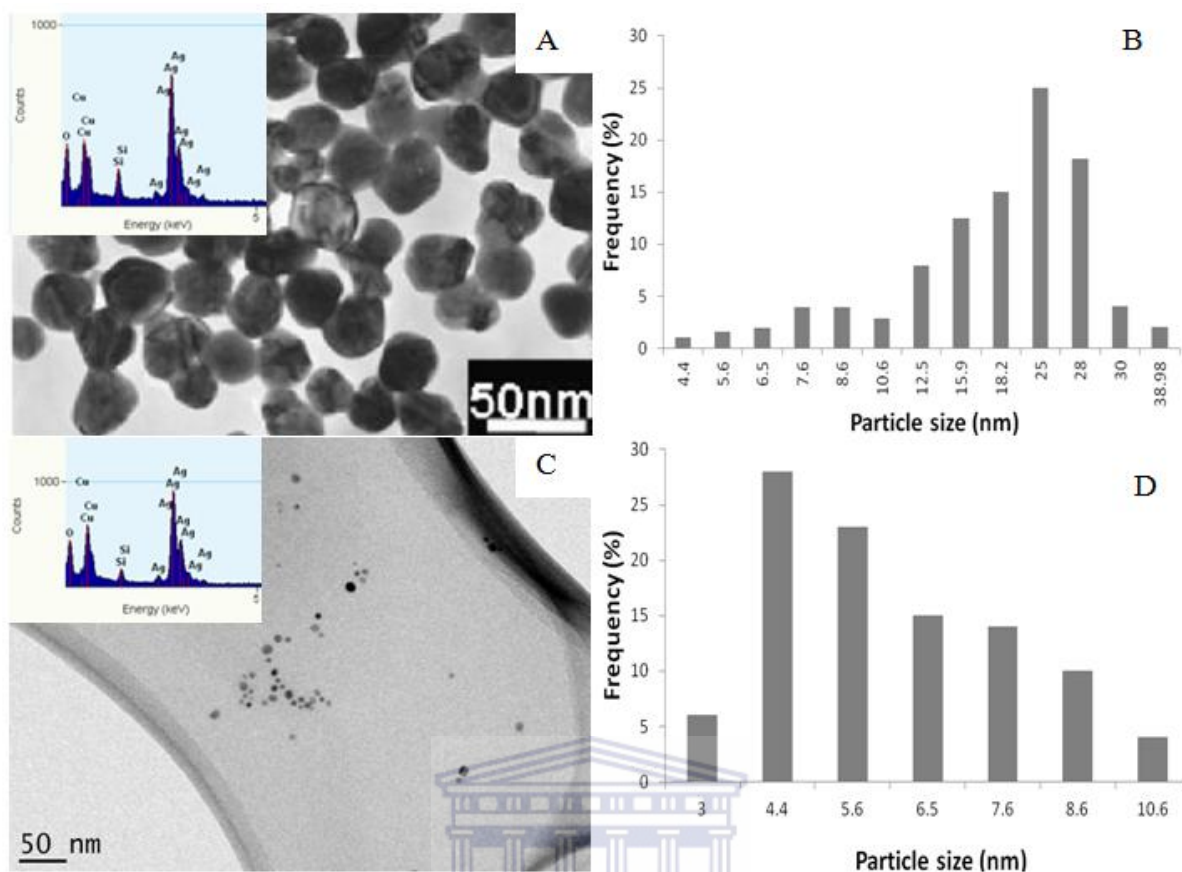
Figure 3.13: Transmission electron micrographs of silver nanoparticles.
A) TEM image with EDS spectra of AgNPs synthesised by ascorbic acid as reducing agent. B) The size distribution of AgNPs synthesised by ascorbic acid as reducing agent. C) TEM image with EDS spectra of AgNPs synthesised by sodium borohydride as reducing agent. D) The size distribution of AgNPs synthesised by sodium borohydride as reducing agent.

The UV-vis spectroscopy determined the average particle size of AgNPs synthesised by ascorbic acid (AA5) or sodium borohydride (BB3) to be 22.6 nm and 7.3 nm respectively [Table 3.2 and Table 3.6]. Transmission electron microscopic images revealed silver nanoparticles synthesised by ascorbic acid were relatively larger with a wider size distribution (15.4±11.15 nm) compared to nanoparticles synthesised by sodium borohydride which were small and uniform in size (6.6±2.6 nm). Both syntheses produced spherical particles that were confirmed by EDS to be silver nanoparticles. The EDS spectrum has a strong signal in the silver region with a typical optical absorption band peaked nearly at 3 KeV confirming the metallic silver nanoparticles due to surface plasmon resonance. The nanoparticles had an oxide layer as indicated by the presence of a distinct oxygen peak. The

EDS spectra also presented with copper (Cu) and carbon (C) which is derived from the copper grids coated with a carbon film that was used in the analysis, as described in section 2.4.2. The peak for silicon (Si) in the EDS spectra originates from the detector and other parts of the microscope which may have been exited by the X-rays in the analysis. Sample BB3 was used for further analysis.

3.2.4. Investigating the effect of light

3.2.4.1.   The effect of light exposure on AgNPs in motion

Sample BB3 (synthesis described in section 2.2.2.1) was exposed to light for 0, 6 and 12 hours as described in section 2.2.3. Figure 3.14 shows TEM images of AgNPs (samples S1, S2 and S3) that were exposed to light for different periods of time (0, 6 and 12 h respectively) while stirring. Figure 3.14, shows a high resolution image of a single silver nanoparticle that was expose to light for 6 hours while stirring (sample S2).
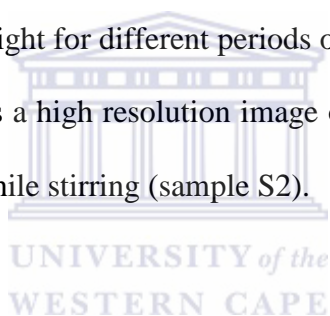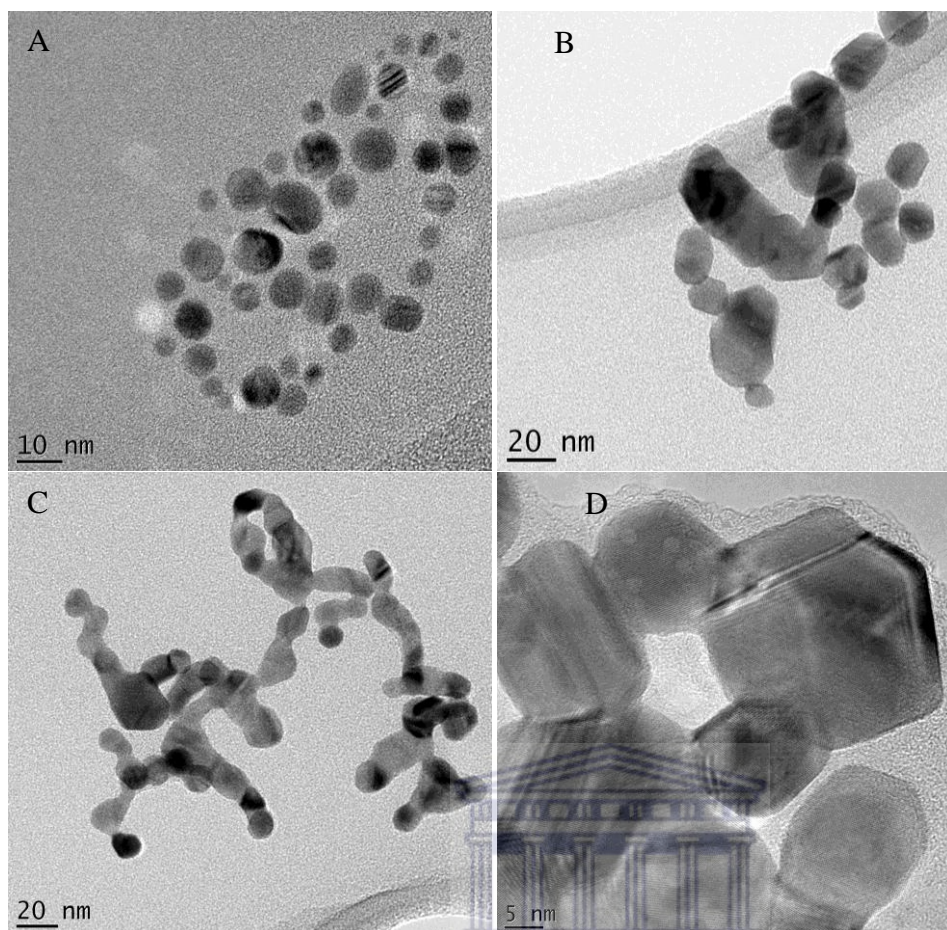
Figure 3.14: The morphological changes that AgNPs develop when exposed to light (while stirring).
A) The TEM images of spherical AgNPs that were not exposed to light (S1). B) The TEM images of icosahedral AgNPs that were exposed to light for 6 hours (S2). C) The TEM images of AgNPs that were exposed to light for 12 hours (S3). D) The high resolution TEM images of icosahedral AgNPs that were exposed to light for 6 hours (S2).

Exposing the particles to light for 6 h changed particle shape without a significant alteration of size. The 6±1.8 nm spherical AgNPs increased in size to 6±2 nm icosahedral AgNPs within 6 h of exposure to light (while stirring) [Figure 3.14 (B)]. However, the particles agglomerated into strings by 12 h of light exposure making it difficult to determine their shape and size [Figure 3.14 C]. Stirring the AgNPs caused particle agglomeration. Cao, (2004) explain this phenomenon by stating that small particles have a high surface to volume ratio and therefore are highly reactive. Allowing the reaction of sodium borohydride to occur over a long time and constantly stirring would promote nanoparticles interaction and ultimately agglomeration.

3.2.4.2. The effect of light exposure on stationary AgNPs

Figure 3.15 represents the TEM images of AgNPs that were exposed to light for different periods of time (0, 6 and 12 hours for S4, S5 and S6 respectively) without stirring.
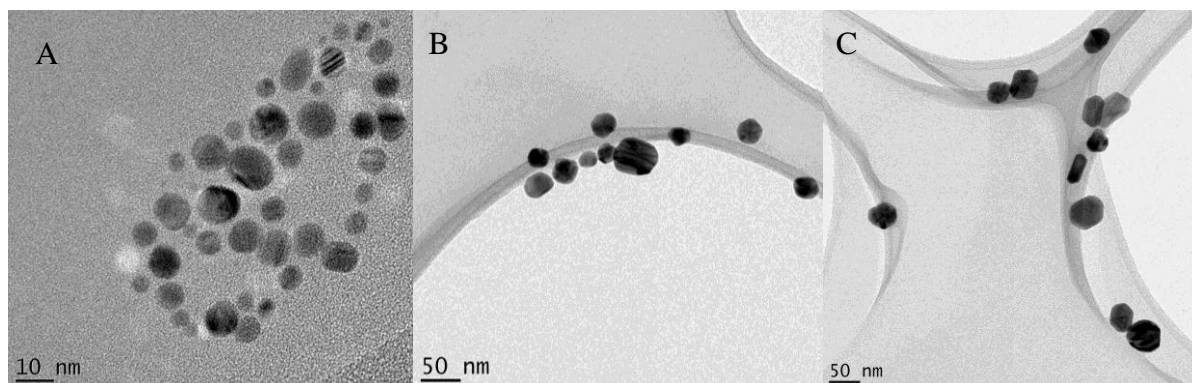
Figure 3.15: The morphological changes that stationary AgNPs develop when exposed to light.
A) The TEM images of spherical AgNPs that were not exposed to light (S4). B) The TEM images of spheres, icosahedral and irregular AgNPs that were exposed to light for 6 hours (S5).C) The TEM images of spheres, icosahedral, tubes and irregular AgNPs that were exposed to light for 12 hours (S6).

The particles increased in sizes but did not show signs of particle collision or agglomeration. Exposing the particles for 6 h (without stirring) did not change particle shape rather increased their size. Increasing the light exposure time to 12 h caused an increase in particles size and altered their morphology to form rods, spheres and icosahedral shapes. This indicated that light has a shape changing effect on the AgNPs at a much slower rate when the particles are stationary. Keeping the AgNPs stationary delayed the shape change period and it also favoured the formation of different shapes, with a wide size distribution.

3.2.5. Concentration and purification of the silver nanoparticles

3.2.5.1. The effect of up-scaling the concentration of silver from 100 μg/ml to 1 mg/ml

Samples BB3 and BB14 were synthesised as described in 2.2.2.1 and 2.3.1 respectively. Sample BB14 (1 g/L AgNPs) was ten times concentrated than sample BB3 (100 mg/L

AgNPs). Figure 3.16 shows the optical properties of samples BB3 (100 mg/L AgNPs) and BB14 (1 g/L) after 24 hours of storage at 4 °C.
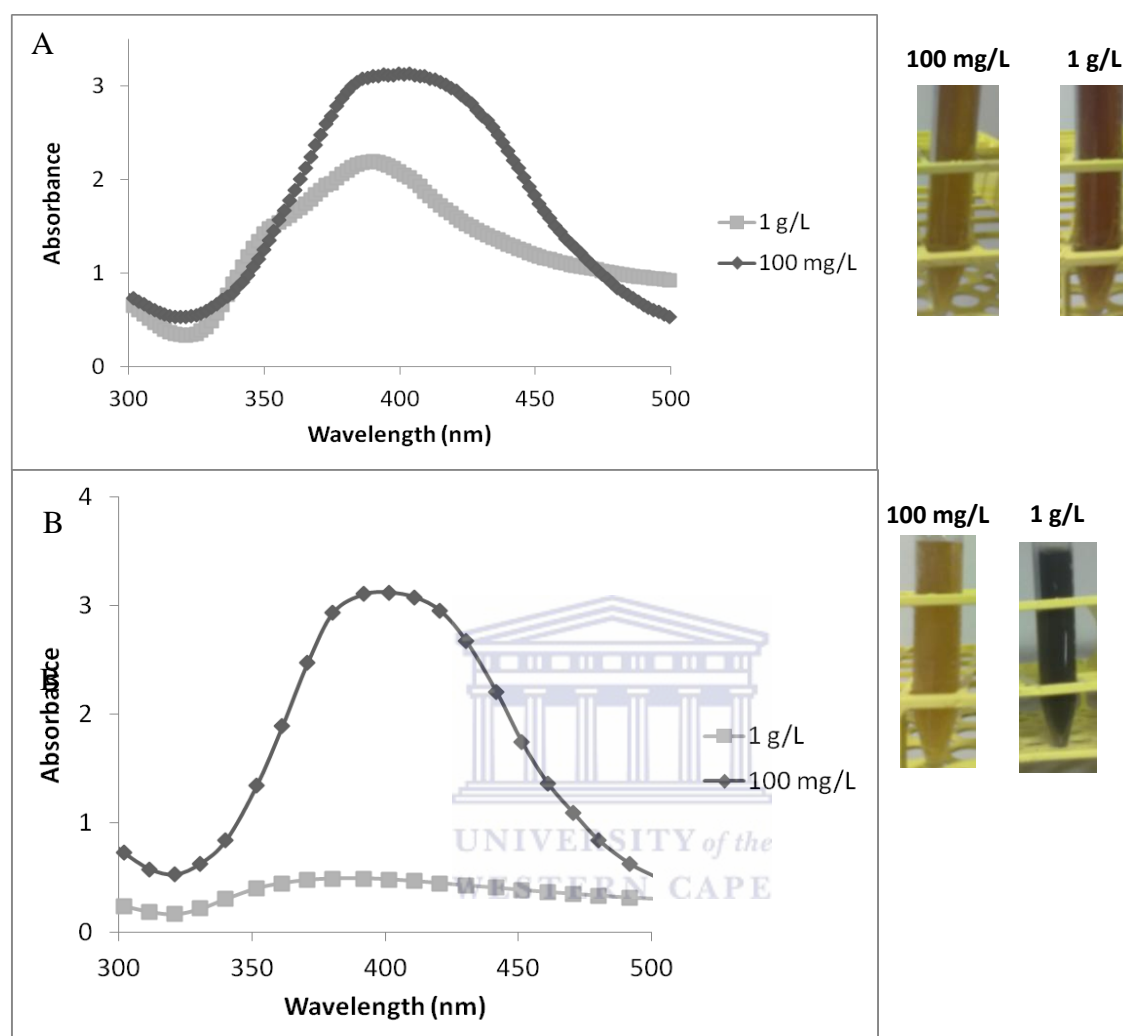
Figure 3.16: The optical properties of 1 g/L AgNPs and 100 mg/L AgNPs after 24 h storage.
A) The colour and UV-vis spectra of AgNPs immediately after synthesis. B) The colour change and UV-vis spectra of AgNPs after 24 h of storage at 4 °C.

UV-vis spectroscopy analysis, immediately after the synthesis, showed low absorption intensity in 1 g/L AgNPs (2.25 a.u.) compared to the 100 mg/L AgNPs (3.2 a.u.) [Figure 3.16 (B)]. Then there was a visual colour change in the 1 g/L AgNPs after 24 h storage, from yellow to black [Figure 3.16]. Furthermore the 1 g/L AgNPs did not absorb after 24 h of storage proving complete depletion of the AgNPs after 24 h. The 100 mg/L AgNPs remained stable after 24 h of storage at 4 °C [Figure 3.16 (B)].

3.2.5.2. Concentrating and purification of silver nanoparticles using the Freeze-dry method

Following the difficulty in producing a concentrated stock of AgNPs (>100 mg/L), other methods such as freeze-drying and centrifugation were undertaken. The Sample BB3 was freshly prepared then either centrifuged at 1300 rpm for 30 minutes or freeze dried at -50 °C for 120 h as described in section 2.2.2.1 The AgNPs could not be purified by the centrifuge method since they remained in suspension [Figure 3.17].
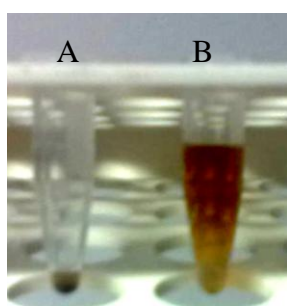
Figure 3.17: Investigating the effect of centrifuge conditions on the AgNPs.
A) The AgNPs stabilised with citric acid (precipitated). B) AgNPs stabilised with PVP (remained in suspension) after the centrifuge step.
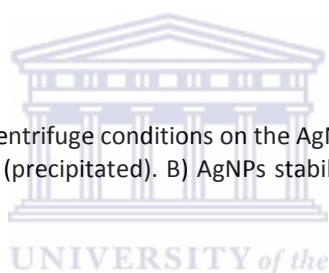
The colloidal suspension was successfully freeze-dried to form a black powder of AgNPs. The AgNPs were then characterised before and after freeze-drying to investigate the effect of freeze-drying on the morphology and size of AgNPs. Figure 3.18 shows the TEM images of AgNPs before the [Figure 3.18 (A)] and after [Figure 3.18 (B)] freeze-drying.
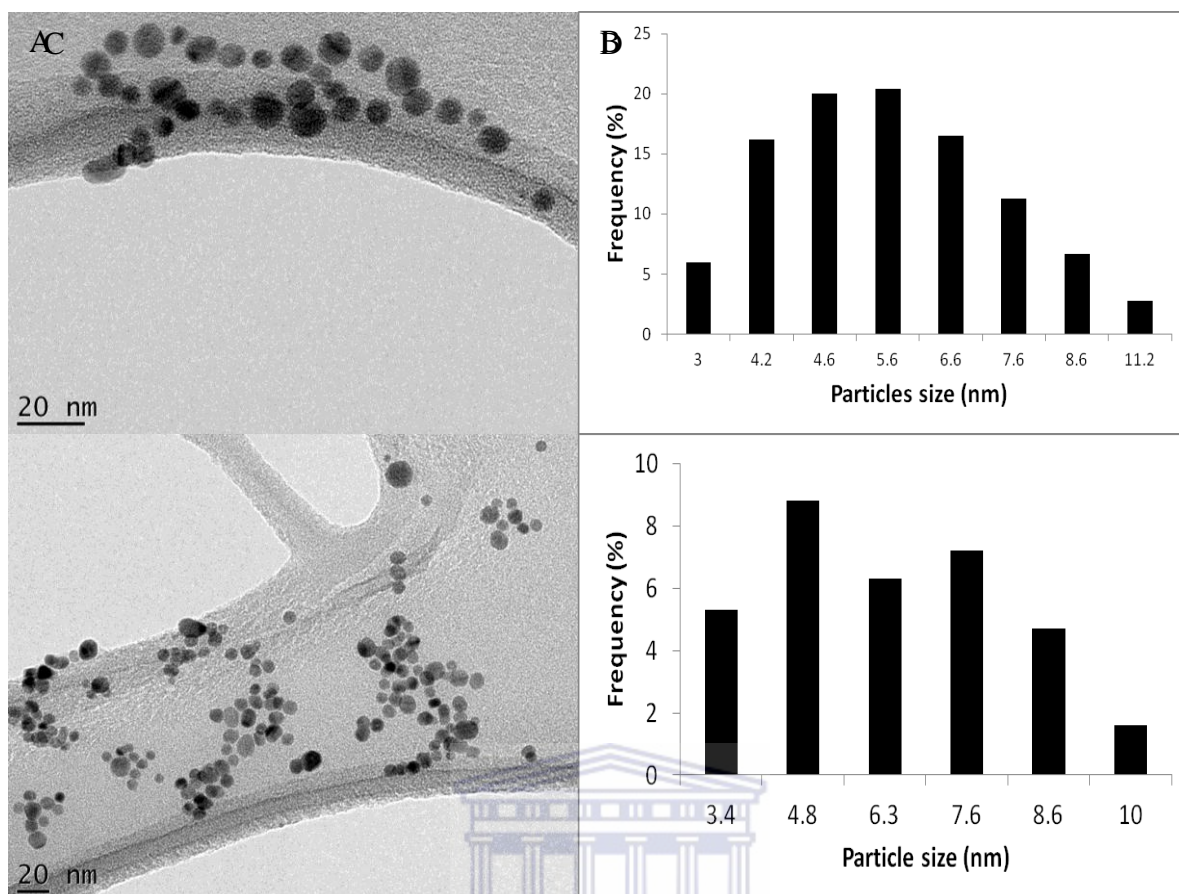
Figure 3.18: Investigating the effect of the freeze-drying conditions on the AgNPs.
A) The TEM images of AgNPs before the freeze-drying. B) Size distribution of AgNPs before the freeze-drying.
C) The TEM images of AgNPs after freeze-dying. D) Size distribution of AgNPs after the freeze-drying.

The freeze-dry conditions did not alter the size and morphology of the AgNPs although the particle size distribution was slightly affected.

3.2.6. The assessment of the compatibility of the silver nanoparticles for its biological application

Sample BB3 was freshly prepared and its stability was checked at the bacterial growth conditions which included constant shaking the solution at a pH 7.4 for 24 h in a 37 ⁰C incubator.
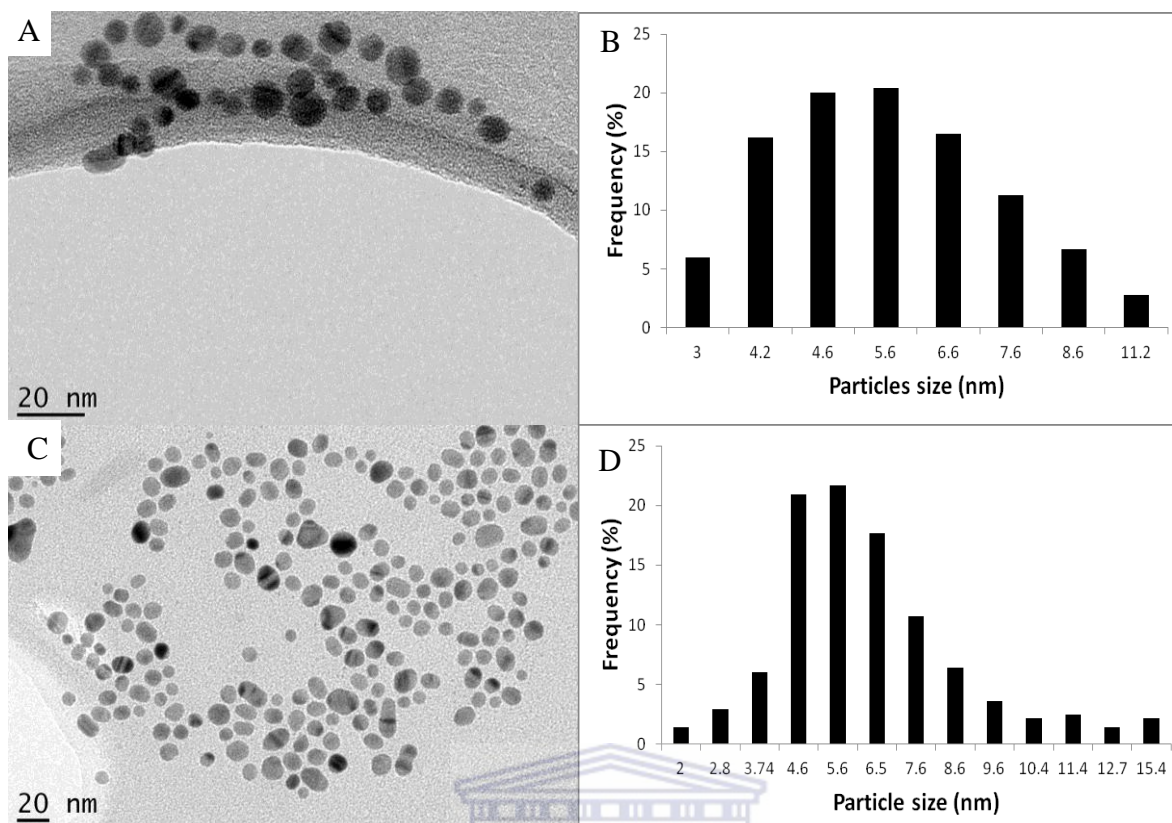
Figure 3.19: Investigating the effect of bacterial incubation conditions on the AgNPs.
A) The TEM images of AgNPs before the incubation. B) Size distribution of AgNPs before the incubation. C) The TEM images of AgNPs after 24 h incubation. D) Size distribution of AgNPs after the 24 h incubation.

The incubation conditions did not alter the size and morphology of the AgNPs although the particle size distribution was slightly affected [Figure 3.19].

3.3. Analysis of Silver nanoparticles using EDS

The EDS analysis of sample BB3 in Table 3.11 shows that there are trace elements in the colloidal suspension but these elements were present in such minute concentration that they could not be revealed by the EDS spectra. If the background effect of copper and carbon is removed a localised EDS analysis predicts 7.22 %, 6.75 %, 5.32 % and 80.69 % of boron, oxygen, sodium and silver.

Table 3. 11: EDS analysis of a localised spot identifyied to be silver nanoparticle .

Element	EDS (Weight %)	EDS (Atomic %)
B	7.22	32.28
O	6.75	20.38

Na	5.32	11.19
Ag	80.69	36.13

3.4 Discussion

The degree of light absorption and scattering is dependent on the size of the AgNPs. The UV-visible absorption spectra of all AgNPs synthesised in this study were often symmetric dipole resonant modes which indicated the formation of uniform AgNPs, smaller than 50 nm. The nanoparticles experienced an uniform electric field because they were smaller than the wavelength of light (Gao *et al*., 2011). If the AgNPs were larger than 50 nm the UV-vis spectra would have had an additional shoulder peak called the quadrupolar resonant mode (Evanoff & Chumanov, 2004; Kumbhar *et al*., 2005).

However, synthesis with the different reducing agent produced nanoparticles of different sizes. This uniform electric field deflects with increase in nanoparticle size therefore contributing to a Red-shifting towards the visible region and broadening of the spectrum (Cao, 2004; Chou *et al*., 2005). The nanoparticles synthesised by ascorbic acid were bigger (absorbing at the wavelength of 430 nm) compared to those synthesised by sodium borohydride (absorbing at the wavelength of 390 nm). Sodium borohydride, a strong reducing agent, instantly results in ±4 nm seeds; whereas ascorbic acid, a weak reducing agent, has a slow rate of formation of new nuclei which allows for rapid aggregation giving rise to a small number of large particles (Cao, 2004; Chou *et al*., 2005; Solomon *et al* 2007). This was observed in the duration and size of AgNPs produced by each synthesis method (ascorbic acid or sodium borohydride based). Ascorbic acid needed enough time with silver to effectively form AgNPs hence the ascorbic acid synthesis took 30 minute compared to sodium borohydride which took a few minutes to complete. Sodium borohydride produced

smaller silver nanoparticles with uniform size and morphology (spherical 6±1.8 nm AgNPs) compared to ascorbic acid that produced big particles with a wide size distribution (15±11.15 nm AgNPs). TEM images showed that both synthesis methods produced spherical AgNPs.

 Particle maturation was solely controlled by exposure of the AgNPs to light. Stirring AgNPs in the light exposure caused particle agglomeration that was not evident in AgNPs that were kept stationary. Cao, (2004) explains this phenomenon by stating that small nanoparticles (less than 20 nm) have high surface to volume ratio causing them to be more chemically, physically and thermodynamically unstable and stirring them enhanced these properties resulting in particle agglomeration. These properties on the other hand aided in the formation of uniform icosahedral AgNPs (within 6 h), but not stirring AgNP solution resulted in different shapes of AgNPs over a longer maturation period (12 hours).

The synthesised AgNPs should be sustained by the solvents', protic or aprotic properties ionic strength, and polarity, pH and inter-particle interactions to remain stable. The reducing agents used in this study, ascorbic acid and sodium borohydride, have high efficacy for the reduction of Ag^+ at alkaline pH, where the zeta potential of silver is around -35 mV. The surface charge majorly contributes to the inter-particle forces and can be altered by a certain pH. When all particles in suspension are uniformly charged (positively, negative or neutrally), they repel each other therefore prevent agglomeration. The silver maximum zeta potentials (±35 mV) are estimated to be around pH 2 and pH 10.5 and the point of zero charge (pzc) is around pH 5.5 (Overbreek, 1952; Hunter, 1987; Shaw 1992; Larson & Attard, 2000). In the current study the alkaline reducing agent (sodium borohydride) favoured an alkaline stabiliser (PVP) whereas an acidic reducing agent (ascorbic acid) preferred an acidic stabiliser (citric acid). Synthesis at point of zero charge (pH 5.5) produces nanoparticles with a charge distribution that resembles a bell shape (some negatively charged while others are positively charged) therefore the positively and negatively charged particles will be attracted

to each other and clump together forming globular structures (Larson & Attard, 2000). This phenomenon was evident when the synthesis (both ascorbic acid and sodium borohydride based) was controlled at pH 5.5 (pzc), whereas nanoparticles with high zeta potential (pH 9-10.5) were smaller and more stable. The addition of citric acid as a stabilising agent in the sodium borohydride based synthesis altered the pH to around the pzc therefore causing agglomeration, but PVP did not alter the pH and resulted in stable, small and uniform AgNPs. The opposite was viewed in the ascorbic acid based synthesis.

The kinetic stabilisation also required a delicate balance in the concentrations of stabilising agent for a successful control of size and size-distribution of AgNPs. PVP is a hydrophobic polymer that covalently attaches to the surface of the particle. The polymers in the case of partially covered particles (low concentration of PVP) tend to interpenetrate in order to reduce the unoccupied space between polymers therefore reducing the thickness of the stabilising agent protective layer, causing the particles to interact resulting in particle agglomeration (Cao, 2004; Travan *et al.*, 2011; Gao *et al.*, 2011). While when particles were 100% covered (high concentration of PVP) there was minimal to no interaction because the distance between the particles was longer than twice the thickness of the stabilising agent protective layer, therefore particles repeled each other preventing agglomeration.

Chapter 4

Investigating the antibacterial properties of silver nanoparticles

4.1.   Minimum inhibitory concentration

Minimum inhibitory concentration (MIC) is defined as the lowest concentration at which there is no visible growth. Sample BB3 which produced smaller and uniform AgNPs (6 ± 1.8 nm) was chosen for the antibacterial study. The silver nanoparticles were prepared by reducing silver nitrate with sodium borohydride then stabilising the AgNPs with PVP as detailed in section 2.2.2.1.

There were difficulties in purifying the nanoparticles from by-products such as the sodium and boron introduced by the reducing agent compound ($NaBH_4$), the nitrate introduced by the silver precursor ($AgNO_3$) and the PVP that coats the nanoparticles. Thus the effect of these by-products on bacterial growth was investigated by treating the bacteria with a solution containing only the respective amount of by-products expected to be in an AgNPs colloidal suspension. To investigate the efficiency of AgNPs over silver ions, bacterial strains were treated with $AgNO_3$ at the predicted amount of silver as calculated from the amount in AgNPs suspensions.

Bacterial (*B. cereus, C. metallidurans, E. coli* 1699*, M. smegmatis* or *S. epidermidis)* inoculums (at OD $\pm$ 0.045) were treated with different concentrations of either by-products or Ag^+ or AgNPs (0, 10, 20, 30, 40, 50, 60, 70 mg/L) then incubated at 37 ^{o}C for 24 h as described in section 2.5.2.2. Bacterial growth was determined by measuring turbidity (optical density, OD) at 600 nm spectrophotometrically. Lack of turbidity corresponded to either very low bacterial growth or complete inhibition.

4.1.1. The effect of by-products, silver ions and silver nanoparticles on the growth of *B. cereus*

Figure 4.1 shows the effect of by-products, silver ions and silver nanoparticles (0 mg/L – 70 mg/L) on the growth of *B. cereus* after 24 h incubation.

Figure 4.1: The effect of by-products, silver ions and silver nanoparticles on the growth of *B. cereus*.
B. cereus was cultured with or without different concentrations (0-70 mg/L) of by-products, silver ions (Ag$^+$), or silver nanoparticles (AgNPs) colloidal suspension for 24 h.

Table 4.1 presents the actual effect of AgNPs by deducting the percentage bacterial growth inhibition as a result of by-products from the percentage bacterial growth inhibition post treatment with AgNPs colloidal suspension.

Table 4.1: The effect of AgNPs on *B. cereus*.

[Ag] mg/L	Inhibitory effect of By-products (%)	Inhibitory effect of Colloidal suspension (%)	Inhibitory effect of AgNPs (%)
0	0	0	0
10	10	12.5	2.5
20	0	0	0
30	0	0	0
40	16.13	18.75	2.62
50	12.9	0	0
60	3.23	0	0
70	17.42	0	0

Figure 4.1 showed that by-products, silver ions and silver nanoparticles colloidal suspension have no inhibitory effect on the growth of *B. cereus.* Table 4.1 shows a dose independent inhibition following treatment with by-products (in 50, 60 and 70 mg/L AgNPs colloidal suspension inhibited the growth of *B. cereus* by 12.9, 3.23 and 17.42 % respectively) which is not evident in the treatment with AgNPs colloidal suspension, suggesting batch to batch variation.

4.1.2. The effect of by-products, silver ions and silver nanoparticles on the growth of *C. metallidurans*

Figure 4.2 shows the effect of by-products, silver ions and silver nanoparticles (0 mg/L – 70 mg/L) on the growth of *C. metallidurans* after 24 h incubation.

Figure 4.2: The effect of by-products, silver ions and silver nanoparticles on the growth of *C. metallidurans.*
C. metallidurans was cultured with or without different concentrations (0-70 mg/L) of by-products, silver ions (Ag^{+}), or silver nanoparticles (AgNPs) in suspension for 24 h.

Table 4.2 presents the actual effect of AgNPs by deducting the percentage bacteria growth inhibition as a result of by-products from the percentage bacterial growth inhibition post treatment with AgNPs colloidal suspension.

Table 4. 2: The effect of AgNPs on *C. metallidurans.*

[Ag] mg/L	Inhibitory effect of By-products (%)	Inhibitory effect of Colloidal suspension (%)	Inhibitory effect of AgNPs (%)
0	0	0	0
10	20	50	30
20	25	70	45
30	30	75	45
40	32	80	48
50	35	100	65
60	40	100	60
70	42	100	58

C. metallidurans showed a dose dependent growth inhibition following treatment with by-product. The by-product in 10, 20, 30, 40, 50, 60 and 70 mg/L AgNPs suspension reduced the growth of *C. metallidurans* by 20, 25, 30, 32, 35, 40 and 42 % respectively. Although the bacterium was sensitive to the by-products, more inhibition was evident when treating with AgNPs colloidal suspension. *C. metallidurans* growth inhibition in the presence of silver nanoparticles also showed a dose dependent pattern. Ten milligram per litre AgNPs reduced 50 % of *C. metallidurans* within 24 h incubation. The bacterial growth gradually decreased by 75, 85 and 90 % when the bacterium was exposed to 20, 30 and 40 mg/L AgNPs colloidal suspension respectively. *C. metallidurans* was completely eradicated by 50 mg/L AgNPs in suspension which was then determined to be the MIC [Figure 4.2]. AgNPs in the absence of by-products also showed a dose dependent inhibitory effect on *C. metallidurans* [Table 4.2]. Silver nanoparticles inhibited *C. metallidurans* in a manner where 10, 20, 30, 40, and 50 mg/L AgNPs reduced 30, 45, 45, 48, and 65 % of the bacteria after 24 h incubation [Table 4.2]. *C. metallidurans* was completely inhibited by low concentration of silver ions (10 mg/L).

4.1.3. The effect of by-products, silver ions and silver nanoparticles on the growth of *E. coli*

Figure 4.3 shows the effect of by-products, silver ions and silver nanoparticles colloidal suspension (0 mg/L – 70 mg/L) on the growth of *E. coli* after 24 h incubation.
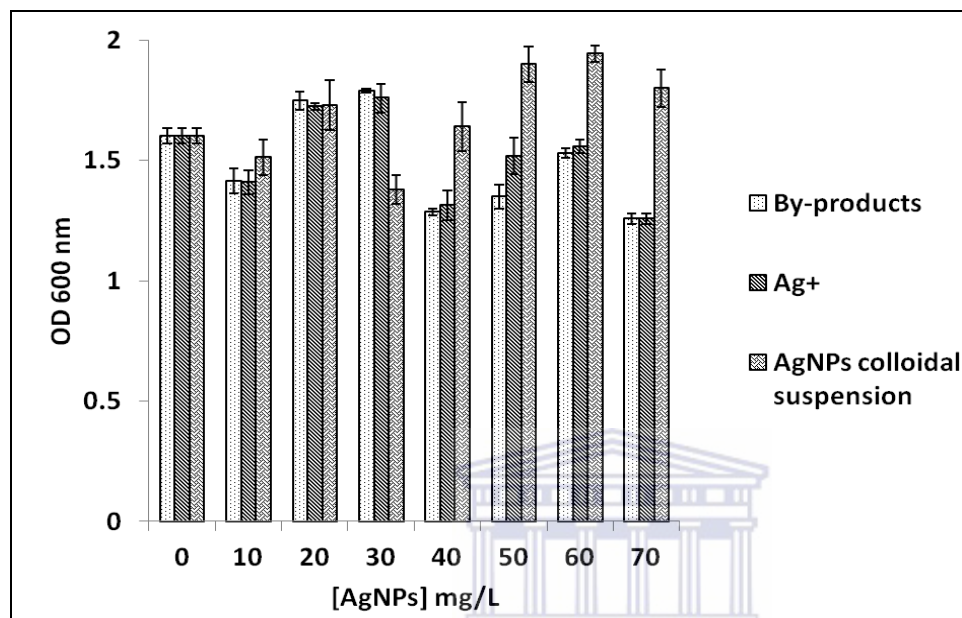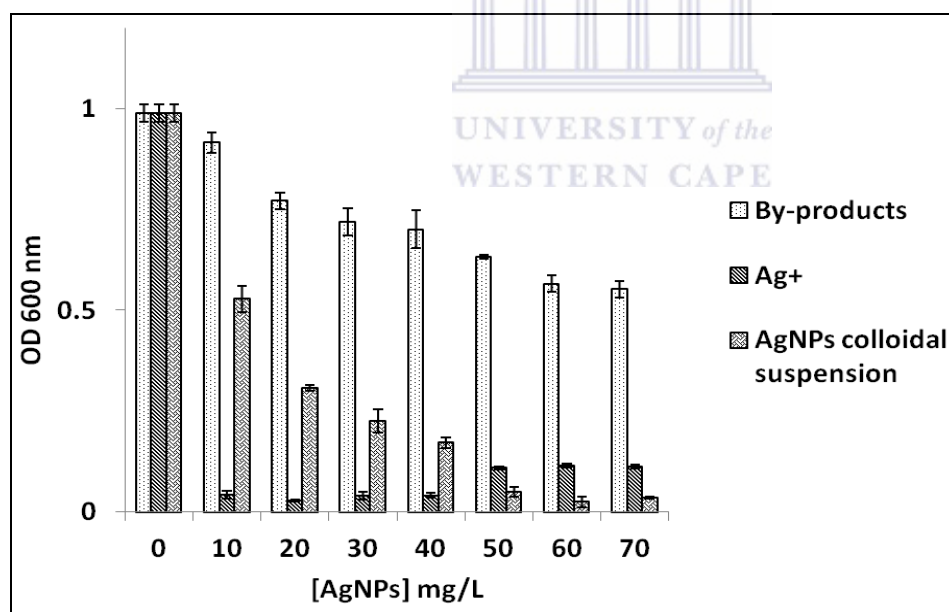

Figure 4.3: The effect of by-products, silver ions and silver nanoparticles on the growth of *E. coli*. *E. coli* was cultured with or without different concentrations (0-70 mg/L) of by-products, silver ions (Ag^{+}), or silver nanoparticles (AgNPs) in suspension for 24 h.

Table 4.3 presents the actual effect of AgNPs on *E. coli*, by deducting the percentage bacteria growth inhibition due to by-products from the percentage bacterial growth inhibition post treatment with AgNPs colloidal suspension.

Table 4.3: The effect of AgNPs on *E. coli*.

[Ag] mg/L	Inhibitory effect of By-products (%)	Inhibitory effect of Colloidal suspension (%)	Inhibitory effect of AgNPs (%)
0	0	0	0
10	11.76	29.41	17.65
20	17.64	100	82.36
30	18	100	82
40	20.59	100	79.41
50	38.24	100	61.76
60	46.7	100	53.3
70	50	100	50

The treatment with by-product solution inhibited *E. coli* growth in a dose dependent manner. The by-products in 10, 20, 30, 40, 50, 60 and 70 mg/L AgNPs suspension reduced the growth of *E. coli* by 11.76, 17.64, 18, 20.59, 38.24, 46.7 and 50 % respectively. Nevertheless the bacterium was more sensitive to AgNPs colloidal suspension, meaning that the silver nanoparticles had an adverse effect on *E. coli*. Ten-milligram AgNPs in suspension was successful in inhibiting 29.41 % of the bacteria and the increase of concentration to 20 mg/L resulted in complete inhibition of *E. coli* growth. The MIC of 20 mg/L AgNPs colloidal suspension was mostly a result of AgNPs (82.36 %) since the by-product could only account for 17.64 % growth inhibition [Table 4.3]. Low concentrations of silver ions (10 mg/L) inhibited the growth of *E. coli* completely.

4.1.4. The effect of by-products, silver ions and silver nanoparticles on the growth of *M. smegmatis*

Figure 4.4 shows the effect of by-products, silver ions and silver nanoparticles (0 mg/L – 70 mg/L) upon the growth of *M. smegmatis* after 24 h incubation.

Figure 4.4: The effect of by-products, silver ions and silver nanoparticles on the growth of *M. smegmatis*. *M. smegmatis* was cultured with or without different concentrations (0-70 mg/L) of by-products, silver ions (Ag⁺), or silver nanoparticles (AgNPs) in suspension for 24 h.

Table 4.4 shows the actual effect of AgNPs on the growth of *M. smegmatis,* by deducting the percentage bacteria growth inhibition due to by-products from the percentage bacterial growth inhibition post treatment with AgNPs in suspension.

Table 4.4: The effect of AgNPs on *M. smegmatis.*

[Ag] mg/L	Inhibitory effect of By-products (%)	Inhibitory effect of Colloidal suspension (%)	Inhibitory effect of AgNPs (%)
0	0	0	0
10	0	26.92	26.92
20	10.71	32.69	21.98
30	7.15	42.31	35.16
40	8.57	53.85	45.28
50	14.29	51.92	37.63
60	21.43	53	31.57
70	7	50.5	43.5

By-products showed no significant inhibitory effect on the growth of *M. smegmatis* with respect to the untreated cells (0 mg/L). Table 4.4 shows that *M. smegmatis* has a dose independent sensitivity to the by-products. On the other hand, AgNPs showed a dose dependent inhibition of 26.92, 21.98, 35.16, 45.28, 37.63, 31.57 and 43.5 % bacterial growth when treated with 10, 20, 30, 40, 50, 60 and 70 mg/L AgNPs respectively. Silver ions were successful in maintaining the growth of *M. smegmatis* at low cell numbers, at OD=0.08-0.1, this poses a risk of the bacteria resisting the silver, recuperating and multiplying.

4.1.5. The effect of silver nanoparticles, by-products and silver ions on *S. epidermidis*

Figure 4.5 shows the effect of silver nanoparticles, by-products and silver ions (0 mg/L – 70 mg/L) in the growth of *S. epidermidis* after 24 h incubations.
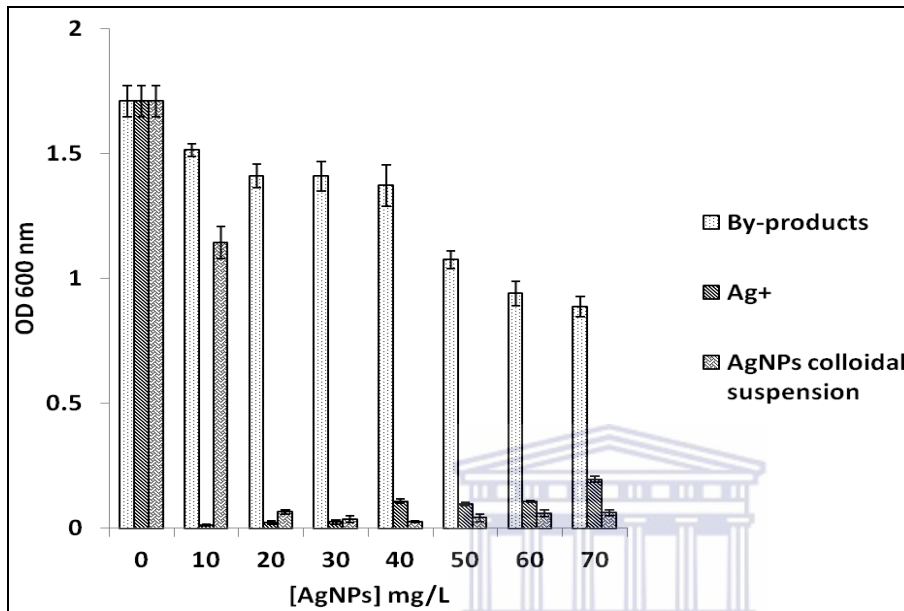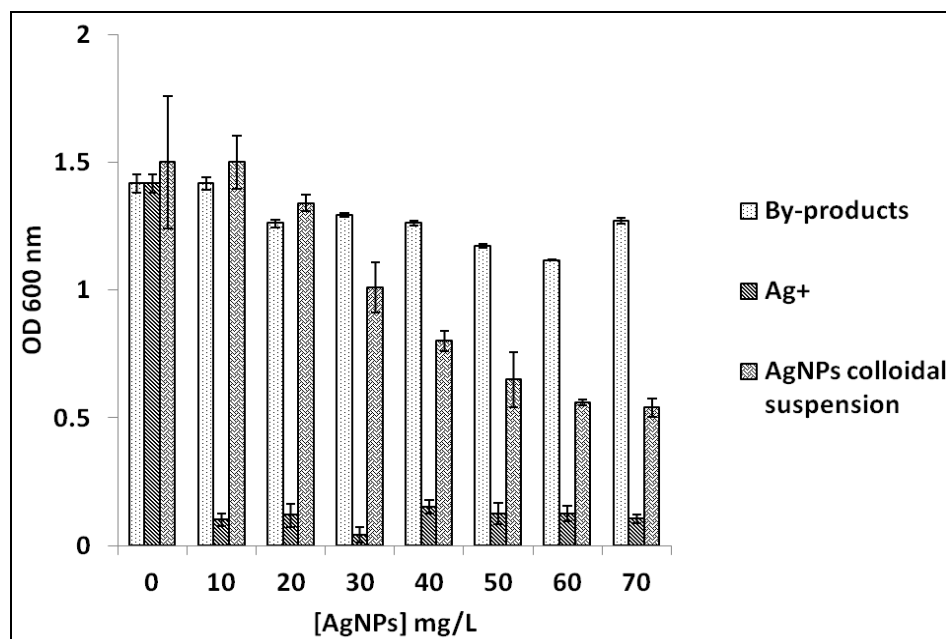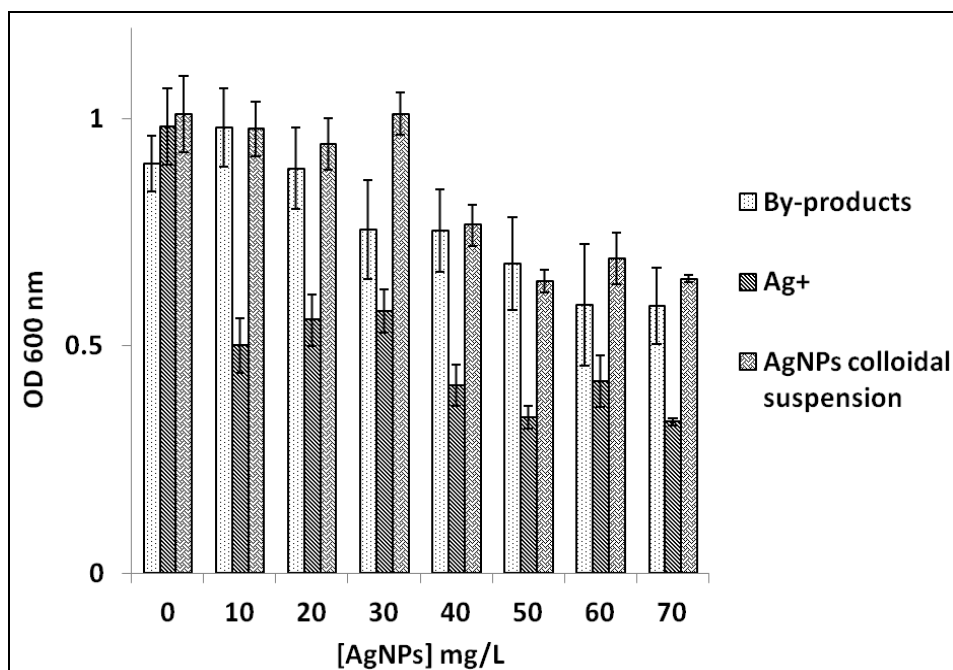
Figure 4.5: The effect of by-products, silver ions and silver nanoparticles on the growth of *S. epidermidis*.
S. epidermidis was cultured with or without different concentrations (0-70 mg/L) of by-products, silver ions (Ag$^+$), or silver nanoparticles (AgNPs) in suspension for 24 h.

Table 4.5 presents the actual effect of AgNPs on the growth of *S. epidermidis*, by deducting the percentage bacteria growth inhibition due to by-products from the percentage bacterial growth inhibition post treatment with AgNPs in suspension.

Table 4.5: The effect of AgNPs on *S. epidermidis*.

[Ag] mg/L	Inhibitory effect of By-products (%)	Inhibitory effect of Colloidal suspension (%)	Inhibitory effect of AgNPs (%)
0	0	0	0
10	0	0	0
20	0	0	0
30	24	0	0
40	24	25	1
50	27	26	0
60	28	25	0
70	27	26	0

S. epidemidis showed a dose dependent sensitivity to the by-product. Table 4.5 illustrated that AgNPs had not inhibitory effect rather the inhibition presented in Figure 4.1 results from the by-products in the colloidal suspension. However, *S. epidermidis* was sensitive to silver ions.

Ten milligram per litre of silver ions reduced 50 % of *S. epidermidis* after 24 h incubation. The increase of Ag^+ concentration from 30 to 70 mg/L inhibited only 55 % of the bacterial growth.

4.2. Growth retardation patterns of bacteria treated with silver nanoparticles

Bacterial growth is a measure of increase in cell mass resulting from cell replication or increase in cell size. The bacteria grows in sigmoidal shape (growth curve) with a lag phase (bacteria adapts to new environment, minimal cell division, maximum metabolism, synthesis of RNA, proteins and other metabolites), log phase (exponential cell division), stationary phase (depletion of nutrients and accumulation of wastes products cell growth rate equals death rate) and death phase (Lodish *et al*., 2000; Staropoli & Alon, 2000; Al-Qadiri *et al*., 2008). As such bacterial growth inhibition at one of these phases following treatment with AgNPs denotes the mode of action of the nanoparticles.

As shown above *B. cereus* and *S. epidermidis* were resistant to AgNPs treatment, whilst *M. smegmatis* showed sensitivity to AgNPs although the MIC was not established. On the contrary *E. coli* and *C. metallidurans* showed sensitivity to AgNPs and the MICs were established at 20 mg/L and 50 mg/L AgNPs in colloidal suspension respectively. The antibacterial effect of AgNPs was further characterised on *E. coli* and *C. metallidurans* as described in section 2.5.2.3. Figure 4.6 shows the growth patterns of *C. metallidurans* and *E. coli,* untreated and treated with AgNPs.
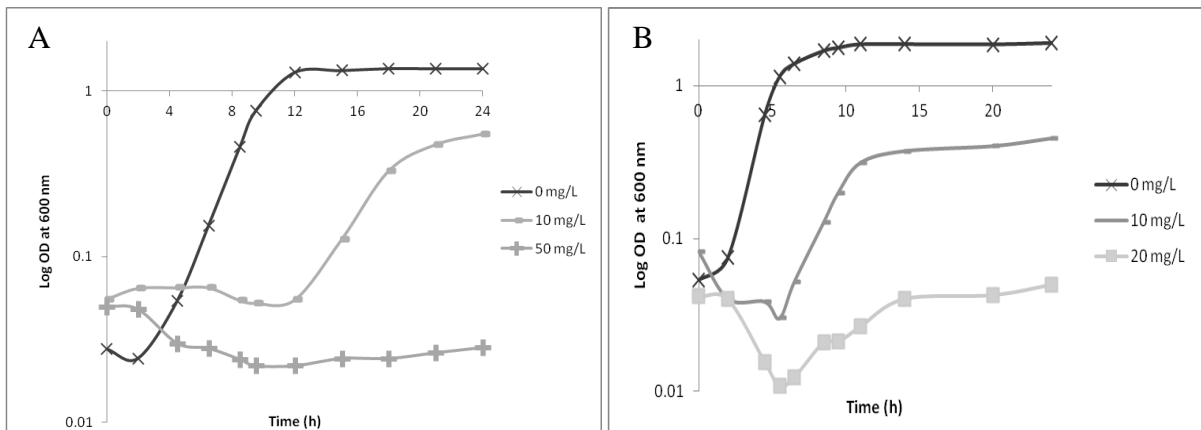
Figure 4.6: Effect of AgNPs on the growth *C. metallidurans and E. coli.*
A) *C. metallidurans* was treated with 0, 10 and 50 mg/L AgNPs and grown at 37 °C in casamino acid- peptone glucose media. B) *E. coli* was treated with 0, 10 and 20 mg/L AgNPs and grown at 37 °C in Lubria broth.

Table 4.6 shows the bacterial growth rates of *E. coli* and *C. metallidurans* following inoculation with AgNPs.

Table 4.6: The bacterial growth rate following exposure to AgNPs.

[AgNPs] (mg/L)	0	10	20	30	40	50
Growth rate of *C. metallidurans* (h)	1.5	6	10	14	16	MIC
Growth rate of *E. coli* (h)	1	3	MIC			

The untreated *C. metallidurans* cells had a short lag phase of 4 h and a log phase that lasted 8 h (with cells multiplying every 1.5 hours) prior to the stationary phase at approximately 12 h of incubation. The treatment with 10 mg/L AgNPs reduced the growth of *C. metallidurans* by up to 50 %. The cells treated with 10 mg/L AgNPs had a prolonged lag phase (from 4 h of untreated compare to 12 h when cells were treated with 10 mg/L AgNPs). The untreated cells had a growth rate of 1.5 h and treating with 10 mg/L AgNPs slowed the doubling time to 6 h. Gradually increasing the concentration of AgNPs by 10 mg/L consistently slowed the growth rate of *C. metallidurans* by ±4 h. Treatment with 50 mg/L AgNPs completely inhibited growth, confirming this to be the MIC.

The untreated *E. coli* cells had a lag phase that lasted 1.5 h while the log phase lasted for 5 h prior to the commencement of the stationary phase after 6 h of incubation. The cells treated with 10 mg/L AgNPs prolonged the lag phase to 8 h compared to the lag phase of the

untreated cells (1.5 h). The lag phase of the *E. coli* cells treated with AgNPs showed a sharp decline in bacterial density (absorbance) which denoted immediate cidal effects. The untreated cells had a growth rate of 1 h whereas the growth rate of cells treated with 10 mg/L AgNPs was 3 h [Table 4.6]. The treatment with 10 mg/L AgNPs reduced the growth of *E. coli* by up to 50 %. The cells that were treated with 20 mg/L AgNPs were completely eradicated proving this concentration to be the MIC.

4.3. TEM characterisation of the morphological alterations caused by silver nanoparticles on *E. coli*

Silver nanoparticles (6±1.8 nm) stabilised with PVP were freshly prepared as detailed in section 2.2.2. *E. coli* was allowed to grow until mid log phase (OD = 0.4) and subsequently the bacterial culture was treated with 20 mg/L AgNPs and allowed to grow for 1 h prior to harvesting for TEM analysis as described in section 2.6. Figure 4.7 shows the transmission electron micrographs of *E. coli* cells grown in LB media at 37 ^{o}C then treated at mid log phase (OD = 0.4) with 20 mg/L AgNPs and then harvested an hour later.
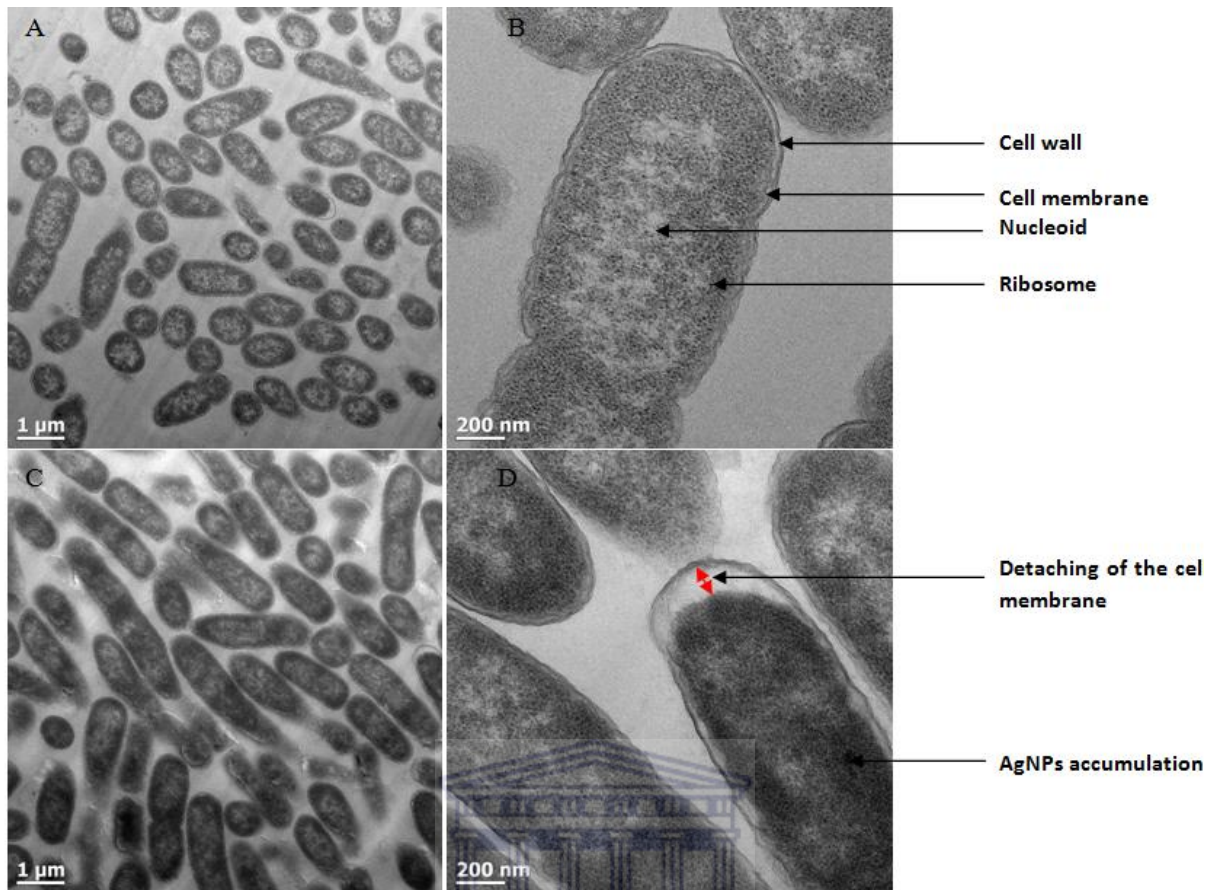
Figure 4.7: Transmission electron micrographs of *E. coli.*
A) *E. coli* grown in LB media and harvested at mid log phase (OD = 0.4). B) A healthy (untreated) *E. coli* cell at log phase. C) *E. coli* grown in LB media then treated with 20 mg/L AgNPs at mid log phase and harvested after an hour. D) *E. coli* distorted by AgNPs.
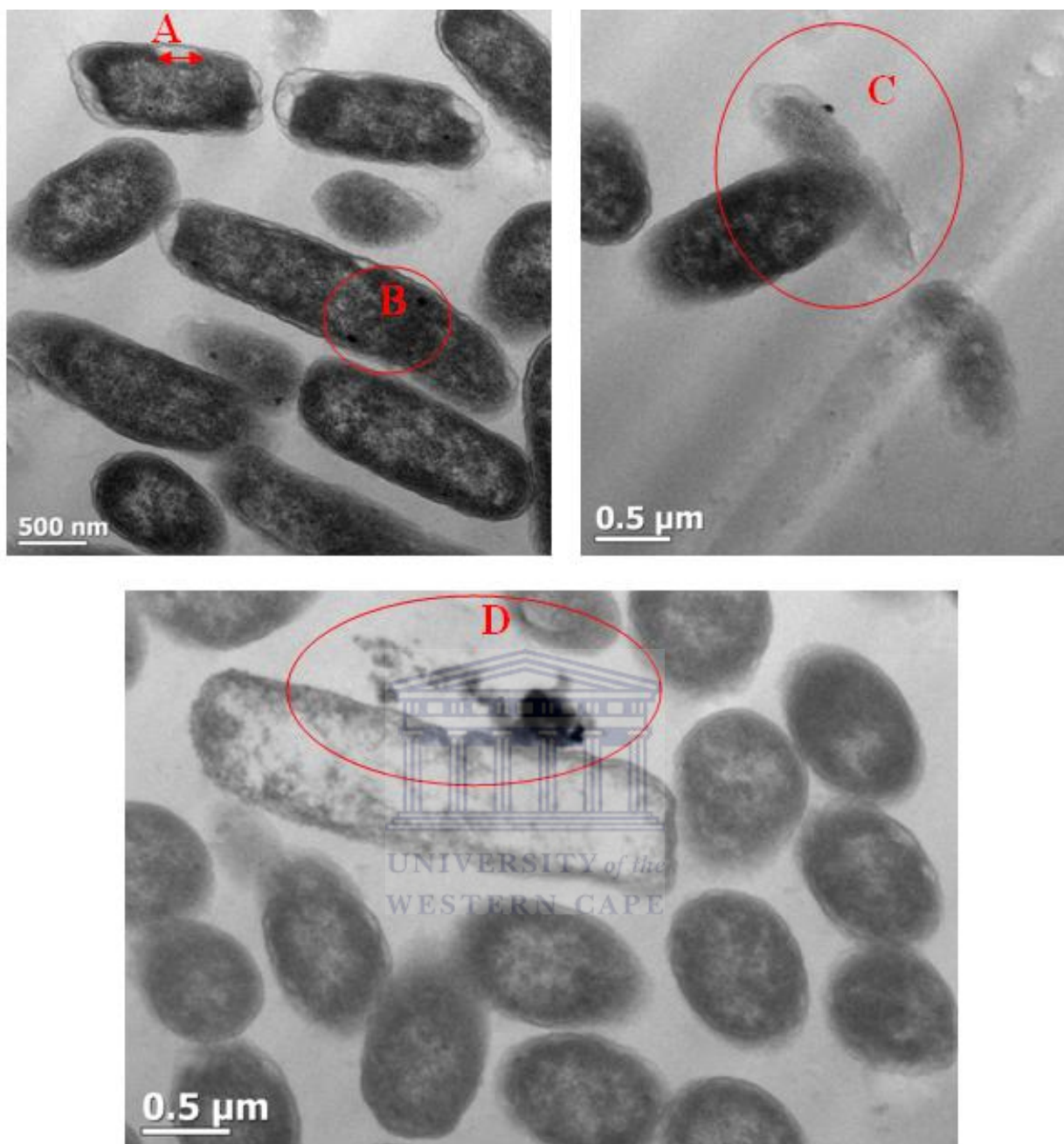
Figure 4.8: Transmission electron micrographs of *E. coli* treated with 20 mg/L AgNPs.
A) Detaching of the cytoplasmic membrane from the cell wall. B) Accumulation of AgNPs within the bacterial cell. C) Cell leakage. D) Cell leakage.

The black spots within the cells [Figure 4.8 (B)] were analysed using localised EDS coupled to TEM, as described in section 2.4.3. Figure 4.9 shows the EDS spectra of the black spot within the *E. coli* cells following treatment with 20 mg/L AgNPs.
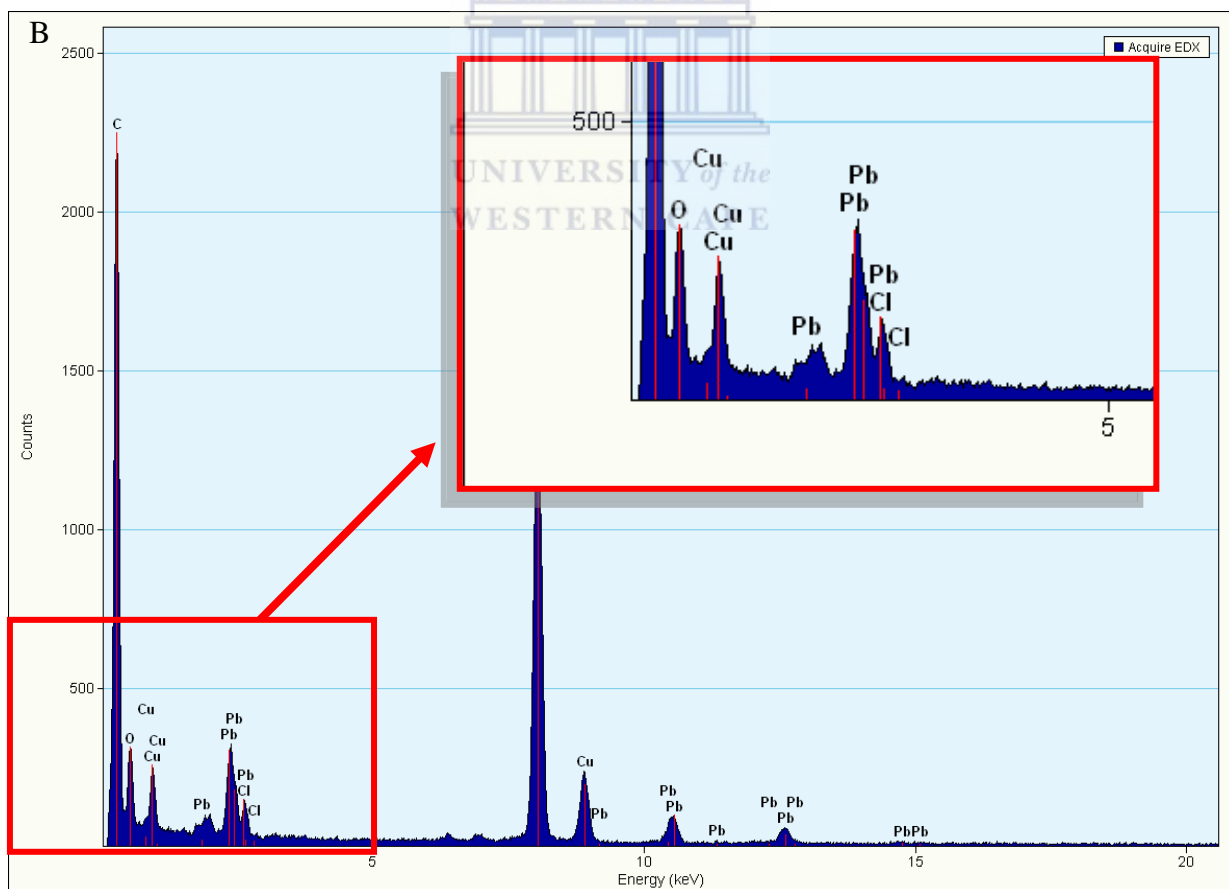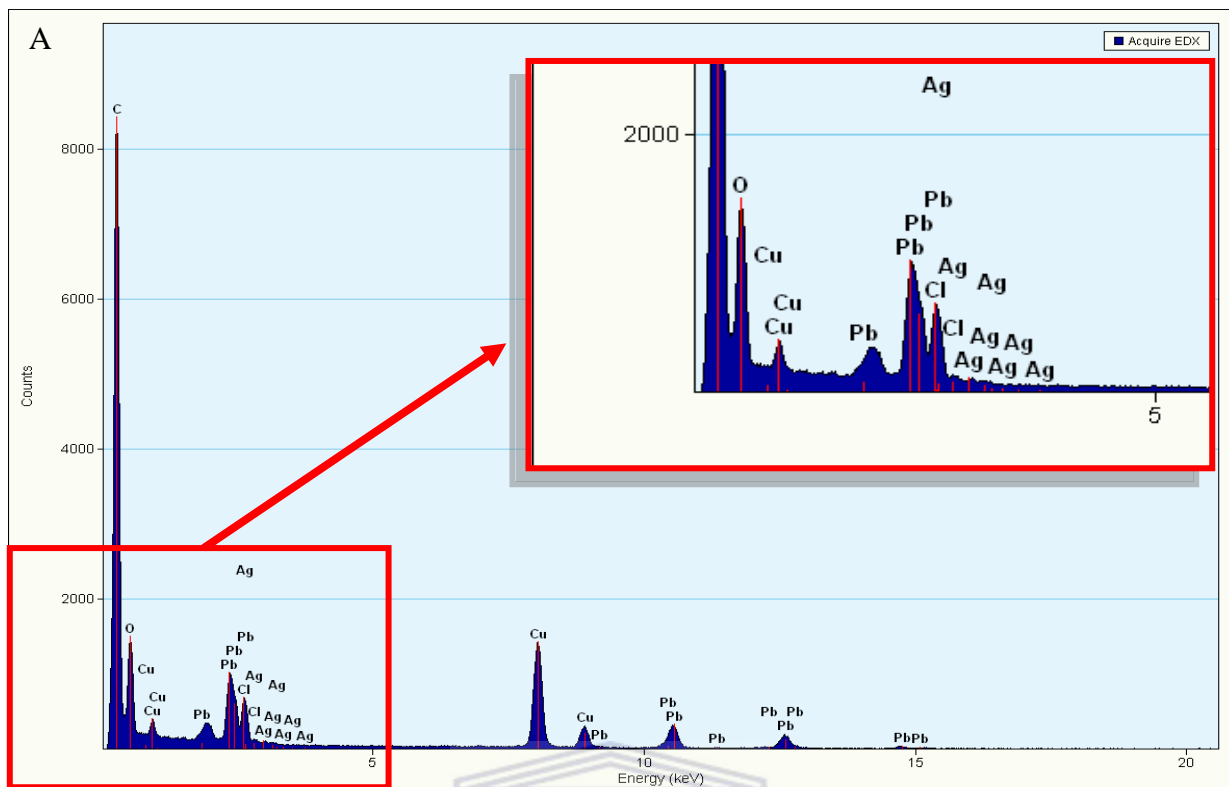
Figure 4.9: The localised EDS spectra *E. coli.*
A) EDS spectrum of the dark spots accumulating inside the *E. coli* cell. B) EDS spectrum taken at a region away from the dark spots accumulating inside the *E. coli* cell.

The cells treated with AgNPs showed distorted morphology such as: cytoplasm membrane detachment from the cell wall (depicting cell shrinkage) [Figure 4.7 D] and elongated cells with septa containing a layer of un-split peptidoglycan (depicting impairment cell division) [Figure 4.7 C compared to Figure 4.7 A]. Figure 4.8 presented cell compartments of untreated cells such as the cell membrane, cell wall, ribosome, nucleoid as intact, whereas the cells treated with 20 mg/L AgNPs resulted in cell shrinkage with the cell membrane detached from the cell wall.. Figure 4.8 C & D showed leakage *E. coli* cellular components following the treatment with AgNPs. The EDS analysis of the dark spots (45±11 nm AgNPs) within *E coli* cells [Figure 4.8 B] proved that nanoparticles accumulated the cells. Figure 4.9 showed EDS spectra that presented with carbon (C) and oxygen (O) which are components of the cell. The cells were stained by lead citrate ($Pb_3(C_6H_5O_7)_2$), hence the presence of lead is abundant. There is a distinct peak of copper (Cu) since the analysis was carried out on a copper grid. The EDS localised to the dark spots [Figure 4.9 (A)] presented with silver X-rays around 3.4 KeV which were absent in Figure 4.9 (B). The X-rays however were not enough to produce a distinct peak because they were surpassed by the other elements present in high quantities.

4.4. Discussion

Previous studies have reported that smaller AgNPs demonstrated stronger antibacterial effects, than bigger particles and mostly surpass silver ions (Morones *et al*., 2005; Choi & Hu, 2008). However, in the current study silver ions were more toxic than the silver nanoparticles synthesised. The MIC as a result of silver ions was established to be 10 mg/L Ag^+ for *C. metallidurans, E. coli* and *M. smegmatis* whereas MIC as a result of silver nanoparticles was 50 mg/L and 20 mg/L AgNPs for *C. metallidurans* and *E. coli* respectively. *M. smegmatis showed sensitivity to the AgNPs however a small population of the bacteria survived* this poses a risk of the bacteria resisting the silver, recuperating and multiplying.

The bacterial strain that showed sensitivity to silver ions also responded to the treatment with AgNPs, supporting literature which states that the mode of action of AgNPs involves, but is not limited to, Ag^+ mode of action (Morones *et al*., 2005; Šileikaite *et al*., 2006). The low toxicity resulting from the treatment with AgNPs compared to the treatment with silver ions could be because of the delay caused by leaching of Ag^+ from AgNPs (oxidation of AgNPs from zero valent silver to silver ions) therefore delaying the Ag^+ mediated mode of action.

The current study is in accordance with literature that gram positive bacteria (*B. cereus* and *S. epidermidis*) or those with an acid fast cell wall (*M. smegmatis*) were resistant to the AgNPs, compared to gram negative bacteria (*E. coli* and *C. metallidurans*) (Morones *et al*., 2005; Cho *et al*., 2005; Kim *et al*., 2007). The complexity of the cell wall aided in the resistance of the bacteria to the by-products, silver nanoparticles and silver ions. The peptidoglycan layer of gram positive bacteria is thicker than that of gram negative bacteria, therefore offering more protection to the cell (Jung *et al*., 2008). *M. smegmatis* resistance of these conditions may result from the acid fast bacterial cell wall.

In contrast, Ruparelia *et al*., (2008) demonstrated that some gram negative bacterial strains (*E. coli* MTCC 739 and MTCC 1687) were much more resistant than gram positive bacteria (*S. aureus*). Therefore it cannot be concluded that the bactericidal effect of nanoparticles is solely dependent on the structure of the bacterial cell wall. In addition, the ability of *B. cereus* to resist silver was explained by Mullen *et al.,* (1989), where *B. cereus* was grown in the presence of 1 mM $AgNO_3$. It was discovered that some *B. cereus* strains are involved in bioremediation and detoxification of silver. The strains reduced 89 % of silver ions to uncharged silver and produced colloidal aggregates that accumulated on the cell surface and occasionally in the cytoplasm (Mullen *et al*., 1989; Ganesh Badu *et al*., 2009). Other *Bacillus* species have also been reported to produce precipitated silver aggregates (nanoparticles) such as *B. licheniformis* (Beveridge *et al*., 1982; Kalishwaralal *et al*., 2008), *B. cereus* PGN1

(Ganesh Babu *et al*., 2009), *B. subtilis* (Beveridge *et al*., 1980) but the mechanism of this reaction is not yet clear. These findings predict that the *B. cereus* strain used in this study is highly resistant, thus rendering AgNPs as an antimicrobial agent inefficient.

S. epidermidis was sensitive to the Ag^+ but the MIC could not be established. Cho *et al*., (2005) reported that the mode of action of Ag^+ involves attachment of Ag^+ to the surface of the bacteria and interaction with the bacterial proteins. The steady bacterial growth, irrespective of the increase in concentration, could mean that the binding or interaction sites of silver on *S. epidermidis* cells were saturated by concentrations as low as 10 mg/L Ag^+ so the increase in concentrations to 70 mg/L Ag^+ did not have an acumulative effect.

Even though there has not been reported resistance incidences in environments where silver is routinely used; such as, burns units in hospitals, silver-coated catheters and dental setting (amalgams contain 35% silver), the resistance shown by *B. cereus* and *S. epidermidis* poses the possibility of the emergence of resistant strains.

The bacterial growth curves revealed a prolonged lag phase on the growth of *E. coli* and *C. metallidurans* following treatment with AgNPs which was consistent with the results published in Ruparelia *et al.,* (2008), where they observed a longer lag phase following treatment of bacteria with AgNPs. They elaborated that a longer lag phase marked the inhibition of cell metabolism, RNA and protein synthesis (Ruparelia *et al*., 2008).

The TEM images showed cell shrinkage and leakage of cellular components. Following the attachment of the nanoparticles, Gade *et al*., (2008) also observed disruption of the bacterial membrane causing leakage and ultimately cell death. Feng *et al*., (2000) also examined the morphological damaged in *E. coli* cell treated with silver species, using electron microscopy (TEM and SEM) and X-ray microanalyses. They reported similar morphological changes such as cytoplasm membrane detachment from the cell wall and impairment of DNA replication. The cellular leakage in Figure 4.8 C & D were similar to the ones determined in

literature to be condensed deoxyribonucleic acid (DNA) molecules that protect nucleic acid from silver ion mediated damage (Feng *et al*., 2000). Jung *et al*., (2008) treated the cells with silver ions and reported similar cell morphological changes. These bacterial cells remained active but in a non-culturable state and eventually died.

The TEM images also showed elongated cells, depicting similar outcomes as shown in a study by Uehara *et al.,* (2009), who found that an *E. coli* mutant that did not express LytM (lysostaphin)-domain containing factors would prepare for cell division but form long cell chains with septa containing a layer of un-split peptidoglycan. This led to the assumption that AgNPs mode of action involved cell division suppression.

The TEM images and EDS analysis showed that *E. coli* cells accumulated the nanoparticles forming 45±11 nm AgNPs agglomerates, whereas the nanoparticles incubated in growth media in the absence of bacteria for 24 h (in rotary shaker) did not change shape or size. This is in line with a study by Ruparelia *et al.,* (2008) which concluded that salts and nutrients did not cause particle agglomeration, rather they facilitated the release of Ag^+ into the media. Therefore the AgNPs interact with the bacterium which interferes with the stabilising agent later resulting in particle agglomeration. Feng *et al*., (2000) also observed electron-dense granules (identified to contain silver and sulfur) that were surrounding the cell wall and some deposited inside the cells, such as the ones identified in the current study using EDS as silver nanoparticles [Figure 4.9]. The AgNPs accumulated in the cytoplasm and in the vicinity of the cell membrane. Morones *et al*., (2005), Gade *et al*., (2008) and Raffin *et al*., (2008) also discovered a size dependent particle penetration and the localization of particles in the ribosome and nucleoid region, which estimates AgNP's mode of action with cellular metabolism and replication impairment.

Nanda *et al*., 2009 reported that Methicillin resistant *Staphylococcus aureus* (MRSA), Methicillin resistant *Staphylococcus epidermidis* (MRSE) and *Streptococcus pyogenes* were

sensitive to silver nanoparticles. The current study also showed that *E. coli* 1699 which is resistant to a wide range of antibiotics showed sensitivity towards AgNPs.

Literature supports that particles with sizes between 1-10 nm have a greater antibacterial activity since they have a larger surface to volume ratio (Baker *et al*., 2005; Panacek *et al*., 2006; Mohan *et al*., 2007; Choi *et al*., 2008). The current study contradicts this statement as the MIC as a result of 6±1.8 nm AgNPs was higher than that which was reported in a study by Kim *et al*., (2007) who used 13.5 ± 2.6 nm (3 nmol L^{-1}) AgNPs to completely inhibit the growth of *E. coli*. However, some studies define MIC as the concentration of the antibacterial agent that has the ability to inhibit the growth of bacteria and the minimum bactericidal concentration (MBC) as the concentration of the antimicrobial agent that can inhibit 99.9 % of bacterial growth. Studies conducted on agar plates have generally had a higher MIC than liquid cultures (Morones *et al*., 2005). AgNPs are highly unstable and this instability increases with a decrease in size, hence different synthesis methods produce nanoparticles with or without an oxide and the layer of stabilising agent. Literature showed that these outer layers can interfere with the antibacterial efficacy. Ruparelia *et al*., (2008) revealed that nanoparticles with an oxide layer produce more ions and have a greater cidal effect compared to nanoparticles without the oxide layer. Cho *et al*., (2005) reported that PVP coated AgNPs were more toxic than those coated with sodium dodecyl sulfate (SDS), even though SDS produces a more stable suspension and concluded that stabilising agents have a tendency to interfere with Ag^{+} release or attachment to the bacterial surface. Irwin *et al*., (2010) investigated the effect of stabilising agents on the efficacy of silver nanoparticles as an antimicrobial agent and came to the conclusion that the PVP layer disrupts the nanoparticle-bacteria interaction therefore decreasing the antimicrobial efficacy. Cho *et al*., 2005 investigated the effect of 8–15 nm AgNPs on *E. coli* and found that SDS-stabilised AgNPs did not have antibacterial effects whereas 100 ppm AgNPs coated with PVP eradicated both

gram positive and gram negative bacteria within 4 hours. The chemical studies showed that SDS had better stabilizing properties compared to PVP, and the chemically stable AgNPs showed no antibacterial activity (Cho *et al*., 2005).

The effect of the by-product enhanced the effect of the AgNPs, since the bacterial strains that were sensitive to the by-product also showed sensitivity to AgNPs in suspension. Half of *C. metallidurans* and *E. coli* population was eradicated by 10 mg/L AgNPs in suspension and the impurities in the 10 mg/L AgNPs suspension accounted for 30 % and 11 % of the growth inhibition of *C. metallidurans* and *E. coli* respectively. *B. cereus* displayed resistance to the treatments with by-products as well as AgNPs. In contrast, Kim *et al*., (2007) conducted a similar study with AgNPs synthesised with sodium borohydride and tested their effect on *E. coli* and *S. aureus*. They designed their control by agglomerating the AgNPs by vigorous stirring and they concluded that the by-products of the AgNPs synthesis did not have significant cidal effect on both strains. The chemical synthesis of metallic nanoparticles can produce stable particles of controlled size and distribution although the purity is compromised by the by-products of the synthesis. Hence, it is necessary to find an absorbent such as zeolites to purify the colloidal suspensions of contaminants. Zeolites have the ability to bind ions and are microparticles in nature which could allow for the purification of nanoparticles by size (Galeano *et al*., 2003).

Chapter 5

Conclusions and Future Prospects

5.1.   The conclusion drawn from the present investigations are as follows:

The present study synthesised small, stable and uniformly dispersed silver nanoparticles. AgNPs were synthesized successfully by chemical reduction of silver nitrate using ascorbic acid and sodium borohydride as reducing agents. The formation of AgNPs was confirmed by UV-vis spectroscopy and TEM coupled with EDS. The average particle size was found to be 15.4 ± 11.15 nm and 6 ± 1.8 nm, for ascorbic acid and sodium borohydride synthesises respectively. Varying the amount of reducing agent had not significant effect on the particle size; however it improved the particle size distribution in the sodium borohydride synthesis. The present study found that small AgNPs were highly unstable and agglomerated within 24 hours if not stabilised, however the addition of stabilising agent caused a slight increase in particle size. Citric acid stabilised the AgNPs synthesised through ascorbic acid oxidation whereas PVP favoured the stability of AgNPs synthesised through sodium borohydride oxidation. Increasing pH showed a significant increase in particle size and narrowed the particle size distribution. Light was the only parameter that changed the shape of the AgNPs. The optimum processing conditions that produced 6 ± 1.8 nm spherical nanoparticles included maintaining the temperature at 0 ᵒC, the pH at 9.78 and the $NaBH_4/Ag/PVP$ ratio at 16:1:10.

Then the antibacterial efficiency of the AgNPs was investigated on *Cupriavidus metallidurans, Staphylococcus epidermidis, Mycobacterium smegmatis, Bacillus cereus and* a multi-drug resistant *Escherichia coli* 1699. Gram-positive (*B. cereus* and *S. epidermidis*) and acid fast bacteria (*M. smegmatis*) showed resistance or tolerance toward the AgNPs compared

to a Gram-negative bacterium (*E. coli* and *C. metallidurans*). *B. cereus* was completely resistant whereas *M. smegmatis* and *S. epidermidis* tolerated the AgNPs. The MIC for *E. coli* and *C. metallidurans* was established to be 20 mg/L and 50 mg/L respectively. When the result was compared with the effect of silver ions on all bacterial strains, nanoparticles were found to be less toxic. This contradicted the literature which states that nanoparticles are more toxic than silver ions (Morones *et al*., 2005); but it is also established that stabilizing agents compromised the antibacterial efficacy of the nanoparticles. The TEM coupled with EDS showed accumulation of AgNPs inside the *E. coli* cells grown in presence of AgNPs. However, the mode of binding and entry could not be established. The AgNPs treated cells presented with cell shrinking, cell leakage and retarded cell division.

Although there has not been any reported clinical incidence of silver resistance, following increased number of silver-based products in the environment and the large number of bacterial strains that are not sensitive to silver nanoparticles resistance can emerge. The WHO requires an antimicrobial agent to inhibit a wide range of microorganisms at concentrations that will not be harmful to the environment. Therefore implementation of chemically synthesised AgNPs-based water treatment methods would not be ecologically sound since this antimicrobial agent could not eradicate all microorganisms at the maximum concentration that a human body can take (100 mg/L).

5.2. The present study encountered the following limitations:

- Only a single set of stable (PVP), small, uniformly distributed and spherical AgNPs were used to investigate the antimicrobial properties of the AgNPs. A comparative study of the antimicrobial effect of unsterilized, large, different sized or shaped AgNPs would have drawn a substantial conclusion.

- As the antimicrobial activity of the AgNPs were performed on a few strains (*C. metallidurans, S. epidermidis, M. smegmatis, B. cereus* and *E. coli*) under similar conditions and at commencement of lag phase, the results might be different for other microorganisms under different conditions. However, the results obtained in this study can be used as a model for other microorganisms.

5.3. The present research work leaves the following future prospects:

- This study has provided the basis for investigating further the attractive features of AgNPs as antimicrobial, antibacterial, antiviral and antifungal agents.

- The mechanism of antimicrobial action presented in this work can be validated by performing flow cytometry and FTIR analysis. In addition the surface location of silver on the bacteria can be analyzed by HR-TEM or SEM a better understanding of the mode of antimicrobial activity of silver.

- More research needs to be done to improve specificity and selectivity of the nanoparticles in order to have a discriminative bacterial cidal effect; such as exploring AgNPs synthesis methods that do not produce by-products or find ways to purify the by-products that might be toxic to human beings and the environment.

- The nanoparticles couldn't be synthesised at high concentrations (1g/L) because they showed agglomeration even in the presence of a stabilising agent. So other forms of concentrating AgNPs such as ultra centrifuge should be explored.

Chapter 6

References

Al-Qadiri H.M., Al-Alami N.I., Lin M., Al-holly M., Cavinato A.G., Rasco B.A., 2008. Studying of the bacterial growth phases using Fourier transform infrared spectroscopy and multivariate analysis. *Journal of Rapid Methods and Automation in Microbiology*, *16*:73-89.

Apetroaie-Constantin C., Mikkola R., Andersson M.A., Teplova V., Suominen I., Johansson T., Salkinoja-Salonen M., 2008. *Bacillus subtilis* and *B. mojavensis* strains connected to food poisoning produce the heat stable toxin amylopsin. *Journal of Applied Microbiology*, 106:1976-1985.

Baker C., Pradhan A., Pakstis L., Pochan D.J., Shah S.I. 2005. Synthesis and antibacterial properties of silver nanoparticles. *Journal of Nanoscience and Nanotechnology*, 5:244-249.

Beri R.K., More P., Bharate B.G., Khanna P.K., 2010. Band-gap engineering of ZnSe quantum dots via a non-TOP green synthesis by use of organometallic selenium compound. *Current Applied Physics*, 10:553-556.

Beveridge T.J., Forsberg C.W., Doyle R.J., 1982. Major sites of metal binding in *Bacillus licheniformis* walls. *Journal of Bacteriology*, 150:1438-1448.

Beveridge T.J., Murray R.G.E. 1980. Sites of metal deposition in the cell wall of *Bacillus subtilis. Journal of Bacteriology*, 141:876-887.

Bielaszewska M., Mellmann A., Zhang W., Kock R., Fruth A., Bauwens A., Peter G., Karch H., 2011. Characterisation of the *Escherichia coli* strain associated with an outbreak of haemolytic uraemic syndrome in Germany, 2011: a microbiological study. *The Lancet Infectious Diseases*, 11:671-676.

Borm P.J., Kreyling W., 2004. Toxicological hazards of inhaled nanoparticles--potential implications for drug delivery. *Journal of Nanoscience and Nanotechnology*, 4:521-531.

Braydich-Stolle, L., Hussain, S., Schlage,r J.J., Hofmann M.C., 2005. In vitro cytotoxicity of nanoparticles in mammalian germline stem cells. *Toxicological Sciences*, 88:412-419.

Bruins M.R., Kapil S., Oehme F.W., 2000. Microbial resistance to metals in the environment. *Ecotoxicology and Environmental Safety*, 45:198-207.

Burch J., Thomas K., 1998. Water disinfection for developing countries and potential solar thermal pasteurization. *Solar Energy*, 64:87-97.

Burd A., Kwok C.H., Hung S.C., Chan H.S., Gu H., Lam W.K., Li H., 2007. A comparative study of the cytotoxicity of silver-based dressings in monolayer cell, tissue explant, and animal models. *Wound Repair Regeneration*, 15:94-104.

Chen B., Jiao X., Chen D., 2010. Size-controlled and size-designed synthesis of nano/submicrometer Ag particles. *Crystal Growth and Design*, 10:3378-3386.

Cho K., Park J., Osaka T., Park S., 2005. The study of antimicrobial activity and preservative effects of nanosilver ingredient. *Electrochimica Acta*, 51:956-960.

Choi O., Deng K.K., Kim N.J., Ross L., Surampalli R.Y., Hu Z., 2008. The inhibitory effects of silver nanoparticles, silver ions, and silver chloride colloids on microbial growth. *Water Research*, 42:3066-3074.

Choi O., Hu Z., 2008. Size dependent and reactive oxygen species related nanosilver toxicity to nitrifying bacteria. *Environmental Science and Technology*, 42:4583-4588.

Chou K.S., Lu Y.C., Lee H.H., 2005. Effect of alkaline ion on the mechanism and kinetics of chemical reduction of silver. *Materials* Chemistry *and Physics*, 94:429-433.

Dankovich T.A., Gray D.G., 2011. Bactericidal paper impregnated with silver nanoparticles for point-of-use water treatment. *Environmental Science Technology*, 45:1992-1998.

Del Nobile M.A., Cannarsi M., Altieri C., Sinigaglia M., Favia P., Iacoviello G., D'Agostino R., 2004. Effect of Ag-containing nano-composite active packaging system on survival of *Alicyclobacillus acidoterrestris*. *Journal of Food Science*, 69:379-383.

Dibrov P., Dzioba J., Gosink K.K., Ha¨se C.C., 2002. Chemiosmotic mechanism of antimicrobial activity of Ag in *Vibrio cholera*. *Antimicrobial Agents and Chemotherapy*, 46:2668-2670.

DuránI N., MarcatoI P.D., De ContiI R., AlvesI O.L., CostaII F.T.M., BrocchiII M., 2010. Potential use of silver nanoparticles on pathogenic bacteria, their toxicity and possible mechanisms of action. *Journal of the Brazilian Chemical Society*, 21:949-959.

Eisenberg J.N.S., Scott J.C., Porco T., 2007. Integrating disease control strategies: balancing water sanitation and hygiene interventions to reduce diarrheal disease burden. *American Journal of Public Health*, 97:846-852.

Evanoff D.D., Chumanov G., 2004. Size-controlled synthesis of nanoparticles. 2. Measurement of extinction, scattering, and absorption cross sections. *Journal of Physical Chemistry B*, 108:13957-13962.

Falkinham J.O., 2003. Factors influencing the chlorine susceptibility of *Mycobacterium avium*, *Mycobacterium intracellulare*, and *Mycobacterium scrofulaceum*. *Applied Environmental Microbiology*, 69:5685-5689.

Falkinham J.O., 2011. Nontuberculous mycobacteria from household plumbing of patients with nontuberculous mycobacteria disease. *Emerging Infectious Diseases*, 17:419-424.

Falkinham J.O., Norton C.D., Chevallier M.W.L., 2001. Factors influencing numbers of *Mycobacterium avium, Mycobacterium intracellulare*, and Other *Mycobacteria* in drinking water distribution systems. *Applied and Environmental microbiology*, 67:1225-1231.

Feng Q.L., Wu J., Chen G.O., Cui F.Z., Kim T.N., Kim J.O., 2000. A mechanistic study of the antibacterial effect of silver ions on *Escherichia coli* and *Staphylococcus aureus*. *Journal of Biomedical Materials Research*, Part A, 52:662-668.

Fernandez A., Picouet P., Lloret E., 2010. Cellulose-silver nanoparticle hybrid materials to control spoilage-related microflora in absorbent pads located in trays of fresh-cut melon. *International Journal of Food Microbiology*, 142:222-228.

Fox C.L., Modak S.M., 1974. Mechanism of silver sulfadiazine action on burn wound infections. *Antimicrobial Agents and Chemotherapy,* 5:582-588.

From C., Pukall R., Schumann P., Hormaza´bal V., Granum P.E., 2005.Toxin-producing ability among *Bacillus* spp. outside the *Bacillus cereus* group. *Applied and Environmental Microbiology*, 71:1178-1183.

Furkert F.H., Sorensen J.H., Arnoldi J., Robioneck B., Steckel H., 2011. Antimicrobial efficacy of surface-coated external fixation pins. *Current Microbiology*, 62:1743-1751.

Furno F., Morley K.S., Wong B., Sharp B.L., Arnold P.L., Howdle S.M., Bayston R., Brown P.D., Winship P.D., Reid H.J., 2004. Silver nanoparticles and polymeric medical devices: a new approach to prevention of infection? *Antimicrobial Chemotherapy.* 54:1019-1024.

Gade A.K., Bonde P., Ingle A.P., Marcato P.D., Durán N., Rai M.K., 2008. Exploitation of *Aspergillus niger* for synthesis of silver nanoparticles. *Journal of Biobased Materials and Bioenergy*, 2:243-247.

Galeano B., Korff E., Nicholson W.L., 2003. Inactivation of vegetative cells, but not spores, of *Bacillus anthracis, B-cereus*, and *B-subtilis* on stainless steel surfaces coated with an antimicrobial silver- and zinc-containing zeolite formulation. *Applied Environmental Microbiology*, 69:4329-4331.

Ganesh Babu M.M., Gunasekaran P., 2009. Production and structural characterization of silver nanoparticles from *Bacillus cereus* PGN1 isolate. *Colloids and Surfaces B: Biointerfaces*, 74:19-94.

Gleick P.H., 2003. Global freshwater resources: Soft-path solutions for 21st century. *Science*, 302:1524-1528.

Goering R., Dockrell H., Roitt I., Zuckerman M., Wakelin D., 2007. *Mims' medical microbiology.* 4 ed. Mosby-Year Book Europe Ltd.: United Kingdom.

Grant J., Wendelboe A.M., Wendel A., Jepson B., Torres P., Smelser C., Rolfs R.T., 2008. Spinach-associated *Escherichia coli* O157:H7 outbreak, Utah and New Mexico, 2006. *Emerging Infectious Diseases*, 14:1633-1636.

Guggenbichler J.P., Boswald M., Lugauer S., Krall, T., 1999. A new technology of microdispersed silver in polyurethane induces antimicrobial activity in central venous catheters. *Infection*, 27:S16-S23.

Hussain S., Hess K., Gearhart J., Geiss K., Schlager J., 2005. In vitro toxicity of nanoparticles in BRL 3A rat liver cells. *Toxicology In Vitro*, 19:975-983.

Irwin P., Martin J., Nguyen L.H., He Y., Gehring A., Chen C.Y., 2010. Antimicrobial activity of spherical silver nanoparticles prepared using a biocompatible macromolecular capping agent: evidence for induction of a greatly prolonged bacterial lag phase. *Journal of Nanobiotechnology*, 8:1-12.

Jaiswal S., Duffy B., Jaiswal A.K., Stobie N., McHale P., 2010. Enhancement of the antibacterial properties of silver nanoparticles using β-cyclodextrin as a capping agent. *International Journal of Antimicrobial Agents*, 36:280-283.

Jani P., Halbert G.W., Langridge J., Florence A.T., 1990. Nanoparticle uptake by the rat gastrointestinal mucosa: quantitation and particle size dependency. *Journal of Pharmacology and Pharmacotherapeutics*, 42:821-826.

Jiang H., Manolache S., Wong A.C.L., Denes F.S., 2004. Plasma-enhanced deposition of silver nanoparticles onto polymer and metal surfaces for the generation of antimicrobial characteristics. *Journal of Applied Polymer Science*, 93:1411-1422.

Jiang X.C., Chen W.M., Chen C.Y., Xiong S.X., Yu A.B., 2011. Role of temperature in the growth of silver nanoparticles through a synergetic reduction approach. *Nanoscale Research Letters*, 6:1-9.

Johnson N., Revenga C., Echeverria J., 2001. Managing water for people and nature. *Science*, 292:1071-1072.

Jung W.K., Koo H.C., Kim K.W., Shin S., Kim S.H., Park Y.H., 2008. Antibacterial activity and mechanism of action of the silver ion in *Staphylococcus aureus* and *Escherichia coli. Applied and Environmental Microbiology*, 74:2171-2178.

Kahinda J.M., Taigbenu A.E., Boroto J.R., 2007. Domestic rainwater harvesting to improve water supply in rural South Africa. *Physics and Chemistry of the Earth*, 32:1050-1057.

Kalishwaralal K., Ramkumarpandia S.B., Deepak V., Mohammad B., Sangiliyandi G., 2008. Biosynthesis of silver nanocrystals by *Bacillus licheniformis. Colloids and Surfaces B: Biointerfaces*, 65:150-153.

Kim J.S., Kuk E., Yu K.N., Kim J.H., Park S.J., Lee H.J., Kim S.H., Park Y.K., Park Y.H., Hwang C.Y., Kim Y.K., Lee Y.S., Jeong D.H., Cho M.H., 2007. Antimicrobial effects of silver nanoparticles. *Nanomedicine*, 3:95-101.

Kim Y.S., Song M.Y., Park J.D., Song K.S., Ryu H.R., Chung Y.H., Chang H.K., Lee J.H., Oh K.H., Kelman B.J., Hwang I.K., Yu I.J., 2010. Subchronic oral toxicity of silver nanoparticles. *Particle Fibre Toxicology*, 7:20.

Kreilgaard M., 2002. Influence of microemulsions on cutaneous drug delivery. *Advanced Drug Delivery Reviews*, 54:S77-S98.

Kumbhar A.S., Kinnan M.K., Chumanov G., 2005. Multipole plasmon resonances of submicron silver particles. *Journal of the American Chemical Society*, 127:12444-12445.

Lambert L., Mulvey T., 1996. Ernst Ruska (1906–1988), Designer extraordinaire of the electron microscope: A memoir. *Advances in Imaging and Electron Physics*, 95:2-62.

Lehtola M.J., Torvinen E., Kusnetsov J., Pitka¨nen T., Maunula L., von Bonsdorff C., Martikainen P.J., Wilks S.A., Keevil C.W., Miettinen I.T., 2007. Survival of *Mycobacterium avium*, *Legionella pneumophila*, *Escherichia coli*, and Caliciviruses in drinking water-associated biofilms grown under High-Shear Turbulent Flow. *Applied and Environmental Microbiology*, 73:2854-2859.

Leung V., Ko, F., 2011. Biomedical applications of nanofibers. *Polymer Advanced Technology*, 22:350-365.

Lkhagvajav N., Yasab I., Çelik E., Koizhaiganova M., Sari Ö., 2011. Antimicrobial activity of colloidal silver nanoparticles prepared by sol-gel method. *Digest Journal of Nanomaterials and Biostructures*, 6:149-154.

Lodish H., Berk A., Zipursky S.L., Matsudaira P., Baltimore D., Darnell J., 2000. *Molecular Cell Biology*. W.H Freeman and Company: New York.

Lok C., Ho C., Chen R., He Q., Yu W., Sun H., Tam P.K., Chiu J., Che C., 2006. Proteomic analysis of the mode of antibacterial action of silver nanoparticles. *Journal of Proteome Research*, 5:916-924.

Lu X.O., Zhang B.L., Wang Y.B., Zhou X.L., Weng J., Qu S.X., Feng B., Watari F., Ding Y.H., Leng Y., 2011. Nano-Ag-loaded hydroxyapatite coatings on titanium surfaces by electrochemical deposition. *Journal of the Royal Society Interface*, 8:529-539.

McIntyre L., Bernard K., Beniac D., Isaac-Renton J.L., Naseby D.C., 2008. Identification of *Bacillus cereus* group species associated with food poisoning outbreaks in British Columbia, Canada. *Applied and Environmental Microbiology*, 74:7451-7453.

Mergeay M., Monchy S., Vallaeys T., Auquier V., Benotmane A., Bertin P., Taghavi S., Dunn J., van der Lelie D., Wattiez R., 2003. *Ralstonia metallidurans*, a bacterium specifically adapted to toxic metals: towards a catalogue of metal-responsive genes. *FEMS Microbiology Reviews*, 27:385-410.

Mohan Y.M., Lee K., Premkumar T., Geckeler K.E., 2007. Fabrication of curcumin encapsulated PLGA nanoparticles for improved therapeutic effects in metastatic cancer cells. *Polymer*, 48:158-164.

Morones J.R, Elechiguerra J.L., Camacho A., Holt K., Kouri J.B., Ram´ırez J.T., Yacaman M.J., 2005. The bactericidal effect of silver nanoparticles. *Nanotechnology*, 16:2346-2353.

Mullen M.D., Wolf D.C., Ferris F.G., Beveridge T.J., Flemming C.A., Bailey G.W.,1989. Bacterial sorption of heavy metals. *Applied Environmental Microbiology*, 55:3143-3149.

Musee N., Thwala M., Nota N., 2011. The antibacterial effects of engineered nanomaterials: Implications for wastewater treatment plants. *Journal of Environmental Monitoring*, 13:1164-1183.

Nakaoka Y., Nosaka Y., 1997. Electron spin resonance study of radicals produced by photoirradiation on quantized and bulk ZnS particles. *Langmuir*, 13:708-713.

Nanda A., Saravanan M., 2009. Biosynthesis of silver nanoparticles from *Staphylococcus aureus* and its antimicrobial activity against MRSA and MRSE. *Nanomedicine*, 5:452-456.

Oberdorster G., 2001. Pulmonary effects of inhaled ultrafine particles. *International Archives of Occupational and Environmental Health*, 74:1-8.

Pal S., Tak Y.K., Song J.M., 2007. Does the antimicrobial activity of silver nanoparticles depend on the shape of the nanoparticle? A study of the gram-negative bacterium *Escherichia coli*. *Applied Environmental Microbiology*, 73:1712-1720.

Panacek A., Kvıtek L., Prucek R., Kolar M., Vecerova R., Pizurova N., Sharma V.K., Nevecna T., Zboril R., 2006. Silver colloid nanoparticles: synthesis, characterization, and their antibacterial activity. *Journal of Physical Chemistry B*, 110:16248-16243.

Parka H.J., Kim J.Y., Kim J., Lee J.H., Hahn J.S., Gu M.B., Yoon J., 2009. Silver-ion-mediated reactive oxygen species generation affecting bactericidal activity. *Water Research*, 43:1027-1032.

Qin Y., Ji X., Jing J., Liu H., Wu H., Yang W., 2010. Size control over spherical silver nanoparticles by ascorbic acid reduction. *Colloids and Surfaces A: Physicochemical Engineering Aspects*, 372:172-176.

Raffin M., Hussain F., Bhatti T.M., Akhter J.I., Hameed A., Hasan M.M., 2008. Antibacterial characterization of silver nanoparticles against *E. Coli* ATCC-15224. *Journal of Material Science and Technology*, 24:192-196.

Rai M., Yadav A., Gade A., 2009. Silver nanoparticles as a new generation of antimicrobials. *Biotechnology Advances*, 27:76-83.

Reith F., Etschmann B., Grosse C., Moors H., Benotmane M.A., Monsieurs P., Grass G., Doonan C., Vogt S., Lai B., Martinez-Criado G., George G.N., Nies D.H., Mergeay M., Pring A., Southam G., Brugger J.I., 2009. Mechanisms of gold biomineralization in the bacterium *Cupriavidus metallidurans*. *PNAS*, 106:17757-17762.

Rijsberman F.R., 2006. Water scarcity: Fact or fiction? *Agricultural Water Management*, 80:5-22.

Rodgers M.R., Blackstone B.J., Reyes A.L., Covert T.C., 1999. Colonisation of point of use water filters by silver resistant non-tuberculous mycobacteria. *Journal of Clinical Pathology*, 52:629-632.

Rojas L.A., Yáñez C., González M., Lobos S., Smalla K., Seeger M., 2011. Characterization of the metabolically modified heavy metal-resistant *Cupriavidus metallidurans* strain MSR33 generated for mercury bioremediation. *PLoS ONE*, 6:1-10.

Rosarin F.S., Mirunalini S., 2011. Nobel metallic nanoparticles with novel biomedical properties. *Bioanalysis and Biomedicine*, 3:085-091.

Ruparelia J.P., Chatterjee A.K., Duttagupta S.P., Mukherji S., 2008. Strain specificity in antimicrobial activity of silver and copper nanoparticles. A*cta Biomaterialia*, 4:707-716.

Sahoo P.K., Kamal S.S.K., Kumar T.J., Sreedhar B., Singh A.K., Srivastava S.K., 2009. Synthesis of silver nanoparticles using facile wet chemical route. *Defence Science Journal*, 59:447-455.

Sambhy V., MacBride M.M., Peterson B.R., Sen A., 2006. Silver bromide nanoparticle/polymer composites: dual action tunable antimicrobial materials. *American Chemical Society*, 128:9798-9808.

Šileikaite A., Prosycevas I., Puiso J., Juraitis A., Guobiene A., 2006. Analysis of silver nanoparticles produced by chemical reduction of silver salt solution. *Materials Science (Medziagotyra)*, 12:1392-1320.

Solomon S.D., Bahadory M., Jeyarajasingam A.V., Rutkowsky S.A., Boritz C., 2007. Synthesis and study of silver nanoparticles. *Journal of Chemical Education*, 84:322-325.

Sondia I., Salopek-Sondib B., 2004. Silver nanoparticles as antimicrobial agent: a case study on *E. coli* as a model for Gram-negative bacteria. *Colloid and Interface Science*, 275:177-182.
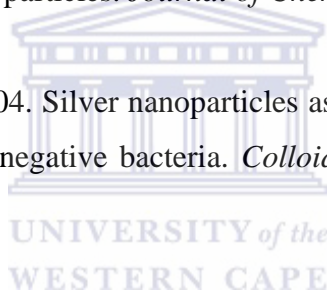
Sreekumari K. R., Sato Y., Kikuchi Y., 2005. Antibacterial metals- a viable solution for bacterial attachment and microbiologically influenced corrosion. *Material Transactions*, 46:1636-1645.

Staropoli J.F., Alon U., 2000. Computerized analysis of chemotaxis at different stages of bacterial growth. *Biophysical Journal*, 78:513-519.

Steed K.A., Falkinham J.O., 2006. Effect of growth in biofilms on chlorine susceptibility of *Mycobacterium avium* and *Mycobacterium intracellulare*. *Applied Environmental Microbiology*, 72:4007-4011.

Sweet M.J., Singleton I., 2011. Silver nanoparticles: a microbial perspective. *Advances in Applied Microbiology*, 77:116-133.

Takenaka S., Karg E., Roth C., Schulz H., Ziesenis A., Heinzmann U., Schramel P., Heyder J., 2001. Pulmonary and systemic distribution of inhaled ultrafine silver particles in rats. *Environmental Health Perspectives*, 109:547-549.

Taylor R.H., Falkinham J.O., Norton C.D., LeChevallier M.W., 2000. Chlorine, chloramine, chlorine dioxide, and ozone susceptibility of *Mycobacterium avium. Applied Environmental Microbiology*, 66:1702-1705.

Tiwari D.K., Behari, J., Sen P., 2008. Application of nanoparticles in waste water treatment. *World Applied Sciences*, 3:417-433.

Torvinen E., Lehtola M.J., Martikainen P.J., Miettinen I.T., 2007. Survival of *Mycobacterium avium* in drinking water biofilms as affected by water flow velocity, availability of phosphorus, and temperature. *Applied Environmental Microbiology*, 73:6201-6207.

Uehara T., Dinh T., Bernhardt T.G., 2009. LytM-Domain factors are required for daughter cell separation and rapid ampicillin-induced lysis in *Escherichia coli. Journal of Biotechnology*, 191:5094-5107.
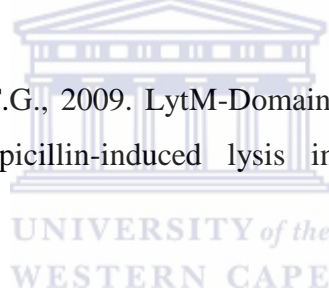
von Reyn C.F., Waddell R.D., Eaton T., Arbeit R.D., Maslow J.N., Barber T.W., Brindle R.J., Gilks C.F., Lumio J., Lahdevirta J., Ranki A., Dawson D., Falkinham J.O., 1993. Isolation of *Mycobacterium avium* complex from water in the United States, Finland, Zaire, and Kenya. *Journal of Clinical Microbiology*, 31:3227-3230.

World Health Organization, 2011. "Guidelines for Drinking-water quality": Available [Online]: http://whqlibdoc.who.int/publications/2011/9789241548151_eng.pdf.

Zhang L., Yu J.C., Yin Yip H., Li Q., Kwong K.W., Xu A., Wong, P.K., 2003. Ambient light reduction strategy to synthesize silver nanoparticles and silver-coated TiO_2 with enhanced photocatalytic and bactericidal activities. *Langmuir*, 19:10372-10380.